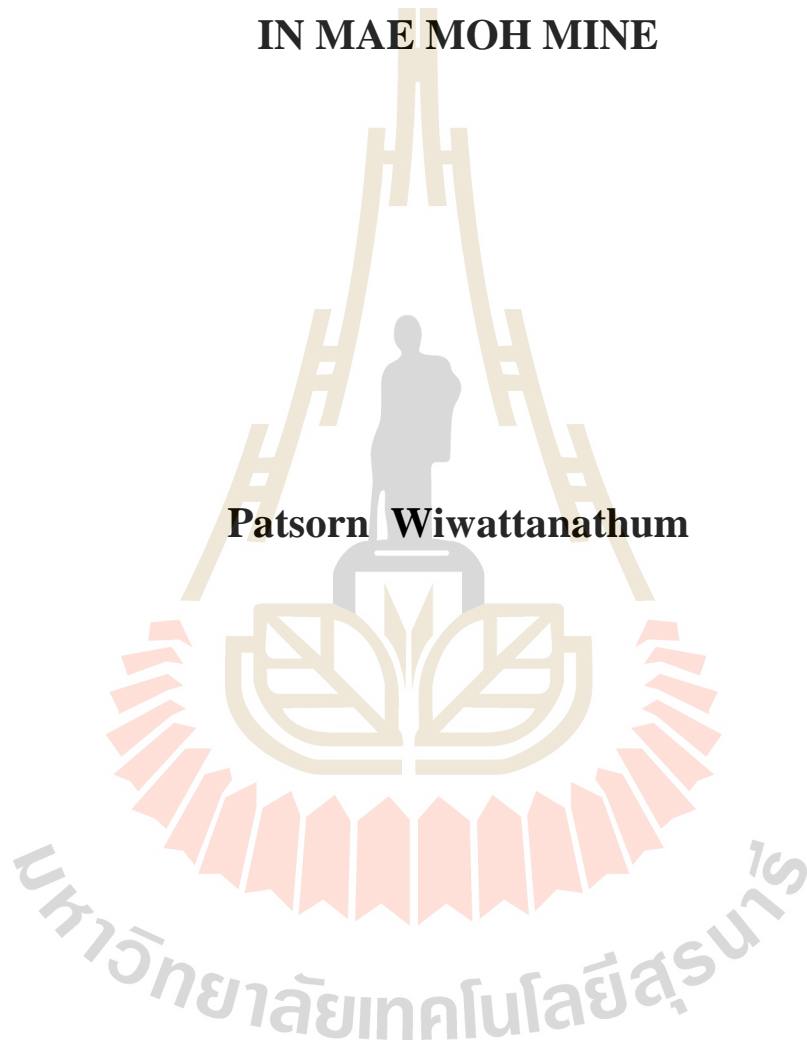


**CONSOLIDATION BEHAVIOR OF PREFABRICATED
VERTICAL DRAINS IMPROVED ULTRA - SOFT MUD
IN MAE MOH MINE**

Patsorn Wiwattanathum



A Thesis Submitted in Partial Fulfillment of the Requirements for the

Degree of Master of Engineering in Civil Engineering

Suranaree University of Technology

Academic Year 2016

พฤติกรรมการอัดตัวคาน้ำของดินโคลนอ่อนมากในเหมืองแม่เมาะที่ปรับปรุง
ด้วยแผ่นระบายน้ำแนวตั้ง



นางสาวภัศรา วิวัฒนาธรรม

วิทยานิพนธ์นี้เป็นส่วนหนึ่งของการศึกษาตามหลักสูตรปริญญาวิศวกรรมศาสตรมหาบัณฑิต

สาขาวิชาวิศวกรรมโยธา

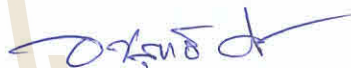
มหาวิทยาลัยเทคโนโลยีสุรนารี

ปีการศึกษา 2559

**CONSOLIDATION BEHAVIOR OF PREFABRICATED VERTICAL
DRAINS IMPROVED ULTRA - SOFT MUD IN MAE MOH MINE**

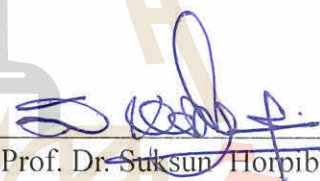
Suranaree University of Technology has approved this thesis submitted in partial fulfillment of the requirements for a Master's Degree.

Thesis Examining Committee



(Assoc. Prof. Dr. Avirut Chinkulkijniwat)

Chairperson



(Prof. Dr. Suksum Horpibulsuk)

Member (Thesis Advisor)



(Asst. Prof. Dr. Pornpot Tanseng)

Member



(Prof. Dr. Sukit Limpijumnong)

Vice Rector for Academic Affairs
and Innovation



(Assoc. Prof. Flt. Lt. Dr. Kontorn Chamniprasart)

Dean of Institute of Engineering

กัศสร วิวัฒนาธรรม : พฤติกรรมการอัดตัวคายน้ำของดิน โคลนอ่อนมากในเมืองแม่เมาะ
ที่ปรับปรุงด้วยแผ่นระบายน้ำแนวตั้ง (CONSOLIDATION BEHAVIOR OF
PREFABRICATED VERTICAL DRAINS IMPROVED ULTRA - SOFT MUDIN MAE
MOH MINE) อาจารย์ที่ปรึกษา : ศาสตราจารย์ ดร.สุขสันต์ หอพิบูลสุข, 113 หน้า

งานวิจัยนี้จึงศึกษาความเป็นไปได้ของการประยุกต์ใช้เทคนิคการให้น้ำหนักบรรทุกร่วมกับ
ระบบระบายน้ำแนวตั้ง ในการลดปริมาณความชื้น และเพิ่มกำลังต้านทานแรงเฉือนของดิน โคลน
ในพื้นที่ Sump1 C1 ของเหมืองแม่เมาะ การไฟฟ้าฝ่ายผลิตแห่งประเทศไทย ด้วยการสร้าง
แบบจำลองกายภาพย่อส่วน(Physical model test) สำหรับการทดสอบการอัดตัวคายน้ำของดิน
โคลนเสริมแผ่นระบายน้ำแนวตั้งที่ต่างขนาดกัน เพื่อหาพารามิเตอร์ของดินและแผ่นระบายน้ำ
แนวตั้ง ผลทดสอบที่ได้จะนำไปเปรียบเทียบกับทฤษฎีของ Hansbo และผลการวิเคราะห์ทางไฟ
ไนท์เอลิเมนต์ทั้งแบบ โมเดลสมมาตรรอบแกนและ โมเดลแบบระนาบ จากผลการศึกษาพบว่าแผ่น
ระบายน้ำแนวตั้งจะช่วยเร่งการทรุดตัวของชั้นดินเหนียวอ่อน โดยค่าการทรุดตัวจะเพิ่มขึ้นตาม
น้ำหนักบรรทุกที่กระทำ ในส่วนของค่าความคั่นน้ำส่วนเกินจะเพิ่มขึ้นอย่างรวดเร็วเมื่อน้ำหนัก
บรรทุกกระทำเช่นเดียวกับค่าการทรุดตัว โดยค่าความคั่นน้ำส่วนเกินในมวลดินตำแหน่งที่อยู่
ใกล้กับขอบเขตที่ระบายน้ำได้ จะระบายได้เร็ว และความคั่นน้ำส่วนเกินที่ตรงกลางถึงทดสอบ
ระบายได้ช้าสุด และตำแหน่งที่อยู่ใกล้กับแผ่นระบายน้ำแนวตั้งจะระบายน้ำได้เร็วกว่าตำแหน่งที่อยู่
ไกล และเมื่อนำผลการทดสอบที่ได้จากห้องปฏิบัติการมาเปรียบเทียบกับผลการวิเคราะห์ทางไฟ
ไนท์เอลิเมนต์พบว่า โมเดลแบบสมมาตรรอบแกนให้ค่าใกล้เคียงกับผลการทดสอบที่ได้จาก
ห้องปฏิบัติการมากกว่าโมเดลแบบระนาบ

สาขาวิชา วิศวกรรมโยธา
ปีการศึกษา 2559

ลายมือชื่อนักศึกษา กัศสร
ลายมือชื่ออาจารย์ที่ปรึกษา สุขสันต์

PATSORN WIWATTANATHUM : CONSOLIDATION BEHAVIOR OF
PREFABRICATED VERTICAL DRAINS IMPROVED ULTRA - SOFT
MUD IN MAE MOH MINE. THESIS ADVISOR : PROF. SUKSUN
HORPIBULSUK, Ph.D., 113 PP.

CONSOLIDATION SETTLEMENT/PREFABRICATED VERTICAL DRAIN/
PHYSICAL MODEL/FINITE ELEMENT ANALYSIS

This research studies the viability of preloading with prefabricated vertical drain (PVD) to improve the mud pond at Sump1 C1, Mae Moh mine of Electricity Generating Authority of Thailand via fully instrumented physical model tests with various PVD dimensions. The consolidation test results obtained from the model tests are compared with Hansbo's solution (unit cell) and finite element analyses using axial symmetry and plane strain models. The study shows that the final settlement of each load increases with the applied vertical stress. The excess pore water pressure increases after the application of vertical load and then rapidly decreases with time. The quick dissipation of excess pore water pressure is observed at the top and bottom of the model ground (double drainage). The highest the excess pore water pressure is found at the middle of the model ground where the excess pore pressure close to the PVD is lower than that far away from the PVD. The comparison between the model test results and finite element analyses shows that the excess pore pressure dissipation is satisfactorily predicted by the axial symmetry model.

School of Civil Engineering

Academic Year 2016

Student's Signature _____

Advisor's Signature _____



ACKNOWLEDGEMENT

The researcher would like to thank everyone who gives the advice, suggestion, and support to successfully complete this study.

I would like to thank Prof. Suksun Horpibulsuk, the advisor, who gave the help in academic matter, suggestion, knowledge, and the review to complete this thesis.

I would like to thank Assoc. Prof. Dr. Avirut Chinkulkijniwat, Chairperson, who gave the knowledge of the academic research.

I would like to thank Asst.Prof.Dr.Pornpot Tanseng, member, who gave the knowledge of the academic research.

Nevertheless, I would like to thank everyone who gave help and support to this research.

Lastly, I would like to thank my parents who always give love and support in everything including the education.

Patsorn Wiwattanathum

TABLE OF CONTENTS

	Page
ABSTRACT (THAI).....	I
ABSTRACT (ENGLISH).....	II
ACKNOWLEDGEMENTS.....	III
TABLE OF CONTENT.....	IV
LIST OF TABLES.....	V
LIST OF FIGURES.....	VI
ACKNOWLEDGEMENT.....	XVI
CHAPTER	
I INTRODUCTION	1
1.1 Statement of the Problems.....	1
1.2 Objectives.....	2
1.3 Scope of Study.....	3
1.4 Expected Benefits.....	3
II Literature Review	4
2.1 General.....	4
2.2 Settlement.....	4
2.3 consolidation.....	19
2.4 Prefabricated vertical drains (PVD).....	42
2.5 Case Study.....	64

TABLE OF CONTENTS (Continued)

III Method	73
3.1 Introduction.....	73
3.2 The sampling and experiment place.....	74
3.3 Basic property test.....	76
3.4 Constructing the tank of physical model test.....	76
3.5 Soil sampling and preparation.....	76
3.6 The duplication of soil layer in the test tank.....	76
3.7 The measuring devices installation and the load adding in physical model test.....	77
3.8 Test conditions.....	80
IV Test Result	81
4.1 Introduction.....	81
4.2 The basic property and engineering property of mud.....	81
4.3 The consolidation behavior of the ultra-soft mud with the prefabricated vertical drain.....	84
4.4 Theoretical and Numerical Analysis.....	89
4.5 Analysis and Discussion.....	107
V Conclusion	109
5.1 Summery.....	109
5.2 Suggestion.....	110
REFERENCES.....	111
BIOGRAPHY.....	113

LIST OF TABLES

Table	Page
2.1 Values of C_s for foundations on clay soil of infinite depth.....	8
2.2 Values of C_s for foundations on clay soil of limited depth (D) above a rigid substratum (Rock)	9
2.3 Range of possible field values of the ratio k_h/k_y for soft clays (Rixner et al.1986).....	56
2.4 Summary of Laboratory Test on Prefabricated Vertical Drains.....	61
2.5 Water content and bulk density of each layer of slurry.....	64
3.1 The sample test.....	80
4.1 The basic property of soil sample.....	82
4.2 Parameter model for the analysis.....	92
4.3 The consolidation time and consolidation settlement of each applied vertical stress and PVD sizes.....	94

LIST OF FIGURES

Figure	Page
2.1 Three phases of settlement for fine-grained soils as function of time.....	6
2.2 Settlement of a mass of soil: (a) before consolidation settlement; (b) after consolidation settlement.....	10
2.3 Time factor as a function of percentage of consolidation (Teng, 962).....	17
2.4 Sketch showing primary consolidation and secondary compression.....	18
2.5 Coefficient of secondary compression; C = ratio of decrease in sample height to initial sample height for one cycle of time on a logarithmic scale following completion consolidation.....	19
2.6 One-dimensional consolidation.....	20
2.7 Drainage path length d	24
2.8 One-dimensional consolidation – Isochromes.....	27
2.9 Average degree of consolidation U_v versus T_v	29
2.10 Oedometer test apparatus.....	31
2.11 Radius of influence of drains.....	38
2.12 Typical vertical drain installation for a highway embankment (Rixner et al., 1986).....	43
2.13 Characteristics of prefabricated drains.....	44
2.14 Schematic of PVD with drain resistances and soil disturbance (Rixner et. Al 1986).....	48

LIST OF FIGURES (Continued)

Figure	Page
2.15 Typical values of vertical discharge capacity (Rixner et. Al 1986).....	30
2.16 Realationship of drain spacing (S) to drain influence zone (D) (Rixner et al, 1986).....	52
2.17 Example of variation of degree of consolidation wih depth for drains with well resistance (Jamiolkowski et al. 1983).....	52
2.18 Influence of finite drain permeability on consolidation rate (Jamiolkowski et al.1983).....	53
2.19 Influence of smear on consolidation rate (Jamiolkowski et al. 1983).....	53
2.20 The filtration mechanism (Vreeken et al, 1983).....	60
2.21 The filtration resistances during filtration (Vreeken et al, 1983).....	60
2.22 Large diameter consolidation cell with soil instruments.....	66
2.23 Sand spreading system used for slurry pond.....	67
2.24 Location of failure area where bursting of slurry.....	68
2.25 Layout of geotextile sheets used to cover failure area of slurry pond.....	68
2.26 Comparison of Settlement Curves.....	70
2.27 Calculated Excess Pore Pressure Variations.....	71
2.28 Lateral Displacement Profiles.....	71
3.1 The research method.....	73
3.2 Mae Moh Mine map.....	74
3.3 Inpit dump area Sump1 C1.....	75

LIST OF FIGURES (Continued)

Figure	Page
3.4 Soil in Sump1 C1.....	75
3.5 Feature of test tank (a) plan of test tank (b) side view of test tank.....	78
3.6 The measuring devices diagram (a) horizontal view (b) vertical view.....	79
4.1 The analysis size of soil.....	83
4.2 The relationship between the void ratio and vertical pressure of mud.....	83
4.3 The relationship between the applied vertical stress and time of the ultra-soft mud with the 5 cm prefabricated vertical drain.....	85
4.4 The relationship between the settlement and time of the ultra-soft mud with 5 cm PVD.....	85
4.5 The relationship between the applied vertical stress and time of the ultra-soft mud with the 10 cm prefabricated vertical drain.....	86
4.6 The relationship between the settlement and time of the ultra-soft mud with 10 cm PVD.....	86
4.7 The relationship between the excess pore water pressure and time of the applied vertical stress at 20 kPa.....	88
4.8 The relationship between the excess pore water pressure and time of the applied vertical stress at 40 kPa.....	88
4.9 The relationship between the excess pore water pressure and time of the applied vertical stress at 80 kPa.....	89

LIST OF FIGURES (Continued)

Figure	Page
4.10 The relationship between the excess pore water pressure and time of the applied vertical stress at 120 kPa.....	89
4.11 Axial symmetry model of ultra-soft mud with PVD for the analysis.....	92
4.12 Plane strain model of ultra-soft mud with PVD for the analysis.....	92
4.13 The relationship between the applied vertical pressure and time; the settlement and time of the ultra-soft mud with 5 cm PVD.....	95
4.14 The relationship between the applied vertical pressure and time; the settlement and time of the ultra-soft mud with 10 cm PVD.....	96
4.15 The change of the excess pore water pressure and the radial distance of PVD sized 5 and 10 cm respectively at 20 kPa.....	98
4.16 The change of the excess pore water pressure and the radial distance of PVD sized 5 and 10 cm respectively at 40 kPa.....	99
4.17 The change of the excess pore water pressure and the radial distance of PVD sized 5 and 10 cm respectively at 80 kPa.....	100
4.18 The change of the excess pore water pressure and the radial distance of PVD sized 5 and 10 cm respectively at 120 kPa.....	101
4.19 The relationship between the excess pore water pressure and depth of the soft mud with PVD sized 5 and 10 cm respectively at 20 kPa.....	103
4.20 The relationship between the excess pore water pressure and depth of the soft mud with PVD sized 5 and 10 cm respectively at 40 kPa.....	104

LIST OF FIGURES (Continued)

Figure	Page
4.21 The relationship between the excess pore water pressure and depth of the soft mud with PVD sized 5 and 10 cm respectively at 80 kPa.....	104
4.22 The relationship between the excess pore water pressure and depth of the soft mud with PVD sized 5 and 10 cm respectively at 120 kPa.....	106
4.23 The relationship between coefficient of consolidation and applied vertical pressure.....	108

CHAPTER 1

INTRODUCTION

1.1 Statement of the Problems

Mae Moh Mine is 4 kilometers in width with 7 kilometers in length. Sump1 C1 is the deepest area around 270 meters depth from the soil level. It is located in the north of Mae Moh Mine with the area about 80,000 square meters. In the north is near the inpit dump of the previous mine; the south is near Sump2 C1. Because Sump1 C1 is a low area, which receives the water flow into the mine for many years, those water flow cause the soil erosion and alluvion. Moreover, there are alluviums under the water with the thickness about 10 meters; the water level is above the alluvium around 5 meters. According to the mine planning and development, the mine will be deeply dug to a depth of approximately 500 meters in the next 37 years and it will be the deepest open pit Lignite mine in the world. From such reason, Sump1 C1 will become the inpit dump. However, the mud in Sump1 C1 possesses high water content, leading to large consolidation settlement and low bearing capacity. Therefore, inpit dump without the improvement of mud properties will cause the instability of mine slope, and the unsafety of workers and machines.

A cost-effective soil improvement technique is pre-loading with vertical drains. The vertical drains reduce the drainage path of the excess pore water pressure and therefore shorten the consolidation time. This technique has been extensively used in earth structure constructions on thick soft soil deposit such as road, airport and

reclaimed area, etc [Chen et al., 2015 and Wu et al., 2015]. For example, Changi east reclamation project in Singapore [Chu et al. (2009) and Bo et al. (1999)] and Suwanaphumi International Airport in Thailand [Seah, Tian Ho (2013)] are successfully constructed using preloading with vertical drains.

This research will study the viability of preloading with vertical drains to improve the mud from Sump1 C1 using fully instrumented physical model tests with various prefabricated vertical drain (PVD) dimensions. The PVD parameters obtained from the model tests will be used to simulate consolidation of the PVD improved mud ground by Finite Element (FE) analysis. The FE analysis results will be compared with measured data and Hansbo's solution (unit cell). The output of this study will lead to a proper design method for mud improvement in the Sump1 C1, Mae Moh Mine

1.2 Objectives

- 1.2.1 to develop a fully instrumented physical model with axial symmetry condition of PVD improved mud
- 1.2.2 to investigate consolidation behavior on PVD improved high water content mud and examine the water content reduction development versus consolidation time
- 1.2.3 to simulate the consolidation behavior development using Plaxis 2D under axial symmetry condition.
- 1.2.4 to suggest a suitable design method for PVD improved mud in Sump 1 C1.

1.3 Scope of Study

The mud samples will be taken from Sump1 C1 of Mae Moh Mine, Lampang.

The mud will be thoroughly mixed with water to attain a water content of approximately twice liquid limit to make a uniform paste. The mud paste will be transferred to a 5 mm thick cylindrical tank with a 500 mm diameter and 1.20 m height. The tank has smooth and neat texture with a bottom drainage hole, which has a faucet and the gap for measuring devices. The measuring devices include pore pressure transducer, linear potentiometers, and earth pressure cells. The measured consolidation data will be compared to the FE analysis by Plaxis 2D and the Hanbo's solution. Based on the critical analysis of the studied results, a design method of PVD improved mud is suggested.

1.4 Expected Benefits

- 1.4.1 the consolidation behavior of the mud in the physical model test
- 1.4.2 the settlement development versus consolidation time of PVD improved mud
- 1.4.3 the simulated consolidation behavior of PVD improved mud including pore water pressure and settlement
- 1.4.3 a suggest design method for PVD improved mud

CHAPTER 2

LITERATURE REVIEW

2.1 General

This chapter reviews literature about the engineering behavior of clay, the settlement, the consolidation including the soil improvement by using prefabricated vertical drain (PVD). Terzaghi's theory of one dimensional consolidation will be used as the base of this research. Moreover, this research will use the feature of prefabricated vertical drain in order to stimulate the consolidation process. Some physical model test and field case history are presented in the end of chapter. The physical model test is conducted to study the settlement and consolidation behavior of slurry soil. The result is then applied to the vertical drain system in the field. For field case history in Singapore called "Changi east land reclamation project", simple method proposed by Chai, Shen, Miura and Bergado (2001) was applied to model PVD improved-subsoil.

2.2 Settlement

2.2.1 Introduction

Structures built on soil are subject to settlement. Some settlement is often in evitable and depending on the circumstances some settlement is tolerable. For example small uniform settlement of a building throughout the floor area might be

tolerable, whereas nonuniform settlement of the same building might not be. Or, settlement of a garage or warehouse building might be tolerable, whereas the same settlement (especially different settlement) of a luxury hotel building would not be because of damage to walls, ceilings, and so on. In any event, knowledge of the causes of settlement and means of computing (or predicting) settlement quantitatively are important to the geotechnical engineer.

Although there are several possible causes of settlement (e.g., dynamic forces, changes in the groundwater table, adjacent excavation, etc.) probably the major cause is compressive deformation of soil beneath a structure. Compressive deformation generally results from reduction in void volume, accompanied by rearrangement of soil grains and compression of the material in the void. If soil is dry, its void ratio is filled with air; and because air is compressible, rearrangement of soil grains can occur rapidly. If soil is saturated, its voids are filled with incompressible water, which must be extruded from the soil mass before soil grains can rearrange themselves. In soil of high permeability (i.e., coarse-grained soils), this process requires a short time interval for completion, and almost all settlement occurs by the time construction is complete. However, in soils of low permeability (i.e., fine-grained soils), the process requires a long time interval for completion. The result is that the strain occurs very slowly; thus, settlement takes place slowly and continues over a long period of time. The latter case (fine grained-grained soil) is of more concern because of long-term uncertainty. Settlement of structures on fine-grained soil generally consists of three phase. The first phase is known as immediate settlement, or volume distortion settlement. As suggested by the expression, immediate settlement occurs rapidly after load is applied. Caused by soil volume distortion, immediate settlement is typically

completed quickly and constitutes a relatively small amount of total settlement in fine-grained soils. Subsequent to immediate settlement, primary consolidation settlement occurs, the result of primary consolidation. (These are commonly referred to simply as consolidation settlement and consolidation, respectively.) Primary consolidation occurs due to extrusion of water from the voids as a result of increased loading. Primary consolidation settlement is very slow and continues over a long period of time. After primary settlement has ended, soil compression and additional associated settlement continue at a very slow rate, the result of plastic readjustment of soil grains due to new, changed stresses in the soil and progressive breaking off of clayey particles and their interparticle bonds. This phenomenon is known as secondary compression, and associated settlement is called secondary compression settlement. Figure 2.1 illustrates the three phases of settlement as a function of time.

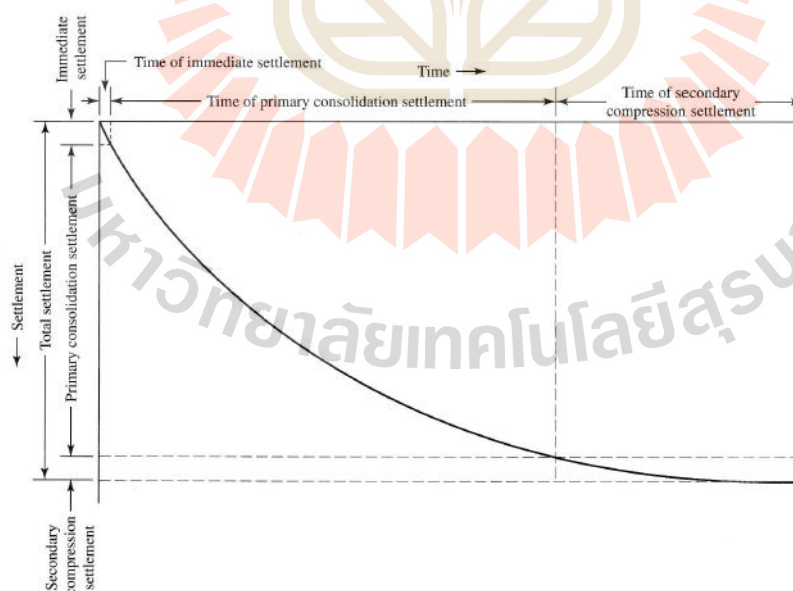


Figure 2.1 Three phases of settlement for fine-grained soils as function of time

2.2.2 Immediate settlement of loads on clay

As noted previously, immediate settlement occurs rapidly, perhaps within hours or days after load is applied. It is caused by soil volume distortion, and it usually constitutes only a small amount of total settlement in fine-grained soils. Immediate settlement may be estimated based on the linear theory of elasticity. Equation (2.1) is applicable.*

$$S_i = C_s q B \frac{1-\mu^2}{E_u} \quad (2.1)$$

- Where S_i = immediate settlement
- C_s = shape and foundation rigidity factor (see Tables 2.1 and 2.2)
- q = magnitude of evenly distributed load acting on the foundation area (total load/foundation area)
- B = width or diameter of foundation
- μ = Poisson's ratio for the applied stress range (assume 0.5 for saturated clays, slightly less for partially saturated)
- E_u = undrained elastic modulus of clay (Young's Modulus or modulus of elasticity)

E_u may be evaluated using the results of undrained triaxial compression test performed on undisturbed soil samples. Values of E_u frequently lie in the range $500c_u$ to $1,500c_u$, where c_u is the soil cohesion shear strength as determined from the undrained tests. The lower range is for clays of high plasticity and where foundation loads are large, while the higher range is for clays of low plasticity and where foundation loading is low.

Table 2.1 Values of C_s for foundations on clay soil of infinite depth

Shape	Center	Corner	Edge at Middle of Long Side	Average
Flexible foundation:				
Circular	1.00	—	0.64	0.85
Square	1.12	0.56	0.76	0.95
Rectangular:				
$L/B = 2$	1.53	0.76	1.12	1.30
$L/B = 5$	2.10	1.05	1.68	1.82
$L/B = 10$	2.56	1.28	2.10	2.24
Rigid foundation:				
Circular	0.79	—	0.79	0.79
Square	0.82	0.82	0.82	0.82
Rectangular:				
$L/B = 2$	1.12	1.12	1.12	1.12
$L/B = 5$	1.60	1.60	1.60	1.60
$L/B = 10$	2.00	2.00	2.00	2.00

^a Soil depth extends greater than $10B$.

Source: D. F. McCarthy, *Essentials of Soil Mechanics and Foundations*, 6th ed., 2002. Reprinted by permission of Pearson Education, Upper Saddle River, NJ.

Table 2.2 Values of C_s for foundations on clay soil of limited depth (D) above a rigid substratum (Rock)

C_s Under Center of Rigid Circular Foundation	Depth to Width Ratio (D/B)	C_{sr} Under Corner of Flexible Rectangular Foundation ^a				
		$L/B = 1$	$L/B = 2$	$L/B = 5$	$L/B = 10$	$L/B = \infty$
0.35	1	0.15	0.12	0.10	0.04	0.04
0.54	2	0.29	0.29	0.27	0.26	0.26
0.69	5	0.44	0.52	0.55	0.54	0.52
0.74	10	0.48	0.64	0.76	0.77	0.73
0.79	∞	0.56	0.76	1.05	1.28	—

^aTo determine C_s for center of a foundation area, divide foundation shape into four equal subrectangles, then assign the B dimension based on the size of one of the subrectangles. Multiply the selected value of C_s by 4 to use with Equation (7-1).
Source: D. F. McCarthy, *Essentials of Soil Mechanics and Foundations*, 6th ed., 2002. Reprinted by permission of Pearson Education, Upper Saddle River, NJ.

2.2.3 Settlement of loads on clay due to primary consolidation

Once the field consolidation line has been defined for a given clayey soil, the total expected primary consolidation settlement of the load on the clay can be determined. Consider Figure 2.2, where a mass of soil is depicted before (Figure 2.2a) and after (Figure 2.2b) consolidation settlement has occurred in a clay layer of initial thickness H . From Figure 2.2,

$$\frac{H}{H} = \frac{H}{H_s + (H_v)_0} \quad (2.2)$$

Where H represents the amount of clay settlement and H_s and $(H_v)_0$ denote the height of solids and initial height of voids, respectively. By definition, the initial void ratio, e_0 in Figure 2.2b, is given by the following:

$$e_0 = \frac{(V_v)_0}{V_s} \quad (2.3)$$

Where $(V_v)_0$ and V_s represent the original volume of voids and the volume of solids, respectively. Because each volume can be replaced by the soil's cross-sectional area

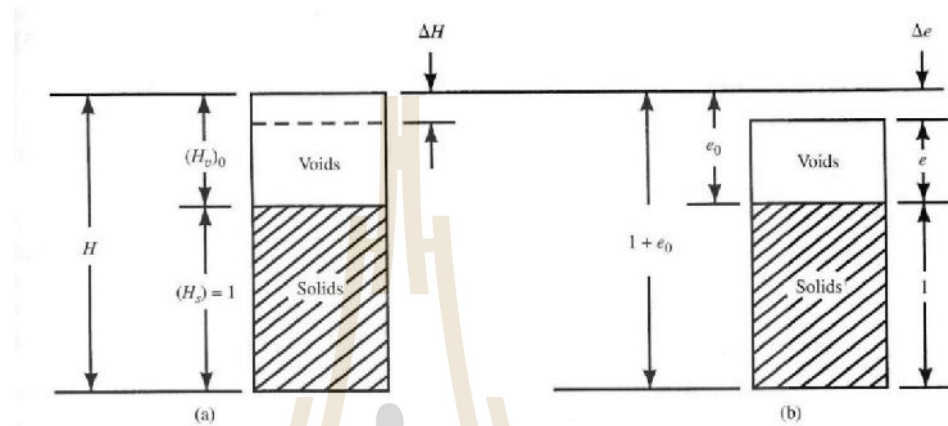


Figure 2.2 Settlement of a mass of soil: (a) before consolidation settlement; (b) after consolidation settlement.

(A) times the height of the soil, this equation can be modified as follows:

$$e = \frac{(A)(H_v)_0}{(A)(H_s)} = \frac{(H_v)_0}{H_s} \quad (2.4)$$

$$e = \frac{H}{H_s} \quad (2.5)$$

Where Δ_e represents the change in void ratio as a result of consolidation settlement. If we let the height of solids equal unity, then Eqs. (2.3), (2.4), and (2.5) become

$$\frac{H}{H} = \frac{H}{1 + (H_v)_0} \quad (2.6)$$

$$e_0 = (H_v)_0 \quad (2.7)$$

$$e = H \quad (2.8)$$

Substituting Eqs. (2.7) and (2.8) into Eq. (2.6) yields

$$\frac{H}{H} = \frac{e}{1 + e_0} \quad (2.9)$$

Or,

$$\frac{H}{H} = \frac{e}{1 + e_0} (H) \quad (2.10)$$

Because $e = e_0 - e$ and $H = \text{settlement } s_c$

$$s_c = \frac{e_1 - e_2}{1 + e_0} (H) \quad (2.11)$$

Where s_c = total settlement due to primary consolidation

e_0 = initial void ratio of the soil in situ

- e = void ratio of the soil corresponding to the total pressure (p) acting at midheight of the consolidating clay layer
- H = thickness of the consolidating clay layer

In practice, the value of e_0 is obtained from the laboratory consolidation test, and the value of e is obtained from the field consolidation line based on total pressure (i.e., effective overburden pressure plus net additional pressure due to the structure—both at midheight of the consolidating clay layer). The value of (H) is obtained from soil exploration.

An alternative equation for computing total expected primary consolidation settlement using the compression index (i.e., slope of the field consolidation line) can be derived by recalling Eq.(2.12)

$$C_c = \frac{e_1 - e_2}{\log(p_2/p_1)} \quad (2.12)$$

Because (p_1, e_1) and (p_2, e_2) can be the coordinates of any two points on the field consolidation line, let

- p_1 = present effective overburden pressure at midheight of the consolidating clay layer (i.e., p_0)
- e_1 = initial void ratio of the soil in situ [i.e., e_0 in Eq. (2.11)]
- p_2 = total pressure acting at midheight of the consolidating clay layer [$p_0 + p$ (i.e., p)]

e_2 = void ratio of the soil corresponding to the total pressure (p) acting at midheight of the consolidating clay layer [i.e., e in Eq. (2.11)]

Making these substitutions in Eq. (2.12) gives the following:

$$C_c = \frac{e_0 - e}{\log(p/p_0)} \quad (2.13)$$

Rearranging this equation results in

$$e_0 - e = C_c [\log(p/p_0)] \quad (2.14)$$

Substituting Eq. (2.14) into Eq. (2.11) yields

$$s_c = \frac{C_c \left[\log \left(\frac{p}{p_0} \right) \right]}{1 + e_0} (H) \quad (2.15)$$

Or

$$s_c = C_c \left(\frac{H}{1 + e_0} \right) \log \frac{p}{p_0} \quad (2.16)$$

Where C_c = slope of the field consolidation line (compression index)

p = total pressure acting at midheight of the consolidating clay layer (= $p_0 + p$)

p_0 = present effective overburden pressure at midheight of the consolidating clay layer

p = net additional pressure at midheight of the consolidating clay layer due to the structure

The value of C_c can be determined by evaluating the slope of the field consolidation line [Eq. (2.12)] or approximated based on the liquid limit. If the latter method is used, computed settlement should be considered as a rough approximation.

The time rate of settlement due to primary consolidation can be computed from the following equation (Terzaghi and Peck, 1967):

$$t = \frac{T_v}{C_v} H^2 \quad (2.17)$$

Where t = time to reach a particular percent of consolidation; percent of consolidation is defined as the ratio of the amount of settlement at a certain time during the process of consolidation to the total settlement due to consolidation

T_v = time factor, a coefficient depending on the particular percent of consolidation

c_v = coefficient of consolidation corresponding to the total pressure ($p = p_0 + p$) acting at midheight of the clay layer

H = thickness of the consolidating clay layer [however, if the clay

layer in Situ is drained on both top and bottom, half the thickness of the layer should be substituted for H in Eq. (2.17)]

In practice, the value of T_v is determined from Figure 2-3, based on the desired percent of consolidation (U), and the value of C_v is determined from the C_v -log p curve based on the total pressure acting at midheight of the clay layer. It will be recalled that the C_v -log p curve is a product of the laboratory consolidation test.

As may be noted from Eq. (2.17), the coefficient of consolidation (C_v) indicates how rapidly (or slowly) the process of consolidation takes place. This consolidation property can also be expressed as follows (Terzaghi et al., 1996)*

$$C_v = \frac{k}{w m_v} \quad (2.18)$$

Where k = coefficient of permeability
 w = unit weight of water
 m_v = coefficient of volume compressibility

The last term can be determined from the following:

$$m_v = \frac{a_v}{1+e} \quad (2.19)$$

Where a_v = coefficient of compressibility

e = void ratio

Substituting Eq. (2.19) into Eq. (2.18) gives the following:

$$C_v = \frac{k(1+e)}{a_v w} \quad (2.20)$$

For small strains, change in the void ratio (Δe) may be taken as directly proportional to change in the effective pressure (Δp). Therefore, a_v in Eq. (2.20) can be expressed in equation form as follows:

$$a_v = \frac{e}{p} \quad (2.21)$$

Values of k , e , and a_v can be evaluated separately and substituted into Eq. (2.20) to find c_v . However, it is common practice to evaluate c_v directly from the results of a laboratory consolidation test.

To summarize the means of finding settlement of loads on clay due to primary consolidation, one can use either Eq. (2.11) or Eq. (2.16) to compute total settlement; then Eq. (2.17) can be used to find the time required to reach a particular percentage of that consolidation settlement. For example, if total settlement due to consolidation is computed to be 3.0 in., the time required for the structure to settle 1.5 in. could be determined from Eq. (2.17) by substituting a value of T_v of 0.196 (along with applicable values of c_v and H). The value of 0.196 is obtained from Figure 2.3 for a

value of U of 50% because the particular settlement being considered (1.5 in.) is 50% of total settlement (3.0 in.).

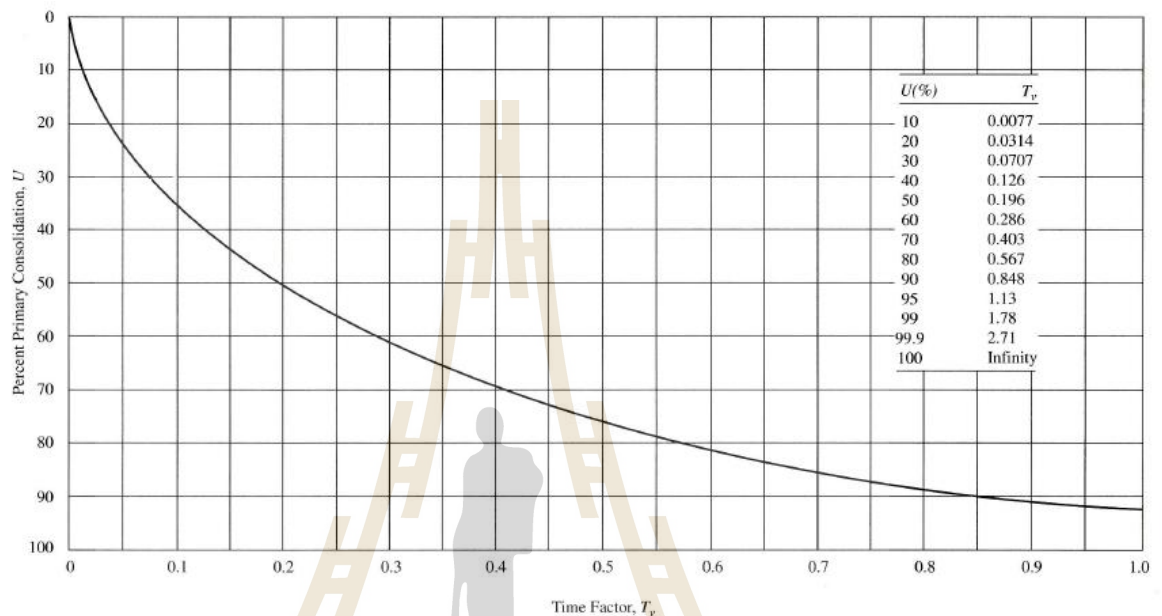


Figure 2.3 Time factor as a function of percentage of consolidation (Teng, 1962)

2.2.4 Settlement of loads on clay due to secondary consolidation

After primary consolidation has ended (i.e., all water has been extruded from the voids in a fine-grained soil) and all primary consolidation settlement has occurred soil compression (and additional associated settlement) continues very slowly at a decreasing rate. This phenomenon is known as secondary compression and perhaps results from plastic readjustment of soil grains due to new stresses in the soil and progressive breaking of clayey particles and their interparticle bonds.

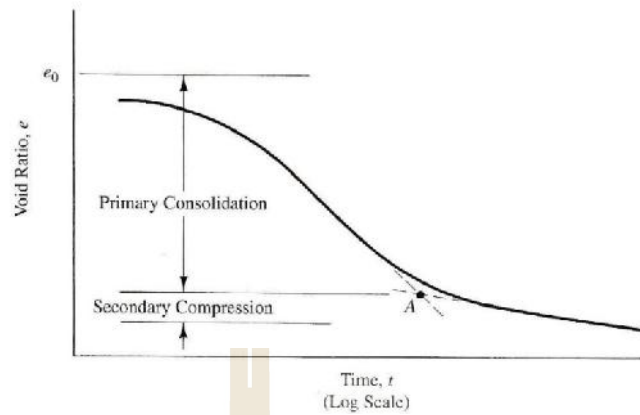


Figure 2.4 Sketch showing primary consolidation and secondary compression.

Figure 2.4 gives a plot of void ratio as a function of the logarithm of time. Clearly, as the void ratio decreases, settlement increases, Secondary compression begins immediately after primary consolidation ends; it appears in Figure 2.4 as a straight line with a relatively flat slope. The void ratio corresponding to the end of primary consolidation (or the beginning of secondary compression) can be determined graphically as the point of intersection of the secondary compression line extended backward and a line tangent to the primary consolidation curve (i.e., point A in Figure 2.4)

Secondary compression settlement can be computed from the following equation (U.S. Department of the Navy, 1971):

$$S_s = C H \log \frac{t_s}{t_p} \quad (2.22)$$

Where S_s = secondary compression settlement

C = coefficient of secondary compression

- H = (initial) thickness of the clay layer
 t_s = life of the structure (or time for which settlement is required)
 t_p = time to completion of primary consolidation

The coefficient of secondary compression (C_c) varies with the clay layer's natural water content and can be determined from Figure 2.5. The amount of secondary compression settlement may be quite significant for highly compressible clays, highly micaceous soils, and organic materials. On the other hand, it is largely insignificant for inorganic clay with moderate compressibility.

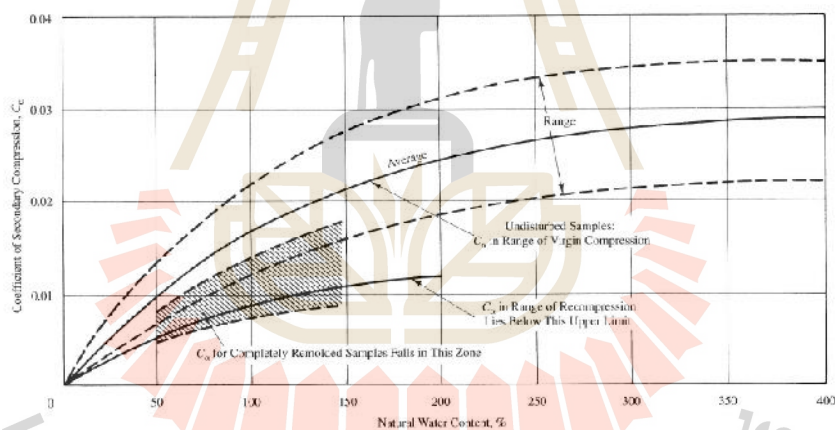


Figure 2.5 Coefficient of secondary compression; C_c = ratio of decrease in sample height to initial sample height for one cycle of time on a logarithmic scale following completion consolidation

2.3 Consolidation

2.3.1 Terzaghi theory of one-dimensional consolidation (Figure 2.6)

The process of consolidation comprises the gradual reduction of the volume of a fully saturated soil with time as water is squeezed out of the pore spaces under an induced or excess pore water pressure. This is coupled with the gradual increase with time of the effective stress within the soil skeleton.

The theory considers the rate at which water is squeezed out of an element of soil and can be used to determine the rates of :

1. volume change of the soil with time
2. settlements at the surface of the soil with time
3. pore pressure dissipation with time

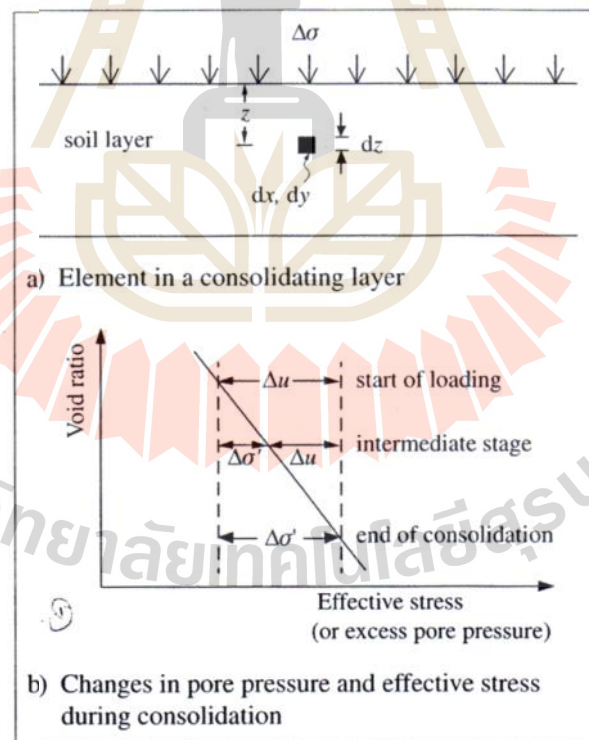


Figure 2.6 One-dimensional consolidation

Several assumptions are made such as the soil is homogeneous and fully saturated and the solid particles and the pore water are incompressible. The tenuous assumptions are that:

1. Compression and flow are one-dimensional. i.e. they are vertical only, whereas significant horizontal flow can occur in layered deposits.
2. Darcy's law is valid at all hydraulic gradients but deviation may occur at low hydraulic gradients.
3. k and m_v remain constant. However, they both usually decrease during consolidation.
4. No secondary compression or creep occurs. If this occurs the void ratio-effective stress relationship is not solely dependent on the consolidation process
5. The load is applied instantaneously and over the whole of the soil layer. However, loads are applied over a construction period and usually do not extend over a wide area in relation to the thickness of the consolidating deposit.

Consider an element of soil in a consolidating layer (Figure 2.6a). The hydraulic gradient across the element is:

$$-\frac{h}{z} = -\frac{1}{w} \frac{u_e}{z} \quad (2.23)$$

where u_e is the excess pore water pressure induced by the applied total stresses. The average velocity of water passing through the element, from Darcy's law:

$$v = -\frac{k}{w} \frac{u_e}{z} \quad (2.24)$$

The velocity gradient across the element:

$$\frac{v}{z} = -\frac{k}{w} \frac{2u_e}{z^2} \quad (2.25)$$

From the equation of continuity

$$\frac{v_x}{x} + \frac{v_z}{z} = 0 \quad (2.26)$$

If volume changes in the soil element are occurring the volume change per unit time can be expressed as:

$$\frac{dv}{dt} = \frac{v}{z} dx dy dz \quad (2.27)$$

$$\frac{dv}{dt} = \frac{k}{w} \frac{2u_e}{z^2} dx dy dz \quad (2.28)$$

This can now be equate to the volume change of the void space in the element. The total volume of the element = $dx dy dz$ so the proportion of voids in the element is:

$$\frac{e}{1+e_0} dx dy dz \quad (2.29)$$

The rate of change of void space with respect to time is then:

$$\frac{1}{1+e_0} \frac{e}{t} dx dy dz \quad (2.30)$$

$$\frac{1}{1+e_0} \left(\frac{e}{t} \right)' dx dy dz \quad (2.31)$$

$$-m_v \frac{u_e}{t} dx dy dz \quad (2.32)$$

Where

$$m_v = \frac{e}{1+e_0} \frac{1}{\gamma}$$

And

$$\left(\frac{e}{t} \right)' = \frac{u_e}{t}$$

which considers the rate of increase of effective stress being equal to the rate of dissipation of the excess pore pressure u_e , as illustrated on Figure 2.6b. Equating 2.28 and 2.32, and dividing by $dx dy dz$ gives:

$$\frac{u_e}{t} = \frac{k}{m_v w} \frac{u_e}{z^2} = c_v \frac{u_e}{z^2} \quad (2.33)$$

where:

c_v is the coefficient of consolidation

m_v is the coefficient of compressibility

k is the coefficient of permeability

2.3.2 Solution of the consolidation equation (Figures 2.7 and 2.8)

The basic differential equation of consolidation gives the relationship between three values, the excess pore pressure u_e , the depth below the surface of the soil layer z and the time t that has elapsed since the instantaneous application of the load. This equation can be expressed in dimension-less terms as:

$$\frac{dU_v}{dT_v} = \frac{d^2U_v}{dz^2} \quad (2.34)$$

z is a dimensionless depth given by:

$$z = z/d \quad (2.35)$$

where z defines the depth below the layer surface of the soil element under consideration. d is the length of drainage path and represents the maximum distance a molecule of water would have to travel to escape from the soil layer and depends on the permeability at the boundaries. This is illustrated in Figure 2.7 where for a half-closed layer d is the full thickness of the soil but for an open layer d is half of the layer thickness.

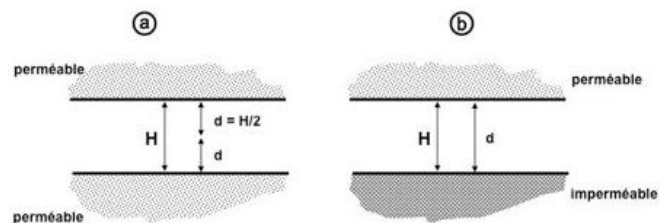


Figure 2.7 Drainage path length, d

T_v is dimensionless time factor given by:

$$T_v = \frac{c_v t}{d^2} \quad (2.36)$$

where c_v is the coefficient of consolidation, given by equation 2.33, t is time elapsed after instantaneous loading and d is the drainage path length.

U_v is the degree of consolidation and represents the proportion of the consolidation process that has taken place at a particular time at a particular location within the layer. It can be defined in three ways. One is the amount of void ratio change that has occurred at the time t compared to the final void ratio change.

$$U_v = \frac{e_0 - e_t}{e_0 - e_f} \quad (2.37)$$

Where:

e_0 = initial void ratio before the instantaneous loading increment was applied

e_t = void ratio at time t from the point of instantaneous loading

e_f = final void ratio at equilibrium under the applied load increment.

It can also be defined as the amount of the excess pore water pressure that has dissipated at the time t compared to the initial excess pore pressure:

$$U_v = \frac{u_i - u_t}{u_i} \quad (2.38)$$

Where:

u_i = initial excess pore pressure

u_t = excess pore pressure at time t

And as the effective stress increase at the time t compared to the final increase in effective stress:

$$U_v = \frac{u_t}{u_i} \quad (2.39)$$

Where:

u_t = increase in effective stress at time t

u_i = final increase in effective stress.

The solution to the dimensionless one-dimensional consolidation equation is given as:

$$U_v = \sum_{m=0}^{\infty} \frac{2}{M} \sin(MZ) e^{-M^2 T_v} \quad (2.40)$$

Where $M = \frac{(2m+1)\pi}{2}$

Although it appears a daunting expression it merely relates the three parameters U_v , Z and T_v and these are conveniently represented as a graph of U_v versus Z for different T_v values, Figure 2.8. The curved lines refer to constant values of time (or T_v) and are called isochrones.

From $Z = 0$ to 2 the diagram represents the state or degree of consolidation at any point in an open soil layer whereas half of the diagram from $Z = 0$ to $Z = 1$ would represent a half-closed layer with an impermeable lower boundary and from $Z = 1$ to $Z = 2$ would represent a half-closed layer with an impermeable upper boundary. The diagram also applies to a uniform distribution of initial excess pore pressure u set up throughout the soil (Case A in Figure 2.9). For triangular distributions (Case B and C) the isochrones would not be symmetrical.

The line $T_v = 0$ in Figure 2.8 represents the instantaneous loading condition (time $t = 0$, see equation 2.14) where $U_v = 0$ since consolidation has not yet commenced. Very soon after commencement of the consolidation process, say $T_v = 0.05$, an element of soil adjacent to the permeable boundaries will have been able to fully consolidate (where $U_v = 1.0$) but for a soil element at the middle of the soil layer consolidation will hardly have started.

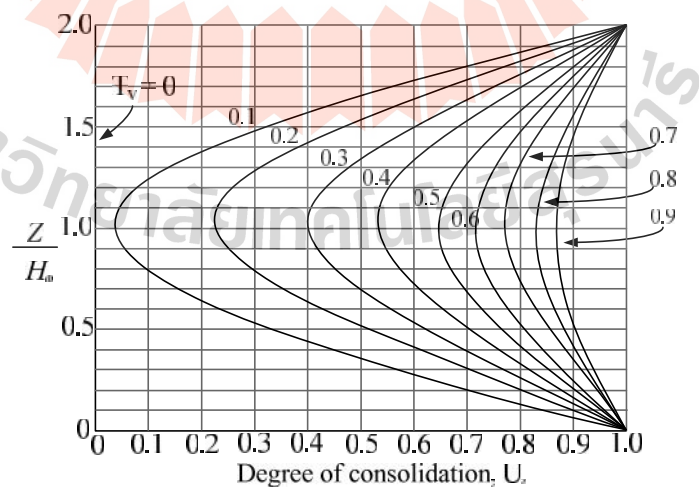


Figure 2.8 One-dimensional consolidation – Isochrones

2.3.3 Average degree of consolidation (Figure 2.9)

When dealing with settlements of loaded areas placed on the surface of a soil layer the average degree of consolidation at a particular time is required, independent of depth z . This is obtained by integrating equation 2.39 with respect to z for a particular T_v value and give:

$$\bar{U}_v = 1 - \sum_{m=0}^{\infty} \frac{2}{M^2} e^{-M^2 T_v} \quad (2.41)$$

Which is an expression relating the average degree of consolidation \bar{U}_v to T_v . The average degree of consolidation defined in terms of settlement is:

$$\bar{U}_v = \frac{s_t}{s_c} \quad (2.42)$$

Where :

s_t = settlement at time t

s_c = final consolidation settlement

There are three relationships between \bar{U}_v and T_v (Curves 1, 2 and 3 in Figure 2.9) depending on the variation of initial excess pore water pressure set up within the soil layer and the permeability of the soil boundaries. The three cases could be produced by:

- Case A – a wide or extensive applied pressure compared to the thickness of the soil layer, such as an embankment, or general lowering of the water table to give a uniform pressure distribution throughout the soil layer.

- Case B – an applied pressure over a small area on the surface of the layer such as a foundation.
- Case C – this could be due to the self-weight of the soil forming an embankment or a hydraulic fill deposit.

Values of \bar{U}_v and T_v are given in Table 2.4 for the three curves and good approximations for the most commonly adopted cases (Curve 1) are:

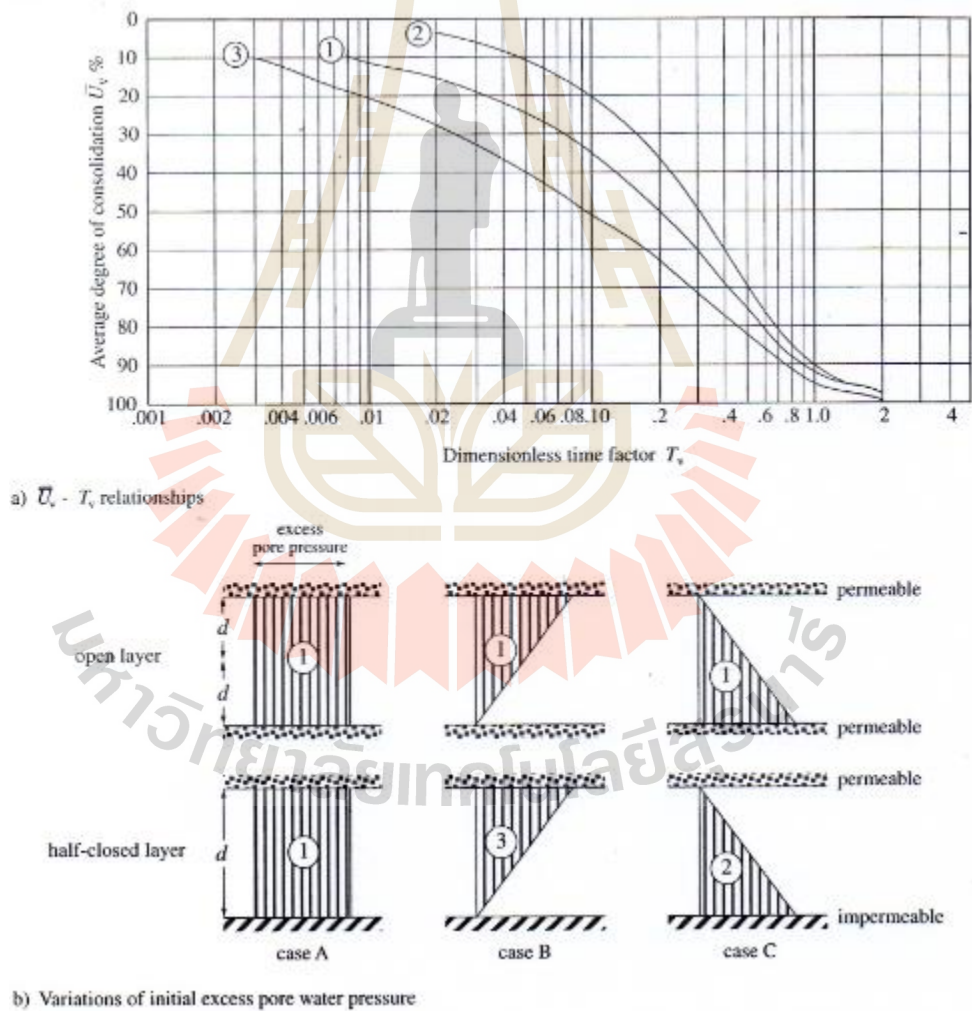


Figure 2.9 Average degree of consolidation \bar{U}_v versus T_v

$$T_v = \frac{1}{4} \left\{ \frac{\bar{U}_v \%}{100} \right\}^2 \quad (2.43)$$

For $\bar{U}_v < 60\%$ And

$$T_v = 1.781 - 0.9331 \log_{10} \{100 - \bar{U}_v \%\} \quad (2.44)$$

For $\bar{U}_v \geq 60\%$

2.3.4 Oedometer test (Figure 2.10)

The recommended test procedure is described in BS 1377:1990 and a cross-section through the apparatus is shown in Figure 2.10. The test was designed to reproduce one-dimensional consolidation by providing:

1. A rigid confining ring to prevent lateral strains and produce K_0 conditions and to prevent lateral drainage thus ensuring one-dimensional drainage conditions. The inner surface must be smooth and coated with low friction as the specimen reduces in thickness.

2. Porous disc top and bottom to act as permeable boundaries.

Coupled with are latively thin specimen this will provide an open Layer (Figure 2.7) and hence the smallest drainage path length. This should enable consolidation under each increment of applied stress to be completed in a manageable time of about 24 hours. A typical specimen height is 19 or 20 mm with diameters of 75 or 100 mm. With thicker specimens the confining ring surface could produce excessive friction during loading and excessive

disturbance during specimen preparation and the time required for consolidation would be increased. On the other hand, the specimen should be at least five times thicker than the largest particle diameter to avoid interference effects.

3. A rigid loading platen to provide equal settlement.
4. A water container to immerse the specimen and porous stones to ensure full saturation. All of the metallic components must therefore be non-corrodible. The water is added after installation of the specimen and assembling the load frame since some soils may have a tendency to swell in the presence of water and others may settle rapidly due to structural collapse on wetting. This behavior should be investigated separately.

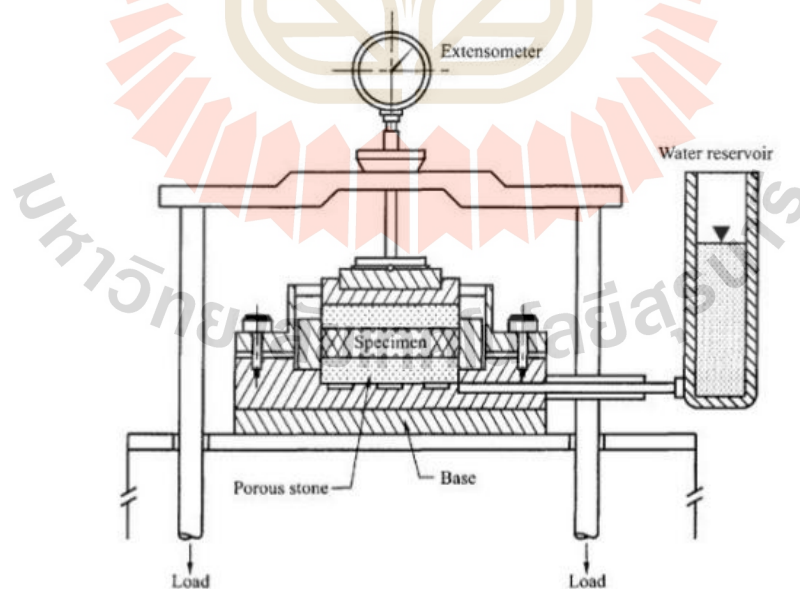


Figure 2.10 Oedometer test apparatus

Loading is applied through a loading yoke or load hanger and a counter-balanced lever system with a load ratio of around 10:1 so that a relatively small mass on the hanger can produce the large stresses required on the specimen.

An initial pressure is applied to return the specimen to near its in situ effective stress p'_0 to act as a starting point for reloading or swelling. This stress will depend on the stress history the soil has been subjected to.

Each pressure increment above p'_0 requires about 24 hours of application so to make the test manageable and economical 4 to 6 increments of loading and 1 or 2 larger unloading increments are normally chosen using the following suggested sequence: 6 , 12 , 25 , 50 , 100, 200 , 400 , 800 , 1600 , 3200 kN/m²

Smaller increments may be adopted for samples taken from shallow depths and for small applied stresses from the structure. If the soil is overconsolidated loading should continue into the normal compression region so that a measure of the preconsolidation pressure can be obtained.

The change in thickness of the specimen (either compression or swelling) is measured by a dial gauge or a displacement transducer impinging on the loading yoke. Readings must be taken at frequent intervals initially when the specimen is rapidly changing in thickness followed by less frequent intervals. This should give sufficient data when plotting thickness against square root or log time.

Nowadays, it is much more convenient to use displacement transducers attached to an automatic recording device so that continual reading are obtained irrespective of the working hours of the laboratory. If the test is only required to measure primary consolidation then the reading can be plotted to assess whether this process has been completed when it will be permissible to apply the next increment of pressure. This may occur within the same day for some soils.

From the oedometer test results a number of soil properties can be determined:

1. The initial and final moisture contents, bulk density, dry density and degree of saturation.
2. Void ratio at the end of each pressure increment.
3. Compression index, c_s for normally consolidated soil
4. Swelling index, c_s for overconsolidated soil
5. Coefficient of volume compressibility, m_v , for each loading increment (not unloading) above p_0' .
6. Coefficient of consolidation, c_v , for each loading increment above p_0' .

The initial moisture content $w_0\%$ can be obtained from the trimmings around the specimen and the final moisture content $w_f\%$ can be obtained from the specimen itself at the end of the test.

The initial bulk density is given by:

$$= \frac{m_0 \times 10000}{AH_0} \quad (2.45)$$

Where :

m_0 = initial wet mass of specimen (g)

A = area of specimen (mm^2)

H_0 = initial height of specimen (mm) The initial dry density is obtained from:

The initial dry density is obtained from:

$$d = \frac{\times 100}{100 + w_0(\%)} \quad (2.46)$$

The initial void ratio is given by:

$$e_0 = \frac{s}{d} - 1 \quad (2.47)$$

Where :

s = particle density (Mg/m^3)

The initial degree of saturation is obtained from:

$$s_{r0} = \frac{w_0 s}{e_0} \quad (2.48)$$

The void ratio at the end of each load increment is determined from:

$$e_f = e_i - \frac{H}{H_i}(1+e_i) \quad (2.49)$$

Where, for each pressure increment:

e_i = initial void ratio

e_f = equilibrium void ratio at the end of consolidation

H_i = initial thickness for the pressure increment (mm)

H = change in thickness over the pressure increment (mm)

The coefficient of volume compressibility m_v , with units of m^2/kN , is obtained for each pressure increment from:

$$m_v = \frac{e_i - e_f}{1 + e_i} \frac{1}{H} = \frac{e - 1}{1 + e_i} \frac{1}{H} \quad (2.50)$$

Or

$$m_v = \frac{H}{\sigma} \frac{1}{H} \quad (2.51)$$

Where σ is the pressure increment (kN/m^2).

The compression index c_c is given by:

$$c_c = (e_1 - e_2) \log_{10} \frac{\sigma_1}{\sigma_2} \quad (2.52)$$

The swelling index c_s is given by:

$$c_s = (e_1 - e_2) \log_{10} \frac{\sigma_1}{\sigma_2} \quad (2.53)$$

Where e_1 is the void ratio at the effective stress σ_1 and e_2 is the void ratio at σ_2 .

c_c represents the gradient of the void ratio-effective stress plot for the normally consolidated line only and c_s represents the gradient of the overconsolidated portion of the reloading line. c_s is referred to as the swelling index because it is used to determine drained heave movements when stresses are removed from a soil. It is not necessary to determine values for each pressure increment, it is preferable to plot void ratio versus effective stress and obtain c_c and c_s from the gradient of each line. Typically, the ratio of the two values is approximately

$$c_c = 0.1 \text{ to } 0.2 c_s \quad (2.54)$$

2.3.5 Two-and three-dimensional consolidation

One-dimensional consolidation will occur beneath a wide load or where the soil layer thickness is small compared to the width of a load such as beneath a large fill area or when the water table is lowered generally. Two-dimensional consolidation will occur beneath a circle, square or rectangle.

One-dimensional consolidation means no horizontal drainage or horizontal strains in any direction (i.e. vertical only) and the one-dimensional consolidation theory described above can be used to obtain the settlement-time relationship. With two-

dimensional consolidation vertical drainage and strains will be accompanied by horizontal drainage and strains in one direction only. Three-dimensional consolidation results in horizontal drainage and strains in all directions so it can be seen that the geometrical shape and size of the load will have a major influence on the rate of settlement.

Conventionally rates of settlement are determined from the one-dimensional theory but Davis and Poulos (1972) have shown that the practical effect of two and three-dimensional conditions are that the time required for consolidation decreases:

1. as the footing area decreases
2. as the soil layer thickness decreases
3. more for square of circular loaded area (three-dimensional) than for strip loading (two-dimensional).
4. as the horizontal permeability increases ($C_H > C_V$)
5. if the underside of the foundation can be considered permeable, e.g. a thin sand layer exists beneath.

2.3.6 Radial consolidation for vertical drains (Figure 2.11)

The time for one-dimensional to take place is inversely proportional consolidation to d^2 , therefore for thick layers of clay settlements of earth structures placed above this type of consolidation take a long time to be completed. By inserting vertical drains at fairly close spacing must shorter horizontal drainage paths are created allowing faster dissipation of pore pressures, removal of pore water and accelerated consolidation settlements.

The original 'sand drains' were formed by sinking boreholes 200-400 mm diameter using cable percussion or flight auger methods through the soil and backfilling with a suitable filter sand. However these could be slow to construct, produce large amounts of spoil and surface damage and be prone to 'waisting'. This is caused by soft clays squeezing into the borehole on removal of the casing leaving a reduced diameter which could prevent adequate drainage. Other techniques include a closed end steel pipe to form a hole although this is prone to producing a disturbed or smear zone around the hole which can reduce the permeability of the soil around the drain.

Prefabricated drains comprising a continuous filter stocking filled pneumatically with sand called sandwicks and installed in a pre-drilled hole can provide a more reliable and cost-effective solution. Since the drain diameter is not a particularly important design parameter, smaller diameters of about 79 mm could be used.

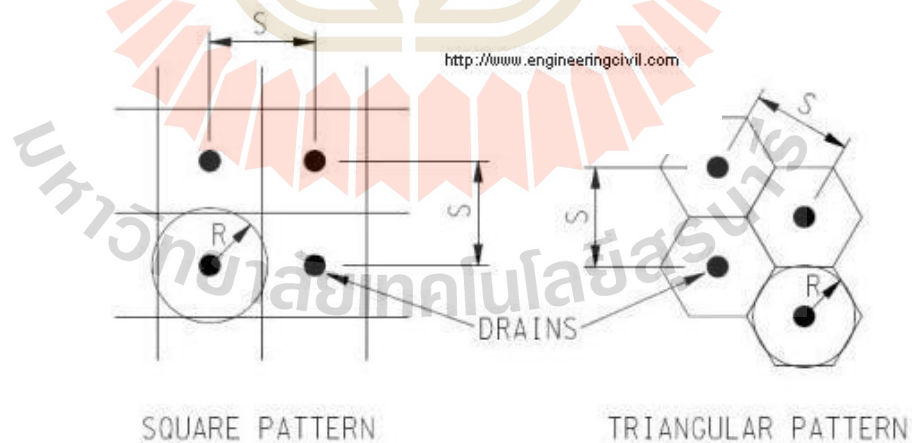


Figure 2.11 Radius of influence of drains

Nowadays, the plastic 'band' drain is commonly used. This consists of a continuous flat plastic core about 60-100 mm wide and 2-5 mm thick which is corrugated to provide vertical drainage channels and wrapped around by a geotextile fabric to act as a filter. The band drain is installed by attaching one end of the band at the bottom of a rectangular steel mandrel with a clip and driving or pushing the mandrel vertically into the soil to the depth required. As the mandrel is withdrawn the clip retains the band drain in the soil which will then squeeze around the drain holding it in place. It is essential that the band drain are maintained vertical within the drainage blanket and not pushed over or constricted otherwise drainage would be impaired. These drains are cheaper, lighter, more robust and quicker to install.

A solution for radial consolidation has been obtained (Barron,1948) by considering Terzaghi's equations for three-dimensional consolidation in polar coordinates as:

$$\frac{u}{t} = c_v \frac{\partial^2 u}{\partial z^2} + \left[c_H \frac{\partial^2 u}{\partial r^2} + \frac{1}{r} \frac{\partial u}{\partial r} \right] \quad (2.55)$$

Overall drainage = vertical drainage + radial drainage

Where:

$$c_v = \frac{k_v}{m_v \gamma_w} \quad \text{and} \quad c_H = \frac{k_H}{m_v \gamma_w} \quad (2.56)$$

The circular drains of radius r_d will have a circular area of influence of radius R

(Figure 2.11) with water moving horizontally towards each drain. In practice, drains

placed in a square grid pattern will have a square area of influence of size s^2 for spacing s . This is equated to a circular area of influence such that $s^2 = R^2$ and:

$$R = 0.564s \quad (2.57)$$

For a triangular pattern:

$$R = 0.525s \quad (2.58)$$

The overall degree of consolidation can be obtained from combination of vertical and radial drainage as:

$$1 - U_c = (1 - U_v)(1 - U_R) \quad (2.59)$$

Where :

U_c = overall or combined degree of consolidation

U_v = average U_v for one-dimensional vertical flow only

U_R = average U_R for radial flow only

Settlements are now related to the overall degree of consolidation as:

$$U_c = \frac{s}{c} \quad (2.60)$$

Values of U_v are obtained from Curve I in Figure 2.8, related to the vertical time factor T_v . Values of U_R are related to a (radial) time factor T_R :

$$T_R = \frac{C_H t}{4R^2} \quad (2.61)$$

But also to the ratio :

$$n = \frac{R}{r_d} \quad (2.62)$$

For design the size or radius of the drain cannot be varied much but this does not matter as it is not as critical as the spacing between the drains. The equivalent diameter of a band drain is determined assuming that it has the same perimeter as a circle.

It has been found that the time t for consolidation varies approximately as:

$$t \propto s^{2.5} \quad (2.63)$$

So the spacing is critical.

Smearing of the soil during installation will affect the horizontal permeability and hence c_H . To allow for this a reduced value, as low as $c_H = c_v$ could be used or smaller drain radius of $r_d/2$ could be used. It has been found that the cost of a drain

installation is inversely proportional to the value of c_v or c_H so care during the site investigation in obtaining a representative value is essential.

Vertical drains can be ineffective:

1. With thin soil layers where sufficient consolidation may be achieved in one dimension (vertical) alone.
2. If c_H is much larger than c_v . Where macro-fabric will permit sufficient drainage horizontally, vertical drains may not be required.
3. If large secondary compressions are likely. Drains only accelerate pore pressure dissipation or primary consolidation so if:

$$\frac{c}{\text{total}} = \frac{\text{consolidation settlement}}{\text{total settlement}} < 0.25 \quad (2.64)$$

then drains may not be viable.

4. Where they are severed due to large horizontal shear deformations around an incipient slip surface.

2.4 Prefabricated vertical drains (PVD)

The Consolidation settlement of soft clay subsoil creates a lot of problem in foundation and infrastructure engineering. Because of the very low clay permeability, the primary consolidation takes a long time to complete. To shorten this consolidation

time, vertical drains are installed together with preloading by surcharge embankment or vacuum pressure. Vertical drains are artificially-created drainage paths which can be installed by one of several methods and which can have a variety of physical characteristics. Figure 2.12 illustrates a typical vertical drain installation for highway embankments. In this method, pore water squeezed out during the consolidation of the clay due to the hydraulic gradient created by the preloading, can flow a lot faster in the horizontal direction toward the drain and then flow freely along the drain vertically towards the permeable drainage layers. Thus, the installation of the vertical drains in the clay reduces the length of the drainage paths and, thereby, reducing the time to complete the consolidation process. Consequently, the higher horizontal permeability of the clay is also taken advantage. Therefore, the purpose of vertical drain installation is twofold. Firstly, to accelerate the consolidation process of the clay subsoil, and secondly to gain rapid strength increase to improve the stability of structures on weak clay foundation.

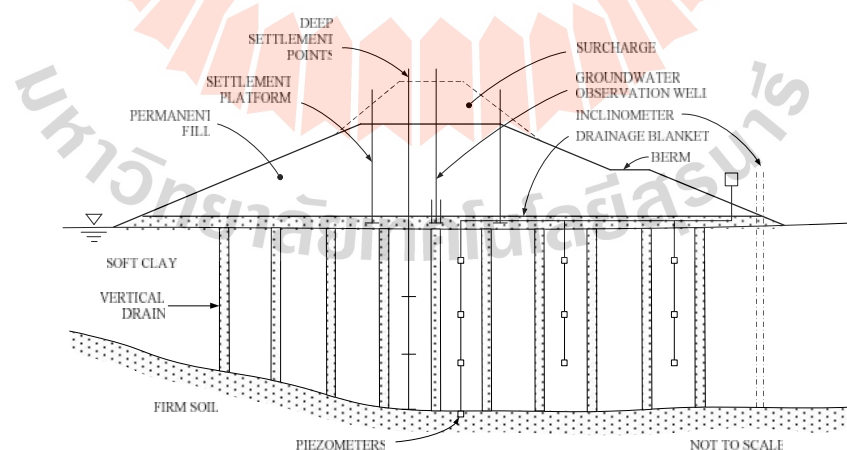


Figure 2.12 Typical vertical drain installation for a highway embankment

(Rixner et al., 1986)

2.4.1 Characteristics of prefabricated drains

A prefabricated vertical drain can be defined as any prefabricated material or

product consisting of synthetic filter jacket surrounding a plastic core having the following characteristics : a) ability to permit porewater in the soil to seep into the drain; b) a means by which the collected porewater can be transmitted along the length of the drain.

The jacket material consists of non-woven polyester or polypropylene geotextile or synthetic paper that function as physical barrier separating the flow channel from the surrounding soft clay soils and a filter to limit the passage of fine particles into the core to prevent clogging. The plastic core serves two vital functions, namely : to support the filter jacket and to provide longitudinal flow paths along the drain even at large lateral pressures.

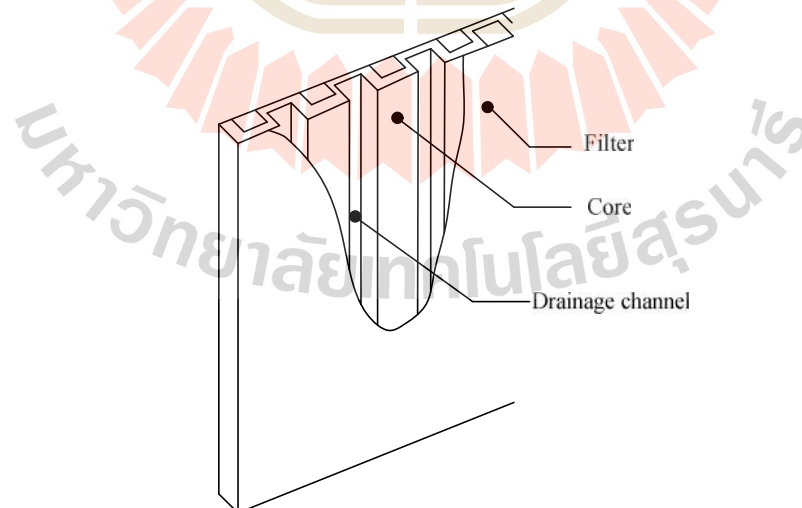


Figure 2.13 Characteristics of prefabricated drains

2.4.2 Consolidation with vertical drain

Barron (1948) presented the first exhaustive solution to the problem of consolidation of a soil cylinder containing a central sand drain. His theory was based on the simplifying assumptions of one-dimensional consolidation theory (Terzaghi, 1943). Barron's theory enable one to solve the problem of consolidation under two condition , namely: (i) free vertical strain assuming that the vertical surface stress remains constant and the surface displacements are non-uniform during the consolidation process; (ii) equal vertical strain assuming that the vertical surface stress is non-uniform.

In the case of equal strain, the differential equation governing the consolidation process is given as:

$$\frac{U}{t} = c_h \left[\left(\frac{\partial^2 u}{\partial r^2} \right) + \frac{1}{r} \left(\frac{\partial u}{\partial r} \right) \right] \quad (2.65)$$

Where u is the average excess pore pressure at any point and at any given time; r is the radial distance of the considered point from the center of the drained soil cylinder; t is the time after an instantaneous increase of the total vertical stress, and c_h is the horizontal coefficient of consolidation. For the case of radial drainage only, the solution of Barron (1948) under ideal conditions (no smear and no well resistance) is as follows:

$$U_h = 1 - \exp \left[\frac{8T_h}{F(n)} \right] \quad (2.66)$$

Where:

$$T_h = \frac{C_h}{D_e} \quad (2.67)$$

$$F(n) = \left[\frac{n^2}{(1-n)} \right] \left[n(n) - \frac{3}{4} + \frac{1}{n^2} \right] \quad (2.68)$$

And D_e is the diameter of the equivalent soil cylinder, d_w is the equivalent diameter of the drain, and n ($n = \frac{D_e}{d_w}$) is the spacing ratio.

Hansbo (1979) modified the equations developed by Barron (1948) for prefabricated drain applications. The modifications dealt mainly with simplifying assumption due to the physical dimensions, characteristics of the prefabricated drains, and effect of PVD installation. The modified general expression for average degree of consolidation is given as:

$$U_h = 1 - \exp \left[\frac{8T_h}{F} \right] \quad (2.69)$$

and

$$F = F(n) + F_s + F_r \quad (2.70)$$

where F is the factor which expresses the additive effect due to the spacing of the drains, $F(n)$; smear effect, F_s ; and well-resistance, F_r . For typical values of the spacing ratio, n , of 20 or more, the spacing factor simplifies to:

$$F(n) = \ln \left[\frac{D_c}{d_w} \right] - \frac{3}{4} \quad (2.71)$$

To account for the effect of soil disturbance during install, a zone of disturbance with a reduced permeability is assumed around the vicinity of the drain, as shown in Figure 2.14. The smear effect factor is given as:

$$F_s = \left[\left(\frac{k_h}{k_s} \right) - 1 \right] \ln \left(\frac{d_s}{d_w} \right) \quad (2.72)$$

Where d_s is the diameter of the disturbed zone around the drain; and k_s is the coefficient of permeability in the horizontal direction in the disturbed zone.

Since the prefabricated vertical drains have limited discharge capacities, Hansbo (1979) developed a drain resistance factor, F_r , assuming that Darcy's law can be applied for flow along the vertical axis of the drain. The well-resistance factor is given as:

$$F_r = z(L-z) \frac{k_h}{q_w} \quad (2.73)$$

Where z is the distance from the drainage end of the drain; L is twice the length of the drain when drainage occurs at one end only; L is equal to the length of the drain when drainage occurs at both ends; k_h is the coefficient of permeability in the horizontal direction in the undisturbed soil; and q_w is the discharge capacity of the drain at hydraulic gradient of 1.

The schematic diagram of PVD with drain resistance and soil disturbance is shown in Figure 2-14. Incorporating the effects of smear and well-resistance, the time, t , to obtain a given degree of consolidation at an assumed spacing of PVD, is given as follows:

$$t = \left(\frac{D_c^2}{8C_h} \right) (F(n) + F_s + F_r) \ln \left(\frac{1}{1-U_h} \right) \quad (2.74)$$

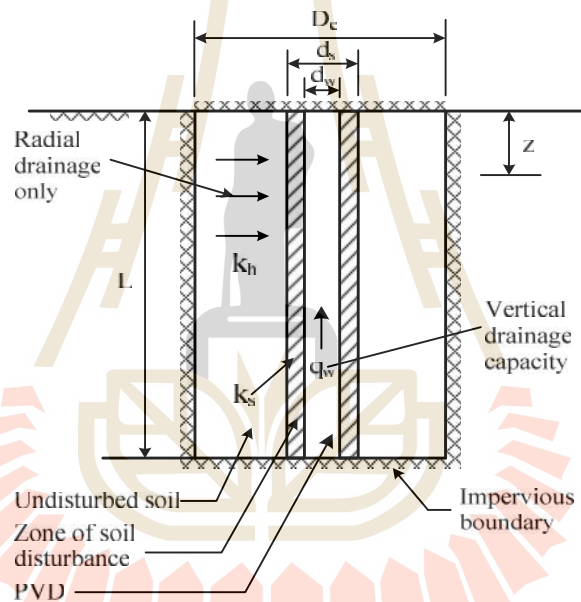


Figure 2.14 Schematic of PVD with drain resistances and soil disturbance
(Rixner et. Al, 1986)

2.4.3 Drain properties

The theory of consolidation with radial drainage assumes that the soil is drained by vertical drain with circular cross section. The equivalent diameter of band-shaped drain is defined as the diameter of circular drain which has the same

theoretical radial drainage performance as the band-shaped drain. Subsequent finite element studies performed by Rixner et al. (1986) and supported by Hansbo (1987) suggested that the equivalent diameter preferable for use in practice can be obtained as:

$$d_w = \frac{(a+b)}{2} \quad (2.75)$$

The relative sizes of these equivalent diameters are compared to the band shaped cross-section of the prefabricated drain by Rixner et al. (1986)

The discharge capacity of prefabricated drains is required to analyze the drain resistance factor and usually obtained from published results reported by manufacturers. Rixner et al. (1986) reported results of vertical discharge capacity tests and those obtained by others, as shown in Figure 2.15. The results demonstrate the major influence of confining pressure.

2.4.4 Drain influence zone

The time to achieve a given percent consolidation is a function of the square of the equivalent diameter of soil cylinder, D_e . This variable is controllable since it is a function of drain spacing and pattern. Vertical drain are usually installed in square or triangular patterns as shown in Figure 2.16. The spacing between drains establishes D_e through the following relationships:

$$D_e = 1.13S \quad (\text{square pattern})$$

$$D_e = 1.05S \quad (\text{triangular pattern})$$

The square pattern has the advantage for easier layout and control. A square pattern is usually preferred. However, the triangular pattern provides more uniform consolidation between drains.

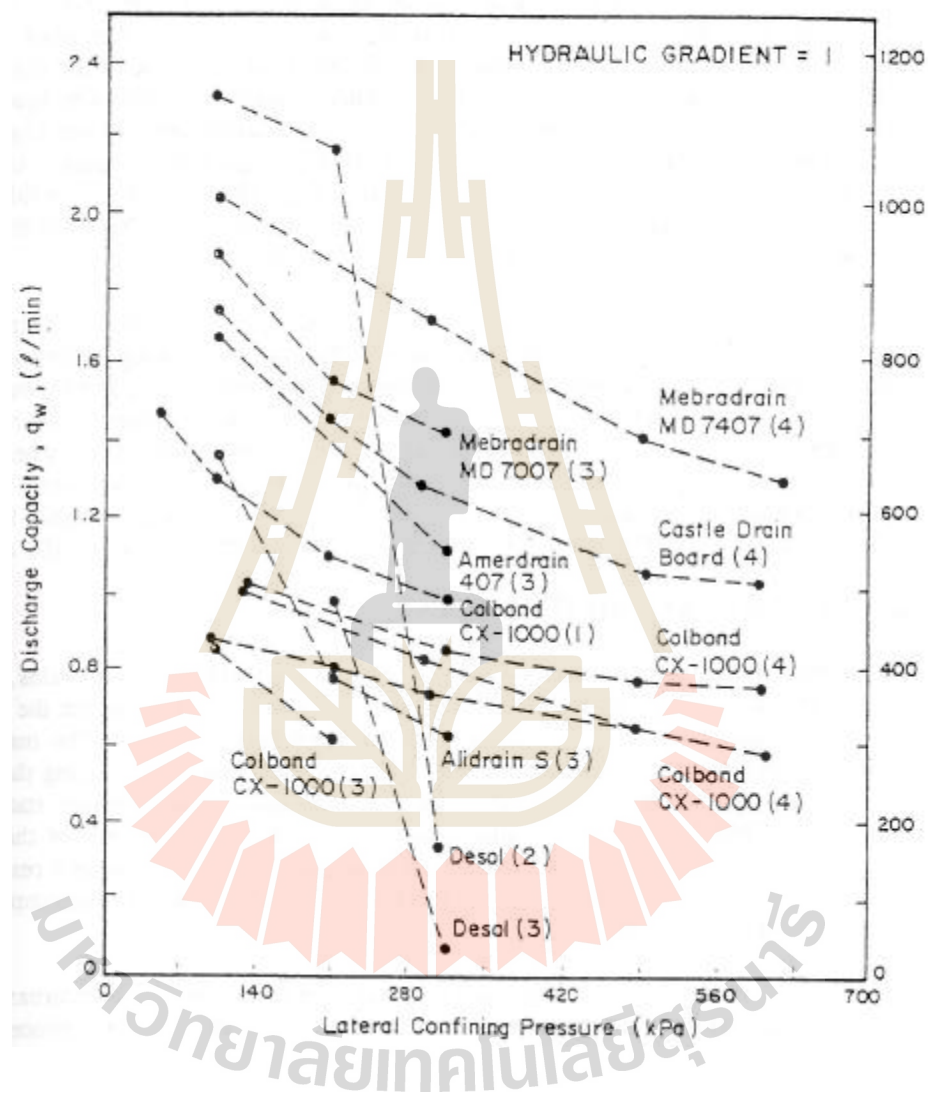


Figure 2.15 Typical values of vertical discharge capacity (Rixner et. Al 1986)

2.4.5 Well resistance

Hansbo (1979, 1981) presented, for equal-strain conditions, a closed-

form solution which allows for ready computation of the effects of well-resistance on drain performance. The finite drain permeability (well-resistance) was considered by imposing on the continuity equation of flow toward the drain. In this assumption, the flow rate in the considered section of the drain is equal to the maximum flow rate which can be discharged through the drain.

The discharge capacity of sand drains depends on the permeability of the sand. The sand used for the drains must be clean with good drainage and filtration characteristic. The discharge capacity of band drains varies considerably depending on the make of the drain and decreases with increasing lateral pressure (Figure 2.17). This is caused by either the squeezing in of the filter sleeve into the core channels reducing the cross-sectional area of the channels, or, for drains without a filter sleeve, the channels themselves are squeezed together. Another important factor is the folding of the drain when subjected to large vertical strains. In this case the channels of flow would be reduced, thus reducing the discharge capacity, the sedimentation of small particles in the flow channels may also decrease the discharge capacity.

The introduction of the well-resistance concept affects the value of the degree of consolidation, U_h , which is no longer constant with depth (Figure 2.17). Taking well-resistance into consideration, the rate of radial consolidation is controlled not only by C_h and D_e but also by the ratio $\frac{q_w}{k_h}$ (Figure 2.18). This factor may play a very important role when prefabricated band drains of great lengths are used with typical values of $\frac{q_w}{k_h}$ less than 500 m^2 where the time necessary to achieve a specific degree

of consolidation is increased (Jamiolkowski et al. 1983). The influence of well-resistance on the consolidation rate increase as the drain length increases. This is illustrated in Figure 2.19 for a typical band-shaped drain ($\frac{q_w}{k_h} = 400 \text{ m}^2$)

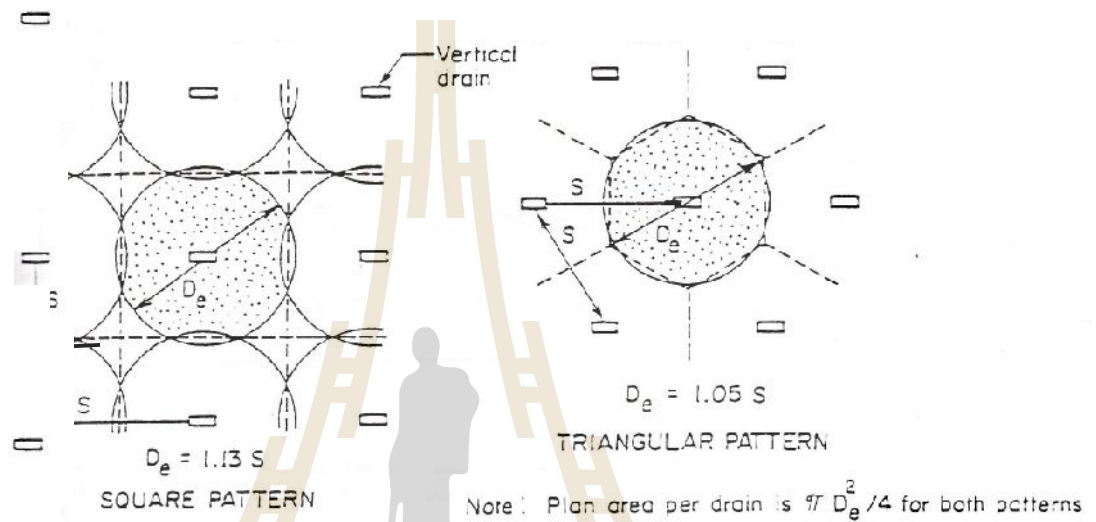


Figure 2.16 Relationship of drain spacing (S) to drain influence zone (D)

(Rixner et al, 1986)

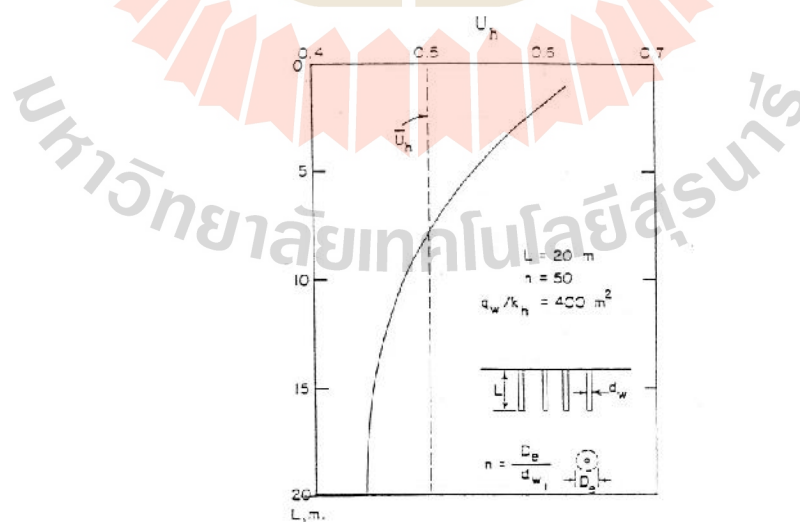


Figure 2.17 Example of variation of degree of consolidation with depth for drains with well resistance (Jamiolkowski et al. 1983)

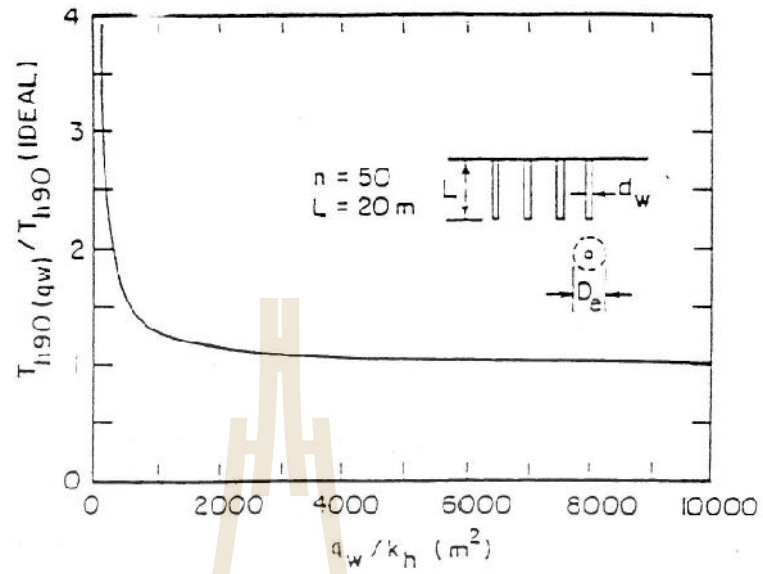


Figure 2.18 Influence of finite drain permeability on consolidation rate
(Jamiolkowski et al. 1983)

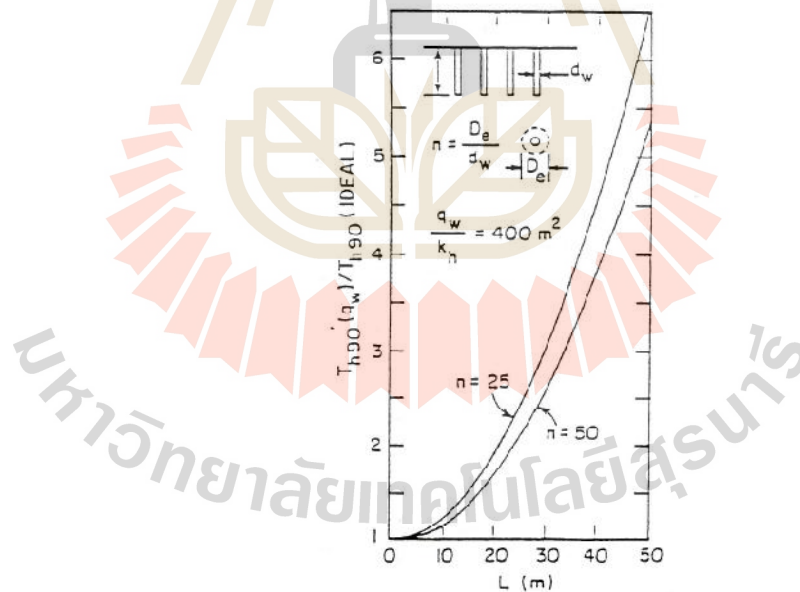


Figure 2.19 Influence of smear on consolidation rate (Jamiolkowski et al.
1983)

2.4.6 Smear effects and Disturbances

Although there are numerous variations in installation equipment for vertical drains, most of the equipment has fairly common features, some of which can directly influence the drain performance. The installation rigs are usually track-mounted boom cranes, the mandrel protects the drain during installation and creates the space for the drain by displacing the soil during the penetration. The mandrel is penetrated into the subsoil using either static or vibratory force. The drain installation results in shear strains and displacement of the soil surrounding the drain.

The installation results in disturbance to the soil around the drain. The disturbance is most dependent on the mandrel size and shape, soil macrofabric, and installation procedure. The mandrel cross-section should be minimized, while at the same time, adequate stiffness of the mandrel is required. Bergado et al. (1991), from a full scale test embankment performance, obtained faster settlement rate in the small mandrel area than in the large mandrel area indicating lesser smeared zone in the former than the latter. For design purposes, it has been evaluated by Jamiolkowski et al. (1981) that the diameter of disturbed zone, d_s , can be related to the cross-sectional dimension of the mandrel as follows:

$$d_s = \frac{(5-6)d_m}{2} \quad (2.76)$$

where d_s is the diameter of a circle with an area equal to the cross-sectional area of the mandrel. Hansbo (1987) recommended the following expression based on the results of Holtz and Holms (1973) and Akagi (1979) :

$$d_s = 2d_m \quad (2.77)$$

This relationship has been verified in the reconstituted soft Bangkok clay by Berdado et al.(1991) using a specially designed laboratory drain testing apparatus. Thus, the influence of smear increases with increasing drain diameter for sand drain or mandrel diameter for prefabricated drains (Hansbo,1981). The performance of PVD is well predicted with smear effect taken into consideration using $k_h/k_y=10$ and $d_s=2d_m$ (Bergado et al. 1993b).

2.4.7 Ratio of horizontal to vertical permeability

For soils with pronounced macrofabric, the ratio of k_h/k_y can be very high, possibly up to 10. This beneficial effect of soil stratification (greater horizontal permeability) can be reduced or completely eliminated in the smeared zone. Thus, the permeability of this zone, k_s , can be put equal to k_v . Bergado et al. (1991) performed oedometer tests on samples taken shortly after drain installation on reconstituted soft Bangkok clay at different distances from the drain. The results closely agreed with the proposal of Hansbo (1987) wherein k_s is equal to k_y in the smeared zone.

2.4.8 Coefficient of horizontal consolidation

The coefficient of radial consolidation can be evaluated from C_v values by means of the approximate relationship:

$$C_h = \left[\frac{k_h}{k_v} \right] C_v \quad (2.78)$$

Table 2.3 Range of possible field values of the ratio k_h/k_y for soft clays (Rixner et al. 1986)

Nature of Clay	k_h/k_y
No or slightly developed macrofabric, essentially homogeneous deposits	1 to 1.5
From fairly well to well developed macrofabric, e.g. sedimentary clays with discontinuous lenses and layers of more permeable material	2 to 4
Varved clays and other deposits containing embedded and more or less continuous permeable layers	3 to 15

Where C_v is the coefficient of vertical consolidation. The ratio of k_h/k_y can be evaluated by back-analysis. Bergado et al. (1992) obtained $\frac{k_h}{k_y} = 4$ to 10 and $C_h(\text{field})/C_h(\text{lab}) = 4$ for the soft Bangkok clay. An average ratio of $C_v(\text{field})/C_v(\text{lab}) = 26$ was also found (Bergado et al. 1990a). A rough estimate of the in-situ anisotropy of the permeability of clays (k_h/k_y) can be made on the basis of the data given by Jamiolkowski et al. (1983), as tabulated in Table 2-4 In-situ piezometer probes and analysis of pore pressure dissipation curves can also be used to evaluate C_h and k_h (Jamiolkowski et al. 1985). In-situ determination of k_h by self-boring permeameters can also be used with laboratory m_v values to calculate C_h using the relationship (Jamiolkowski et al. 1983):

$$C_h = \frac{k_h}{(m_w Y_w)} \quad (2.79)$$

Where γ_w is the unit weight of water and m_v is the coefficient of volume change.

Albakri et al. (1990) obtained C_h values in the field by piezocone tests.

2.4.9 Parameter effects on consolidation time

Taking into consideration the smear effects, the time, t , corresponding to a given degree of consolidation is given as:

$$t = \frac{D_e}{8C_h} \left[\ln \left(\frac{D_e}{d_w} \right) - \frac{3}{4} \right] + \left(\frac{K_h}{K_s} - 1 \right) \ln \left(\frac{d_s}{d_w} \right) \ln \left(\frac{1}{1-U_h} \right) \quad (2.80)$$

2.4.10 Rate of consolidation

The principal objective of soil precompression with vertical drains is to achieve the desired degree of consolidation within a specified period of time. With vertical drains, the overall degree of consolidation, U , is the result of the combined effects of horizontal (radial) and vertical drainage. The combined effect is given by Carallo (1942) as:

$$U = 1 - (1 - U_h)(1 - U_v) \quad (2.81)$$

Where U_h is the average degree of consolidation due to horizontal drainage, and U_v is the corresponding values due to vertical drainage.

2.4.11 Selection of drain type

The primary concerns in the selection of the type of prefabricated drain for a particular project include: equivalent diameter; discharge capacity; filter jacket characteristics and permeability; and material strength, flexibility, and durability.

For common prefabricated drains, d_w ranges from 50 to 75 mm. It is generally inappropriate to use a drain with an equivalent diameter of less than 50 mm (Rixner et al. 1986). Typical values of discharge capacity, q_w are given in Figure 2.15 as a function of lateral confining pressures. Generally, the selected drain should have a vertical discharge capacity of at least $100 \text{ m}^3/\text{yr}$ measured under gradient of one while confined to maximum in-situ effective horizontal stress.

Large permeability of the filter is desired but at the same time small particles should be prevented to pass through the filter. The basic requirement of the permeability criteria is that the geotextile filter must be and must remain more permeable than the adjacent soil (Holtz, 1987). For critical applications and severe conditions:

$$k_{\text{geotextile}} \geq 10 k_{\text{soil}} \quad (2.82)$$

For less critical and less severe situations:

$$k_{\text{geotextile}} = k_{\text{soil}} \quad (2.83)$$

Almost all geotextile filters have sufficient permeability.

The retaining capacity and the resistance of a filter are mainly dependent on the particle size distribution of the soil and the pore pressure distribution of the filter. As illustrated in Figure 2.20, three principal filter mechanisms can be distinguished, namely: cake filtration; blocking filtration, and deep filtration (Vreken et al,1983). Cake filtration takes place if the particles are larger than the filter pores. Blocking filtration occurs if the particles have the same diameter as the filter pores. Deep filtration happens if the particles are smaller than the filter pores and the particles adhere on the filter. Figure 2.21 shows typical pressure development for the different filtration mechanism. The filter resistance is strongly influenced by small soil particles that may be concentrated in or against the filter by the porewater flow. Small particles should pass the filter freely. However, not too many particles should pass, because of risk of sedimentation and subsequent decrease of vertical discharge capacity.

Various laboratory test were performed to determine the PVD performance at a given condition. The comparison of the four types of drains at a given condition is illustrated in Table 2.5. The types of drains used in the tests are as follows

- 1) Drains with separate core and filter
 - Grooved core (A)
 - Studded core (B)
 - Filament core (C)

- 2) Drain with filter fixed to the core
 - Grooved core (D)

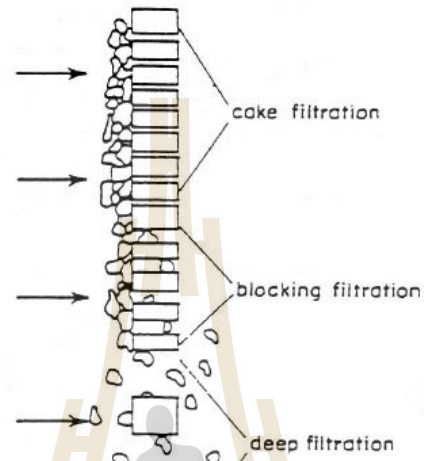


Figure 2.20 The filtration mechanism (Vreeken et al, 1983)

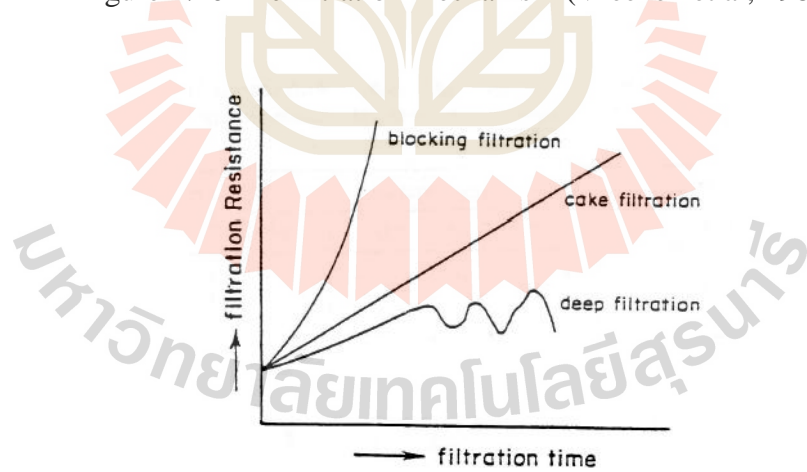


Figure 2.21 The filtration resistances during filtration (Vreeken et al, 1983)

2.4.12 Filter criteria

The first rational approach to deal with filter problems was the work of Terzaghi (1929). While there are slightly differences in opinion concerning quantitative criteria for satisfactory filters, the following rules are widely used:

1) D_{15} size of filter should be at least 5 time larger than the D_{15} of the soil being protected

Table 2.4 Summary of Laboratory Test on Prefabricated Vertical Drains

Type of Test	Comparison of Results
A. Discharge Capacity <ul style="list-style-type: none"> - Straight condition - 20% compression and free bending - 20% compression and one clamped - Twisted at 45° 	<ul style="list-style-type: none"> A > D > B and C A and D > B and C D > A > B and C D > A > B and C
B. Suitability for Safe Installation <ul style="list-style-type: none"> - Grab tensile strength - Trapezoidal tear strength - Puncture resistance - Burst strength 	<ul style="list-style-type: none"> D > A and C > B A and D > B and C D > A and C > B A, C and D > B

2) The D_{15} size of filter should not be larger than 5 time the D_{85} of the protected soil.

These rules are too conservative for clays which have inherent resistance to piping because of their cohesion. As suggested by Cedergreen (1972), the piping ratio (D_{15}/D_{85}) can reach as high as 10 or even higher. Recently, Sherard and Dunnigan (1989) suggested a limiting value of 9 for the piping ratio.

2.4.13 Geotextile filter criterion

The filtration criterion depends on the critical nature of the project and on the severity of hydraulic loading conditions. For less critical applications, the geotextile filter with the largest opening size based on soil retention criterion should be specified. To evaluate the retention ability of the drains accurately, several factors have to be considered such as: electrochemical forces of the geotextile, chemical properties of fibrous structure compound, and soil composition (Kellner et al. 1983). However, the retaining ability of the geotextile is too complicated to be determined. Hence, the rules of thumb are as follows:

$$O_{90} \text{ --- } < 1.7 \text{ to } 3 \quad (\text{Schober and Teindl, 1979}) \quad (2.84)$$

$$O_{50} \text{ --- } < 2 \text{ to } 3 \quad (\text{Carroll, 1983}) \quad (2.85)$$

$$D_{85}$$

$$O_{90}$$

$$--- < 1.3 \text{ to } 1.8 \text{ (Chen and Chen, 1986)} \quad (2.86)$$

 D_{85}
 O_{50}

$$-- < 10 \text{ to } 12 \text{ (Chen and Chen, 1986)} \quad (2.87)$$

 D_{50}

The ratio O_{50}/D_{50} ensures that seepage forces within the filter are reasonably small. The reason to choose the upper bound of O_{50}/D_{50} ratio to be 12 is to prevent fines to enter the core. O_{90} was chosen because it can be measured accurately by mercury intrusion method (Chen and Chen, 1986). Kamon (1983) recognized that clay particles are aggregated with average diameter of 50 to 60 microns (0.05 to 0.06 mm). If the average pore size of the filter is less than 50 microns, the clogging of the filter will not take place. Recently, Bergado (1992) conducted laboratory Experiments for prefabricated band drain. As preliminary guidelines for soft Bangkok clay, the following criteria are recommended:

 O_{90}

$$--- < 2 \text{ to } 3 \quad (2.88)$$

 D_{85}
 O_{50}

$$-- < 18 \text{ to } 24 \quad (2.89)$$

 D_{50}

2.5 Case Study

2.5.1 One dimensional compression of slurry with radial drainage

Bo et al., Arulrajah and Choa (1999) studied the deformation behavior of slurry-like soil due to additional load. The objective of this study is to improve the land in coastal areas and surrounding city areas which is the land on ultra-soft soil like waste ponds and mine tailing ponds. Materials in such waste ponds and mine tailing ponds are extremely soft, and high water content which usually above the liquid limit. A laboratory study with a large diameter consolidation cell (Figure 2.22) equipped with pore water pressure transducers was carried out to find out the deformation behavior of slurry-like soil under a one dimensional vertical load. The fine-grained soil was prepared to a water content of 132% with sea water. This slurry-like soil was placed in four layers and was thoroughly stirred for each layer so as to remove possible air trapped in the soil. The initial thickness of the sample was 750 mm and the diameter was 495 mm. The water content and bulk density of each layer was measured. The value obtain can be found in table 2.5.

Table 2.5 Water content and bulk density of each layer of slurry

Layer No.	Moisture content (%)	Bulk Density (kN/m ³)
1	129.6	13.59
2	133.9	13.60
3	132.7	13.61
4	132.1	13.57
Average	132.0	13.60

Sills (1995) was discovered that for fine grained, high moisture content slurry-like soil flocculated in the fluid, the slurry-like soil may not have a structure capable of taking the transfer of the load from the pore fluid. The soil particles may be bonded together loosely in flocs and aggregates with a very open structure due to electro-chemical interaction. This result in no pore water pressure dissipation and subsequently no effective stress gain will occur. In the mean time, water will only drain out from the flocculated structure through the radial drainage and volume change of the soil will occur; this volume change will be the same as the measured volume of water drained out from the soil. Therefore there is a volumetric strain due to reduction of water alone. Pore water pressure will start to dissipate, in other words consolidation will begin only after the soil has attained a structural density and void ratio which capable of taking over the transfer of load from the water. For this laboratory study, the structural density and void ratio at the beginning of consolidation with 100 kPa load was 14.2 kN/m^3 and 2.68 respectively. It was also confirmed by field tests that, for slurry-like soil, there will be one type of deformation which occurs only due to the draining out of water before the consolidation stage. During this stage, no pore water pressure dissipation will occur and hence no effective stress gain and strength gain will occur. However strain during the no pore water pressure dissipation period was found to be as high as 19% in the laboratory study.

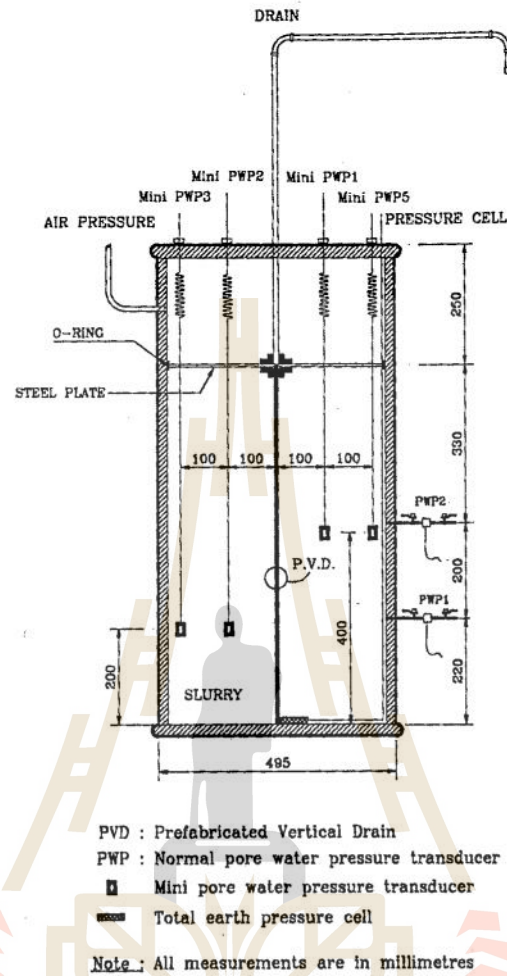


Figure 2.22 Large diameter consolidation cell with soil instruments

2.5.2 Reclamation of a slurry pond in Singapore

The Changi East reclamation project was carried out between 1991 and 2005 to create 2000 ha of land offshore for the extension of the Changi International Airport and other infrastructure developments in Singapore. This project included the reclamation of a 180 ha slurry pond. A containment sand bund was constructed around this borrow pit in 1986 to the crest level of about +5 mCD. Subsequently silt and clay washings from other sand quarrying activities in the eastern part of Singapore were transported through pipelines with water and discharged into this

contained area to form a pond. Therefore the slurry inside the pond consisted mainly of clay and silt. The water content of the slurry varied from 60% to 300%, but was mainly in the range of 120–180%. The bulk density was low, with values ranging from 1.2 to 1.4 Mg/m³.

The method of the reclamation and soil improvement works is

1. Sand placement by spreading

As the top surface of the slurry had little strength, direct hydraulic placement of sandfill on top of the slurry would have caused the slurry to be displaced by the penetration of the sand fill. The sand fill therefore had to be spread in thin layers using a specially designed sand spreader, as shown in Figure 2.23. The sand fill, with a high water to sand ratio, was pumped into the spreader using a suction dredger. Small lifts of 20 cm were used in the first phase of spreading to ensure stability of the fill. When the fill reached an elevation at +2 mCD, a failure in the form of slurry bursting occurred at the location shown in Figure 2.24

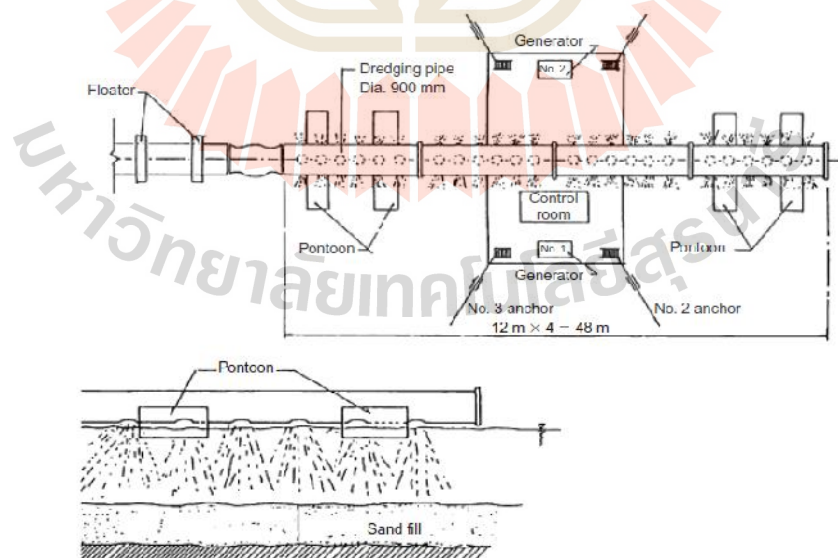


Figure 2.23 Sand spreading system used for slurry pond

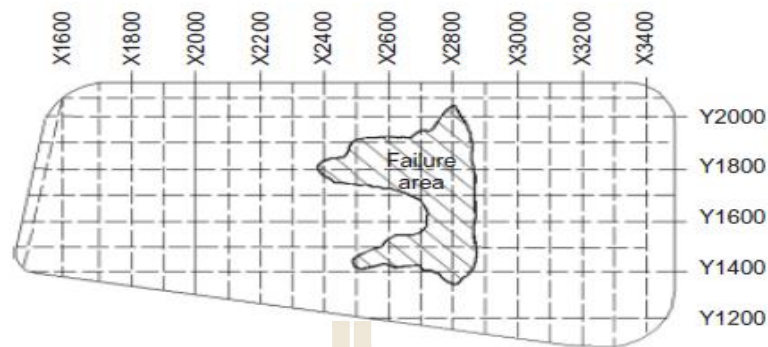


Figure 2.24 Location of failure area where bursting of slurry

2. Remedial measures using geotextile

As a remedial measure, geotextile fabric was used to cover the failure area (Figure 2.25). Two types of woven geotextile were used. The first type, HS150/150 It was placed in a single layer to cover an area 700 m by 300 m a second type, HS100/50. The second type of geotextile was placed in two layers over an area 700 m by 600 m

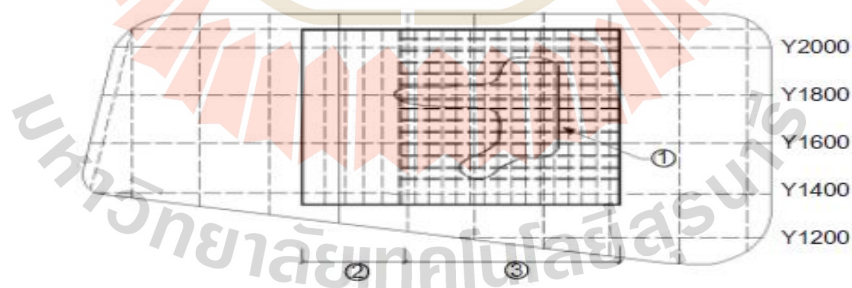


Figure 2.25 Layout of geotextile sheets used to cover failure area of slurry pond

3. Second phase of sand spreading

After placement of the geotextile, sand fill spreading resumed, using

the same Sand spreader, until the ground elevation of +4 mCD was reached.

4. Installation of vertical drains

The surcharge in the first stage was placed to +6 mCD. After Approximately 1.5 m of settlement had taken place, a second pass of vertical drains was installed with the same square grid of 2.0 m in the centre of the square grid of PVDs installed in the first round.

For reclamation over ultra-soft, high water content slurry, direct placement of fill was attempted. However, this was not entirely successful as a failure in the form of a mud burst occurred around the centre of the pond. But geotextile was used as a reinforcement to cover the failed area before fill placement. And this method was proven to be successful.

2.5.3 Simple method of modeling PVD-improved subsoil

Chai et al. (2001) have been studied the effect of Installing prefabricated vertical drains (PVDs) in subsoil is to increase the mass hydraulic conductivity of the subsoil in the vertical direction. Based on this concept, a simple method for modeling PVD improved subsoils is proposed, in which an equivalent vertical hydraulic conductivity k_{ve} for the PVD improved subsoil is explicitly derived. With the proposed simple method, analysis of PVD improved subsoil is the same as that of the unimproved case. The theoretical verification of the simple method was made under 1D condition. The calculated average degree of consolidation and excess pore pressure distribution in the vertical direction using the simple method are compared with existing theoretical solutions (combination of Terzaghi's consolidation theory and Hansbo's solution for PVD consolidation). It has been proved theoretically that, in terms of average degree of consolidation, in the case

of one layer and ignoring the vertical drainage of natural subsoil, the maximum error of the proposed method is 10% compared with Hansbo's solution. For the case of one layer or multilayers and considering both vertical and radial drainages with the parameters adopted here, the maximum error of the proposed method is 5%. The multilayer case was analyzed by FEM method, and the proposed simple method is compared with that of using 1D drainage elements. Then, 2D finite element analyses were conducted for three case histories of embankments on PVD improved subsoils.

The method was applied to analyze test embankments on PVD-improved subsoils in China compared with the results of using the drainage elements method as well as measured data, indicate that the proposed method yielded acceptable results in terms of settlement (Figure 2.26), excess pore pressure (Figure 2.27), and lateral displacement (Figure 2.28). It is recommended that the proposed simple approximate method is a useful tool for engineering practice.

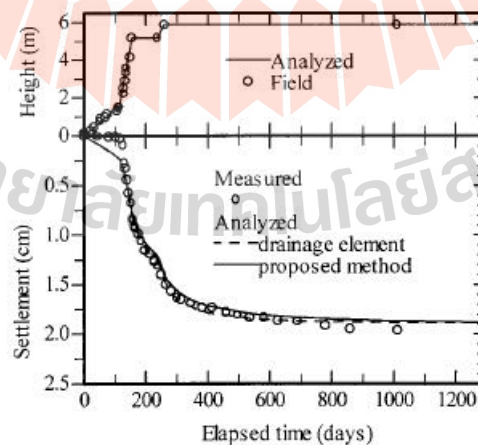


Figure 2.26 Comparison of Settlement Curves

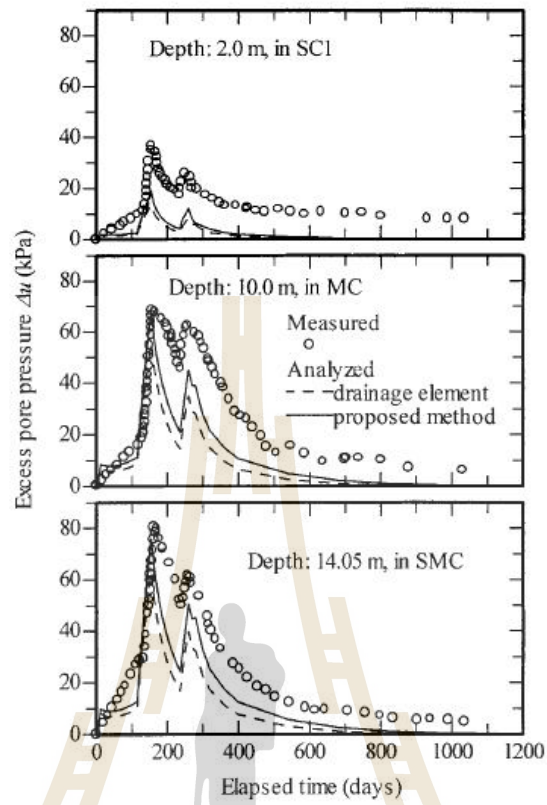


Figure 2.27 Calculated Excess Pore Pressure Variations

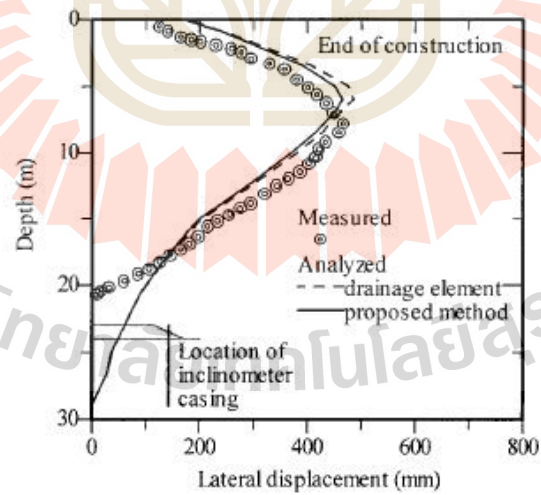


Figure 2.28 Lateral Displacement Profiles

2.5.4 Mae Moh Mine

Mae Moh open pit lignite mine is located at Mae Moh district, Lampang province. Mae Moh Mine far from Bangkok about 630 km and located on the northern side. Geological structure is complicated syncline and has a lot of fault. The lignite beds have 5 seams, which are J, K, Q, R and S (from top bottom respectively). K and Q seam are the most important because of the thickness about 20-30 meters. According to the mine planning and development, the mine will be deeply dug to a depth of approximately 500 meters in the next 37 years and it will be the deepest open pit Lignite mine in the world. From such reason, Sump1 C1 will become the in-pit dump. However, the mud in Sump1 C1 possesses high water content, leading to large consolidation settlement and low bearing capacity. Therefore, in-pit dump without the improvement of mud properties will cause the instability of mine slope, and the unsafely of workers and machines. Unless measures are taken to form drainage paths for the water to exit the rock mass, the groundwater table within the low wall is likely to approach the most adverse condition. For a low wall slope 150 m. high the decrease in safety factor resulting from such continuous recharge is likely to be of the bedding dip by 3°. The equivalent increase in probability of sliding can therefore be estimated from the design curves.

CHAPTER 3

METHOD

3.1 Introduction

This chapter is about the process and the test method include the sampling and experiment place, basic property test, sampling soil preparation, physical model test preparation, measuring devices installation, and stress vertical loading. The research method is shown in Figure 3.1

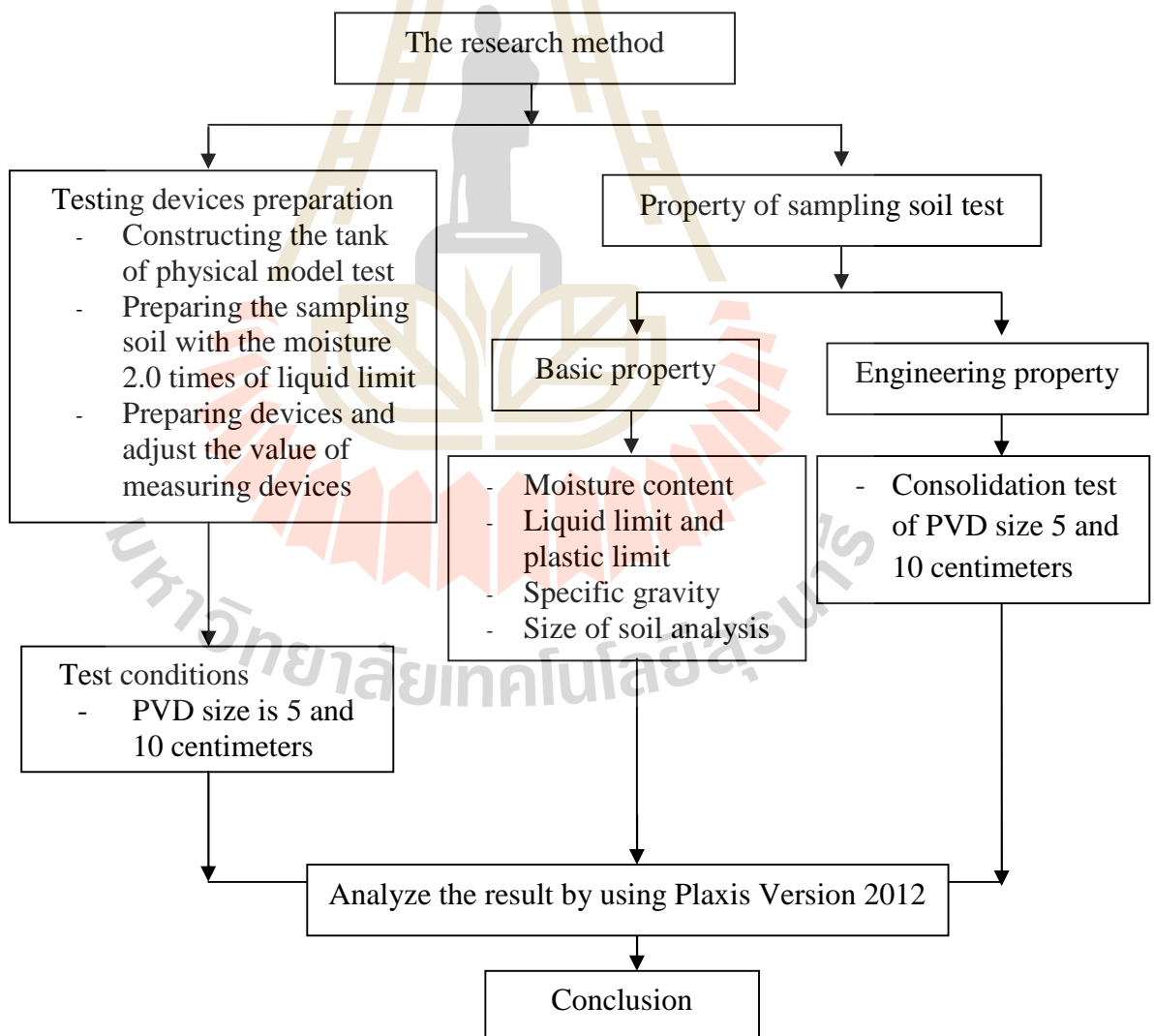


Figure 3.1 The research method

3.2 The sampling and experiment place

The sampling place was Mae Moh Mine; the coal mine in Lampang, (The map of Mae Moh Mine was shown in Figure 3.2). The sampling soil was taken from Sump1 C1; it was the water-received area of Mae Moh Mine was shown in Figure 3.3 and 3.4. The test was hold in the laboratory of Suranaree University of Technology.

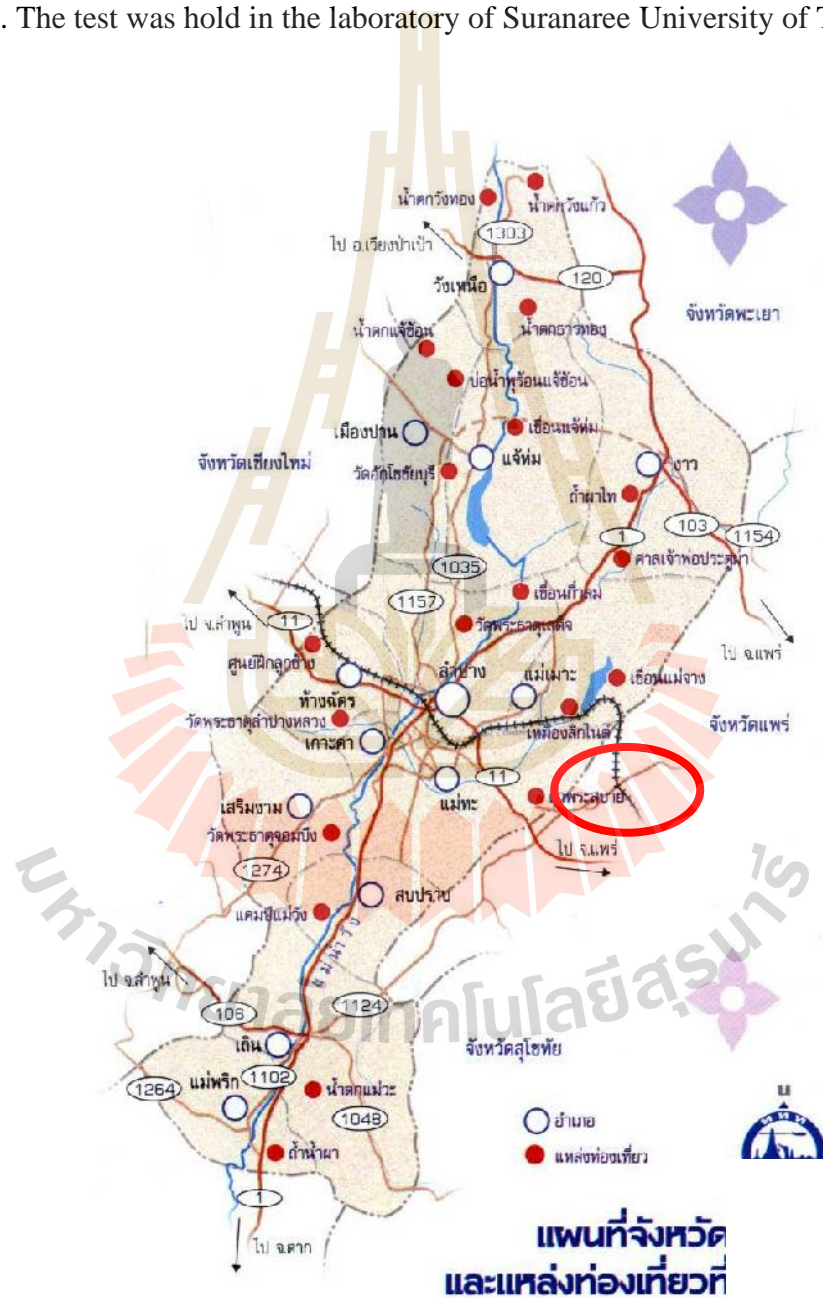


Figure 3.2 Mae Moh Mine map

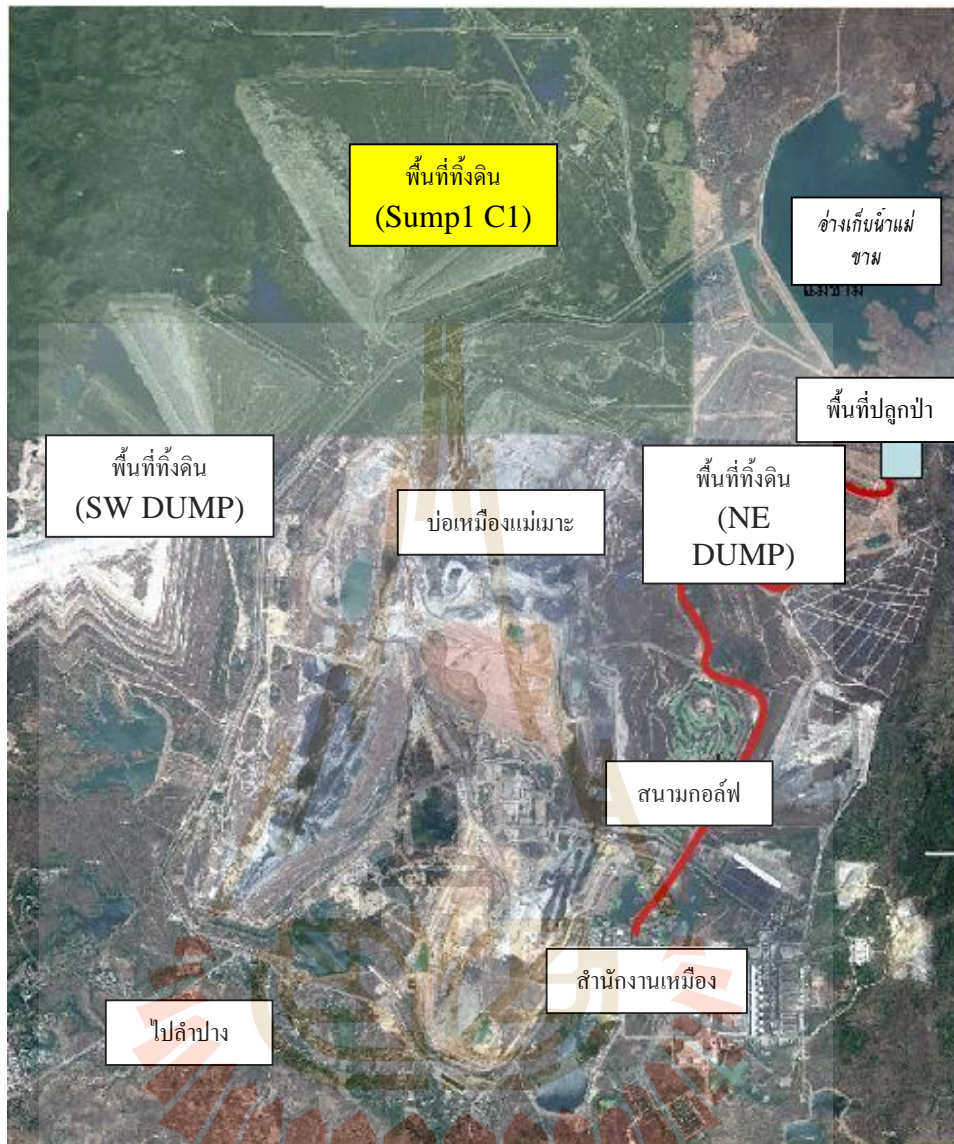


Figure 3.3 Inpit dump area Sump1 C1



Figure 3.4 Soil in Sump1 C1

3.3 Basic property test

Testing the basic property and engineering property of sampling soil as shown below:

- 3.3.1 Specific gravity comply with ASTM D 854
- 3.3.2 Liquid limit and plastic limit test comply with ASTM D 4318
- 3.3.3 Analyze size of soil by using Laser Scattering Particle Size Distribution Analyzer LA-950
- 3.3.4 Consolidation test comply with ASTM D 2435

3.4 Constructing the tank of physical model test

Figure 3.5 (a) and (b) show the feature and size of the test tank. This tank was 5 millimeters thick; 50 centimeters of diameter; 1.20 meters height.

3.5 Soil sampling and preparation

The sampling soil in this research was the clay in Sump1 C1 which is the water-received area of Mae Moh Mine. Pattern of the sampling was disturbed sample by using Backhoe directly dig from the pit. Some of sampling soil was tested for basic property and engineering property. The leftover soil was molded with the moisture 2.0 times of liquid limit in order to put into the tank of symmetry physical model test around an axle.

3.6 The duplication of soil layer in the test tank

The first stage was the installation of pore pressure transducer, linear potentiometers and earth pressure cells. After that, the soil sample which is remolded at 2.0 times of liquid limit was put into the cylindrical stainless steel mold; the geotextile was put on the soil layer. Then, the sand was poured with the 10 cm thick; the pressure loading 0.5 kPa was started and waited for the end of the consolidation of that load. The applied load was 0.5, 1, 1.5, 3, 5, 10, 20, 40, 60, 80 and 120 kPa. The PVD was installed in the middle of the tank after the consolidation due to 10 kPa was finished. Two sizes of PVD were used in this research which were 5 and 10 cm.

3.7 The measuring devices installation and the load adding in physical model test

Figure 3.6 shows the installation of pore pressure transducer, earth pressure cells, and linear variable displacement transducers (LVDT). During the tests, the change of water pressure, stress vertical loading, and the settlement were recorded.

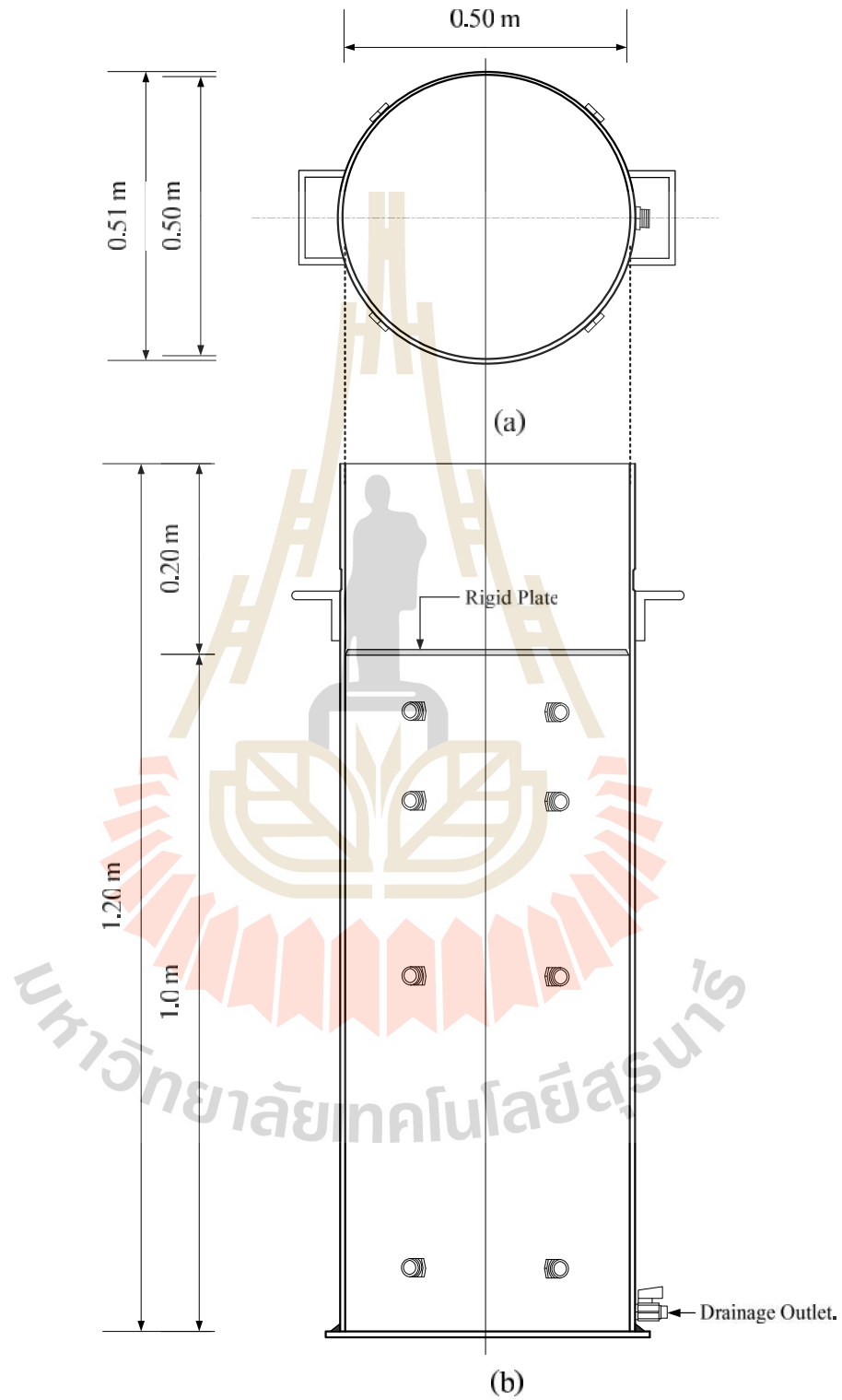


Figure 3.5 Feature of test tank (a) plan of test tank (b) side view of test tank

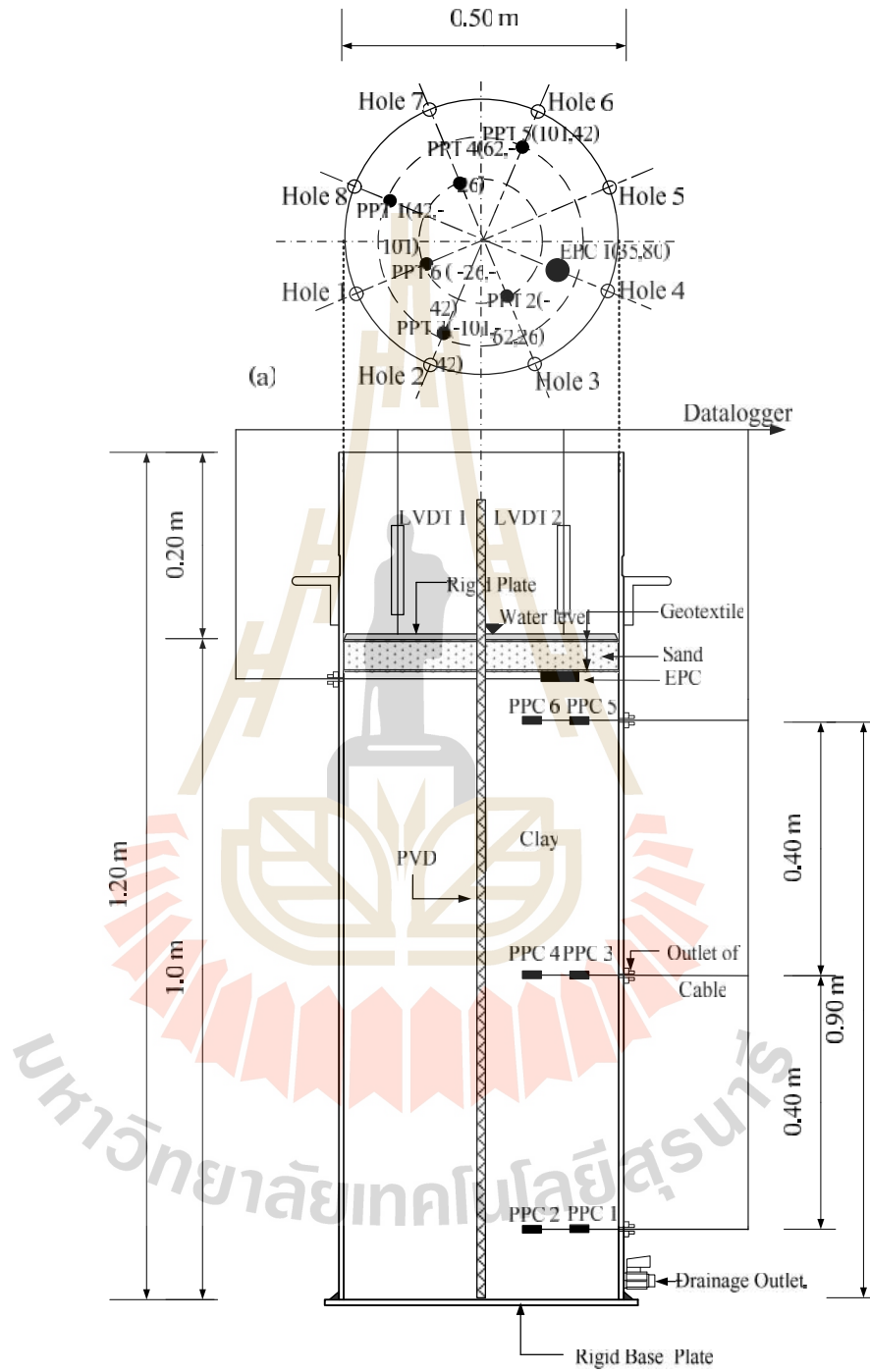


Figure 3.6 The measuring devices diagram (a) horizontal view (b) vertical view

When EPC is Earth Pressure Cell

PPC is Pore Pressure Cell

LVDT is Linear variable displacement transducers

3.8 Test conditions

The test in the laboratory was under 2 conditions included the size of PVD was 5 centimeters and 10 centimeters.

Table 3.1 The sample test

Case.	Size of PVD (cm)	Height of PVD (cm)
1	5	120
2	10	120

CHAPTER 4

TEST RESULTS

4.1 Introduction

This chapter presents the consolidation test results of ultra-soft mud (from the Sump1 C1 of Mae Moh mine) improved by PVD in the physical model test. The settlement and excess pore pressure of the composite ground were also simulated by finite element analysis using PLAXIS program. The consolidation behavior of the ultra-soft mud with PVD was modeled by the numerical analysis with the Plaxis 2D version 8.2 and the simulations were compared with the test results in term of settlement and excess pore water pressure. Comparison was made based on studies from 2D axial symmetry model and plane strain model. The 15-node triangular element was used in the finite element. Finally, the suitable method for this ultra-soft mud is suggested.

4.2 Basic and engineering properties of mud

The mud samples were obtained from Sump1 C1 of Mae Moh Mine, which is the coal mine in Lampang province. The Sump1 C1 is a slurry pond, which has received water flow in Mae Moh Mine. The samples were taken by a backhoe directly from the pond. Basic and engineering property tests on the mud samples were undertaken. The mud sample was remolded at the water content of approximately twice of liquid limit and then transferred to a cylindrical stainless mold.

Table 4.1 shows the basic properties of the mud sample. The specific gravity was 2.61, and the liquid limit and plastic limit were 55% and 27%, respectively.

Figure 4.1 shows the grain size distribution of the mud sample. Soil consisted of 40% sand, 55% silt and 5% clay. The soil was classified as high plasticity silt (MH) according to the Unified Soil Classification System (USCS). Figure 4.2 shows the relationship between void ratio and effective vertical pressure of mud. The compression index (C_c) was 0.5 and swell index (C_s) was 0.1.

Table 4.1 Basic properties of soil sample

G_s	LL	PL	PI	USCS	Particle size distribution: %		
	%	%	%		Sand	Silt	Clay
2.60	55	27	29	CH	40	55	5

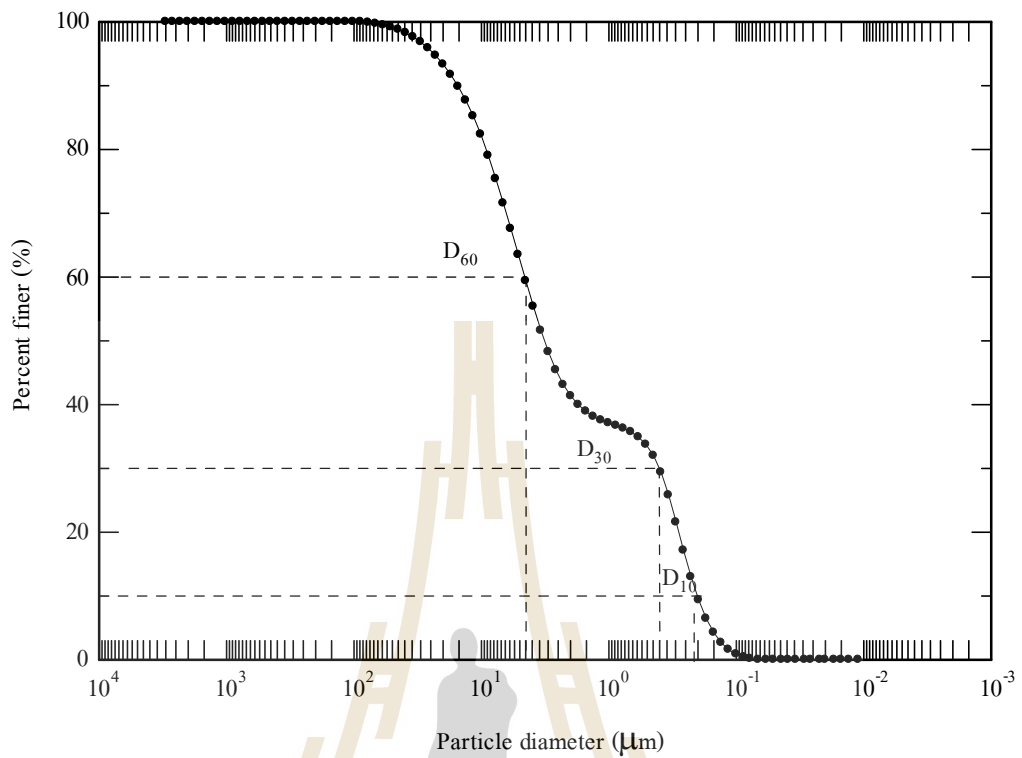


Figure 4.1 grain size distribution of test mud

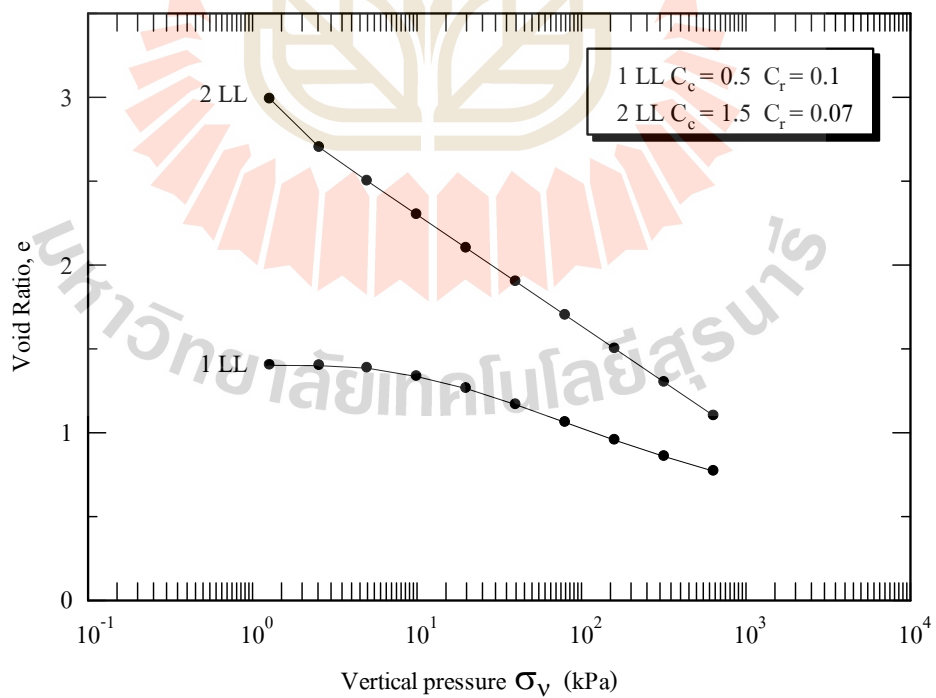


Figure 4.2 Consolidation curves of mud samples at LL and 2LL

4.3 Consolidation behavior of ultra-soft mud with the prefabricated vertical drain

4.3.1 Settlement of ultra-soft mud with the prefabricated vertical drain

Figures 4.3 and 4.4 show the relationship between the applied vertical stress versus time and settlement versus time of the ultra-soft mud improved with a 5 cm PVD respectively. Figures 4.5 and 4.6 show the relationship between the applied vertical stress versus time and settlement versus time of the ultra-soft mud improved with a 10 cm PVD respectively. The vertical stress was applied on the PVD improved mud from 0.5, 1, 1.5, 3, 5 and 10 kPa; i.e., the next loading was applied after the consolidation that was caused by the previous loading was completed. The PVD was installed after 10 kPa consolidation. The vertical stresses from 20, 40, 80 and 120 kPa were then applied on the model ground, respectively. The test result shows that the final settlement of 5 cm and 10 cm PVD are almost the same. It indicates that, the PVD only accelerated the settlement of the ultra-soft mud but the final settlement were more or less the same. In the initial stage, large settlement was observed when the first 20 kPa load was applied to the soil because the pore water was squeezed out of soil element. In other words, the total settlement of the ultra-soft mud with or without PVD is similar and is approximately 66 cm. The settlement rate for 10 cm PVD is faster than the 5 cm PVD of about 37 % because of being higher sectional area.

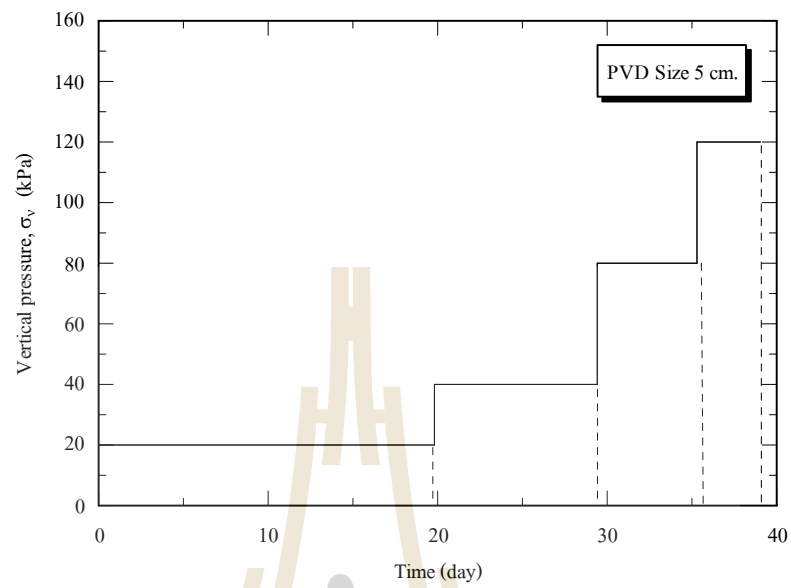


Figure 4.3 The relationship between the applied vertical stress and time of the ultra-soft mud with the 5 cm prefabricated vertical drain

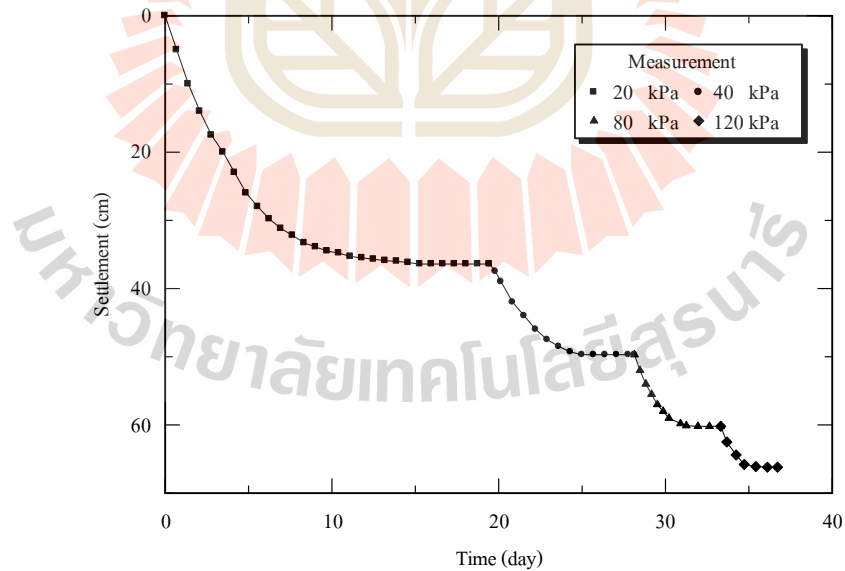


Figure 4.4 The relationship between the settlement and time of the ultra-soft mud with 5 cm PVD.

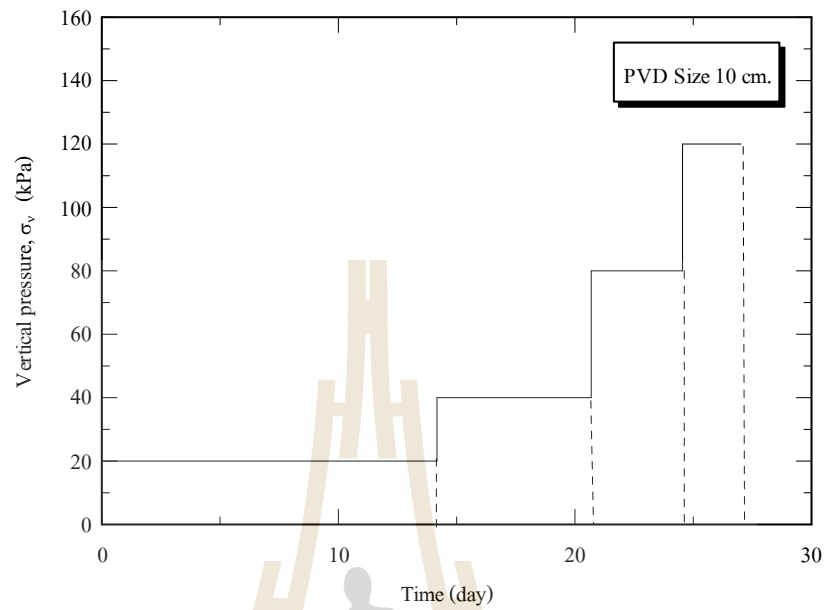


Figure 4.5 The relationship between the applied vertical stress and time of the ultra-soft mud with the 10 cm prefabricated vertical drain.

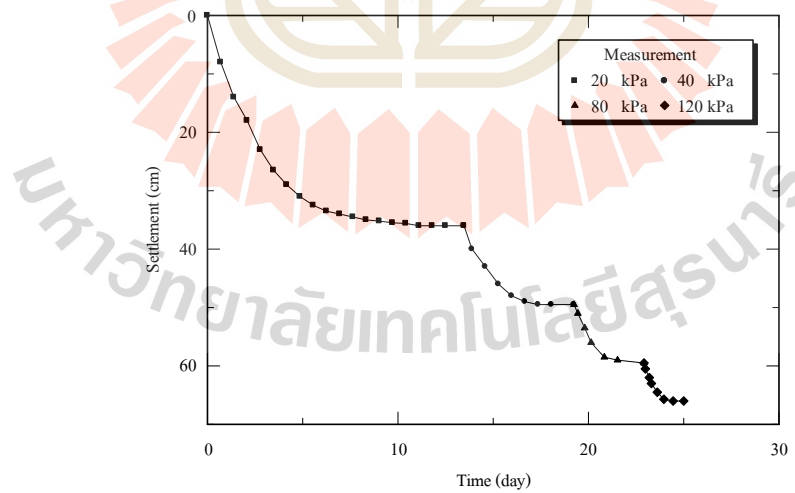


Figure 4.6 The relationship between the settlement and time of the ultra-soft mud with 10 cm PVD.

4.3.2 The excess pore water pressure of ultra-soft mud with prefabricated vertical drain

Figures 4.7 to 4.10 show the relationship between the excess pore water pressure versus time for different applied vertical stresses of two different sizes of PVD (5 and 10 cm). At the initial stage (i.e., at time $t=0$), excess pore water pressure (u) increases immediately and equals the applied vertical stress ($u = \sigma_v$). Then, the water in the void spaces of the clay layer is squeezed out and flowed toward the highly permeable sand layers and PVD, thereby reducing the excess pore water pressure. This, in turn increases the effective stress by an equal amount since $\sigma_v' + u = \sigma_v$. Thus, at any time ($t > 0$), $\sigma_v' > 0$ and $u < \sigma_v$. Theoretically, at the end of consolidation ($t = t_c$), the excess pore water pressure at all depths of the clay layer will be fully dissipated. This process of increase in effective stress in the mud due to the surcharge will result in a settlement which is time-dependent.

With the application of PVD, the water is actually “pushed” into the PVD by different pressure. The water then flows up to the sand layers where it can freely discharge. The use of PVD greatly expedites the consolidation process by shortening the drainage path length, as well as allowing horizontal drainage, which is the preferential direction of flow with highest permeability in naturally horizontally deposited fine-grained sediments. The use of vertical drains in forced consolidation applications can speed the time to reach acceptable levels of bearing capacity.

In the model ground, pore pressure cells PPC 1 and PPC 2 were installed at the bottom, PPC 3 and PPC 4 at the middle, PPC 5 and PPC 6 at the top.

The earth pressure cell was installed at the top of the soil. Moreover, LVDT was installed in order to measure the settlement by having the sand layer at the top and

bottom (double drainage) as shown in Figure 3.6. The consolidation time to release excess pore water pressure of 10 cm PVD is faster than that of the 5 cm PVD of about 60 % because of being higher sectional area. The dissipation of excess pore water pressure near the top and bottom of the model ground (double drainage) is very fast (PPC6, PPC5, PPC2 and PPC1). The dissipation of excess pore pressure at middle of the physical model (PPC4 and PPC3) is the slowest. A comparison of the excess pore pressures at different positions shows that the dissipation of excess pore water pressure at the positions close to the PVD is faster than that at the position faraway.

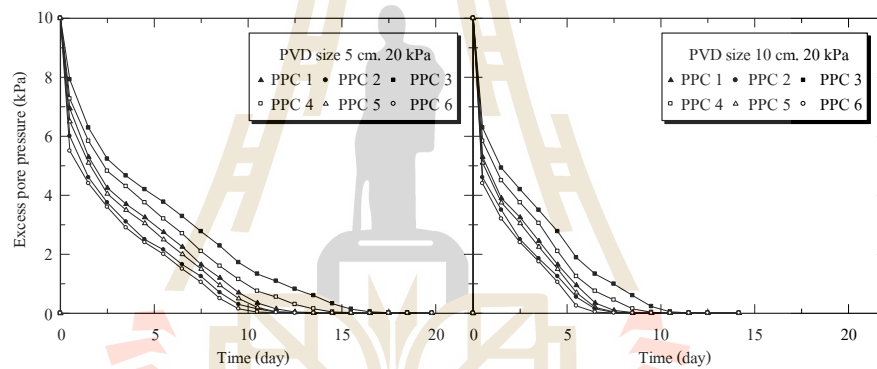


Figure 4.7 The relationship between the excess pore water pressure and time of the applied vertical stress at 20 kPa.

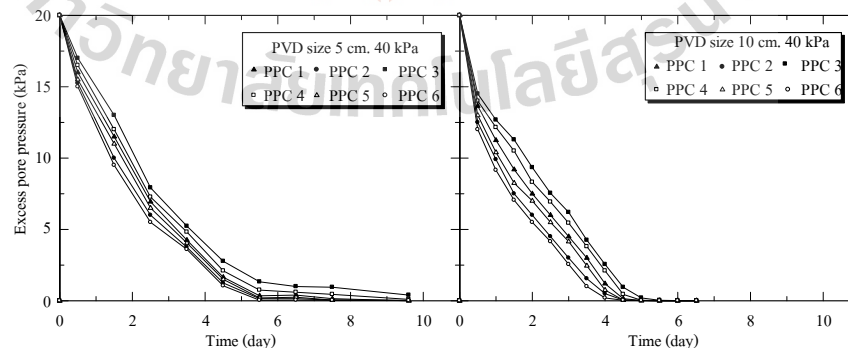


Figure 4.8 The relationship between the excess pore water pressure and time of the applied vertical stress at 40 kPa.

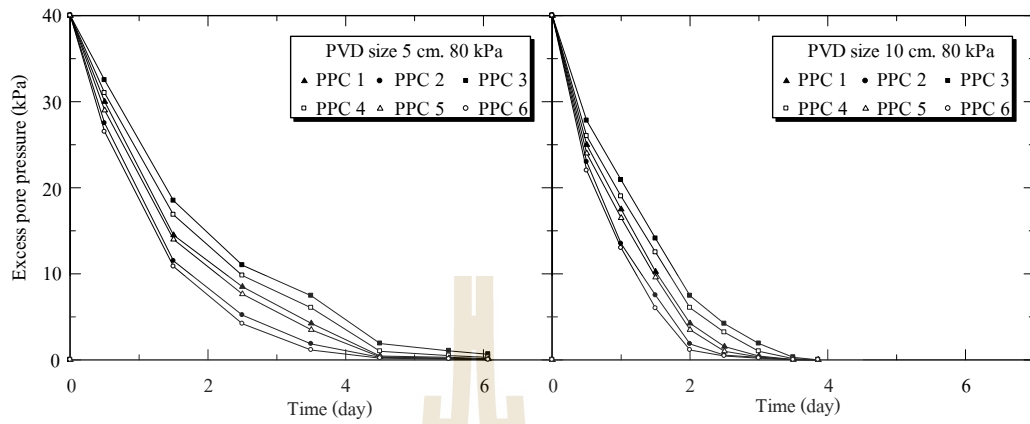


Figure 4.9 The relationship between the excess pore water pressure and time of the applied vertical stress at 80 kPa.

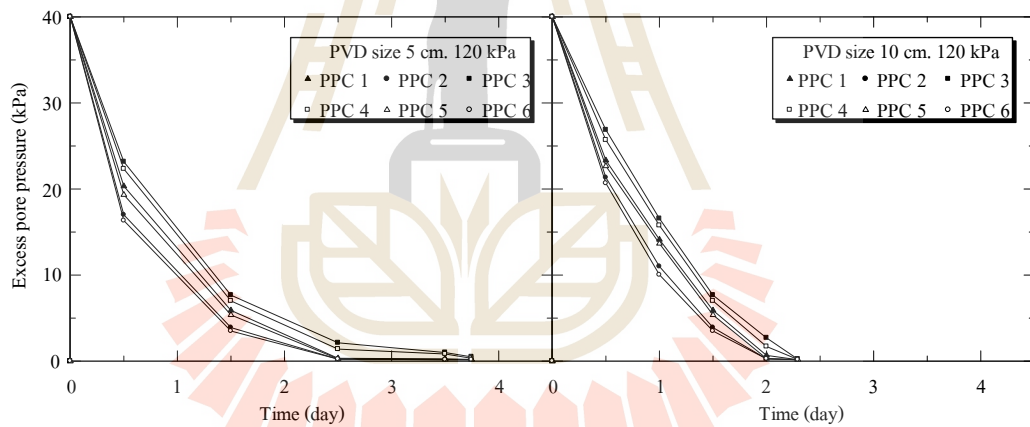


Figure 4.10 The relationship between the excess pore water pressure and time of the applied vertical stress at 120 kPa.

4.4 Theoretical and Numerical Analysis

Consolidation behavior of the ultra-soft mud with PVD can be simulated by the following theoretical and numerical models;

1. Hansbo's Theory

$$U_h = 1 - \exp\left[\frac{-8T_h}{F}\right]$$

where U_h = Degree of horizontal consolidation

$$T_h = \text{Time Factor}\left(\frac{C_h}{D_e^2} t\right)$$

$$F = \text{Factor } (F_n + F_s + F_r)$$

2. Chai's method

$$k_{ve} = \left(1 + \frac{2.5l^2 k_h}{\mu D_e^2 k_v}\right) k_v$$

where k_{ve} = The equivalent of vertical hydraulic conductivity

k_h = Horizontal hydraulic conductivities of the natural soil and smear zone

k_v = Hydraulic conductivity in the vertical direction

3. Axial symmetry model

4. Plane strain model, Hird et al. (1992)

$$\frac{K_{h,ps}}{K_h} = \frac{0.67}{\left[\ln(n) - \frac{3}{4}\right]} \text{ where } n = \frac{d_e}{d_w}$$

where K_h = Horizontal permeability

d_e = Influence zone diameter

D_w = Diameter of drain $\left(\frac{a+b}{2}\right)$

For the numerical analysis (axial symmetry model and plane strain model), consolidation behaviors was simulated using Plaxis 2D version 8.2. The 15-node triangular element was considered in this study. The calculated and measured subsoil responses were compared in terms of settlement and excess pore pressure. The simulated results from each model were also compared with the measured results. Table 4.2 shows the parameter used in the analysis.

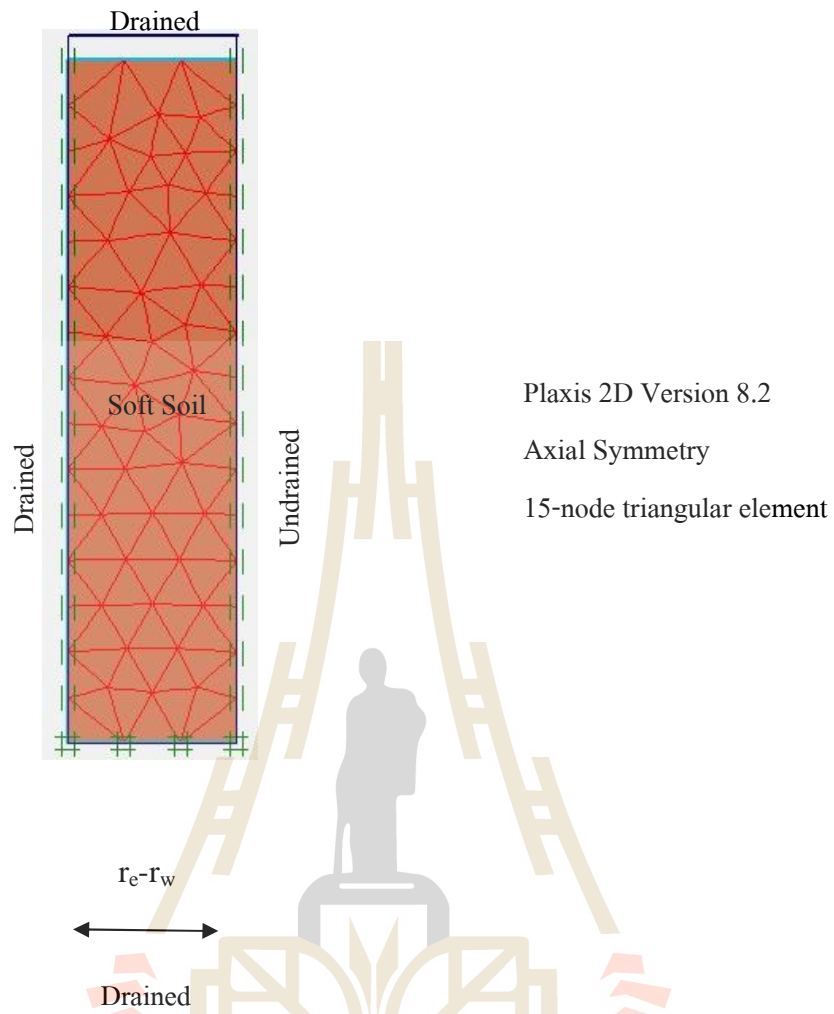
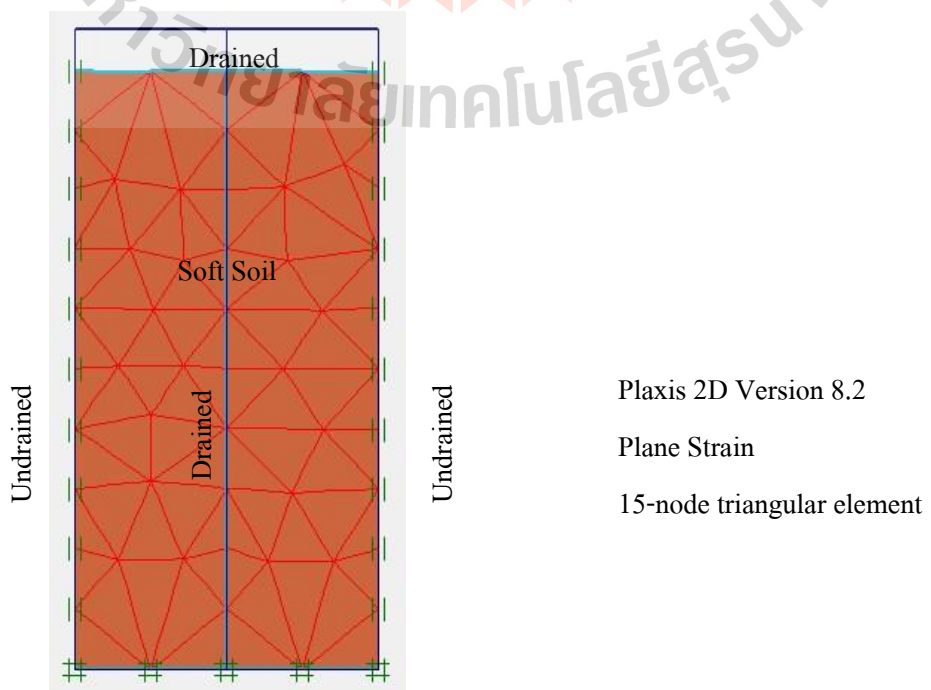


Figure 4.11 Axial symmetry model of ultra-soft mud with PVD for the analysis



β^*	0.2	0.2	0.2	0.2	0.2	0.2	-	-
λ^*	0.02	0.02	0.02	0.02	0.02	0.02	-	-
c'	5	5	5	5	5	5	-	(kN/m ²)
W'	25	25	25	25	25	25	-	o
$r_c - r_w$	0.237	0.225	0.237	0.225	-	-	-	(m)
F	-	-	-	-	-	-	2.19	-

4.4.1 The final settlement and rate of the settlement

Figures 4.13 and 4.14 show the relationship between the measured settlement versus time at various applied vertical stresses for 5 cm PVD and 10 cm PVDs, respectively. For a particular PVD size, the applied vertical stress of 20 kPa provides the highest consolidation time and consolidation settlement and is followed by 40 kPa, 80 kPa and 120 kPa, respectively. The consolidation time and consolidation settlement of each applied vertical stress and PVD sizes are given in Table 4.3

มหาวิทยาลัยเทคโนโลยีสุรนารี

Table 4.3 The consolidation time and consolidation settlement of each applied vertical stress and PVD sizes

PVD Size (cm)	Applied vertical stress (kPa)	Consolidation time (min)	Consolidation settlement (cm)
5	20	28522	37
	40	13830	50
	80	8472	62
	120	4906	66
10	20	20402	37
	40	9387	50
	80	5561	62
	120	2558	66

By comparing the sizes of PVD, the consolidation time of 10 cm PVD is faster than that of 5 cm PVD. However, the final settlement of 5 cm PVD and 10 cm PVD are almost the same. It implies that PVD only accelerated the time of settlement while final settlement does not change with size of PVD

Normally, the calculated variation of vertical compression of the foundation soil with depth is influenced by relative values of the coefficient of compressibility and the permeability and the permeability of different layer, as well as drainage condition. The consolidation settlement with PVD was simulated using 4 methods; 1.Hansbo's Theory 2. Chai's method 3. Axial symmetry model and 4. Plane strain model. The calculated results using Chai's method and Plane strain model found to

have a slightly slower consolidation rate when compared with the measured results. However, the maximum difference between calculated and measured settlement is only about 9% and 6%, respectively. For Hansbo's method, overestimation in consolidation settlement is observed with about 6% difference. Axial symmetry model is the most similar to the measured result, the final settlement at the end of test is about 66 cm and the consolidation time take s40 days and 25 days for 5 and 10 cm PVD, respectively.

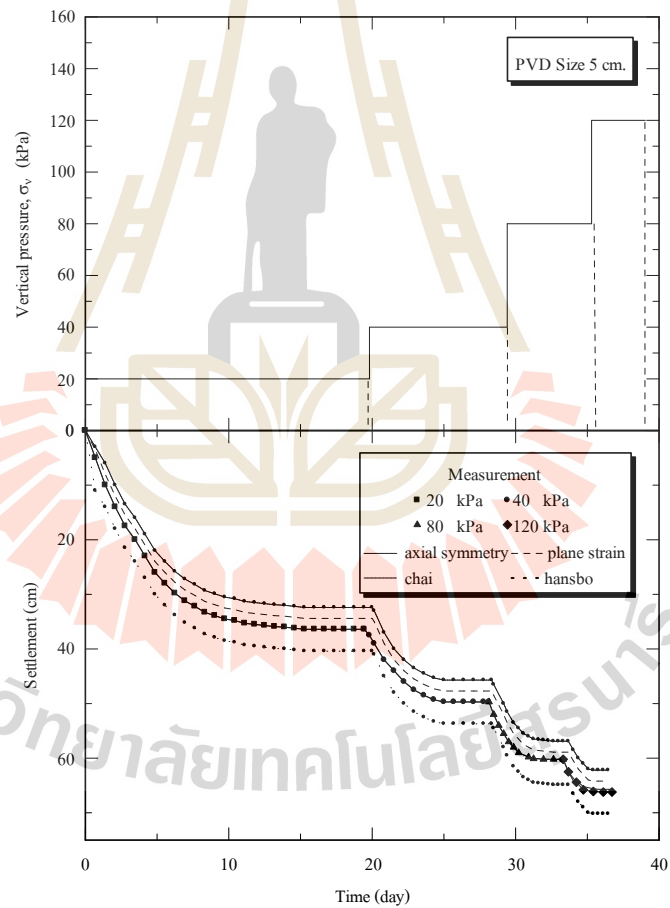


Figure 4.13 The relation between the applied vertical pressure and time; the settlement and time of the ultra-soft mud with 5 cm PVD.

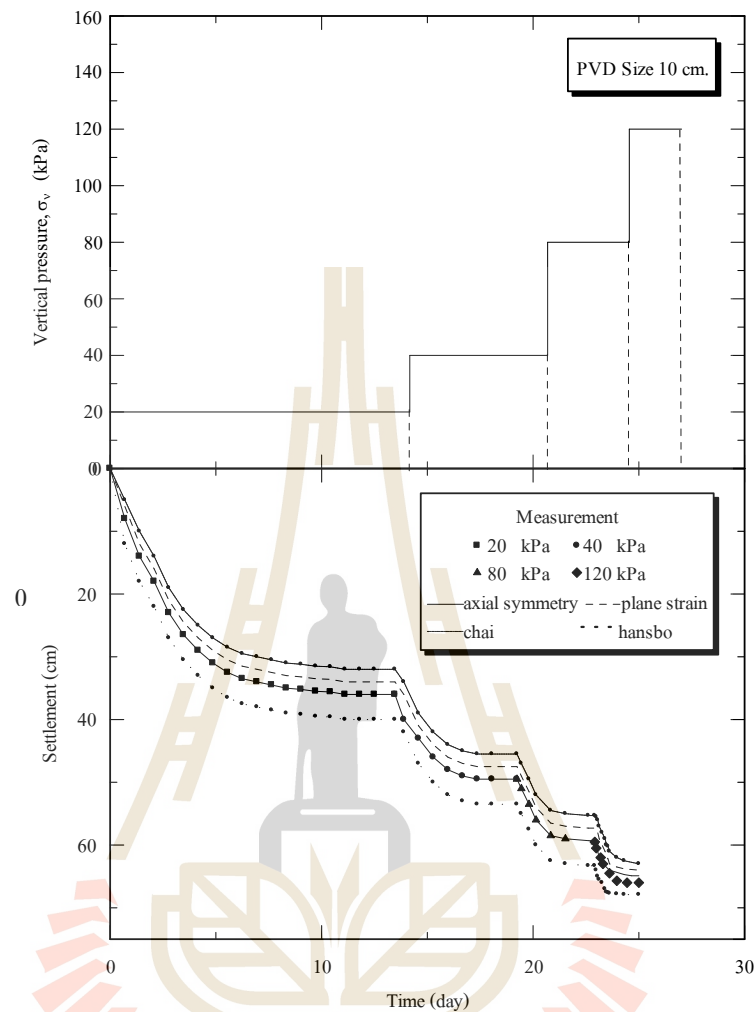


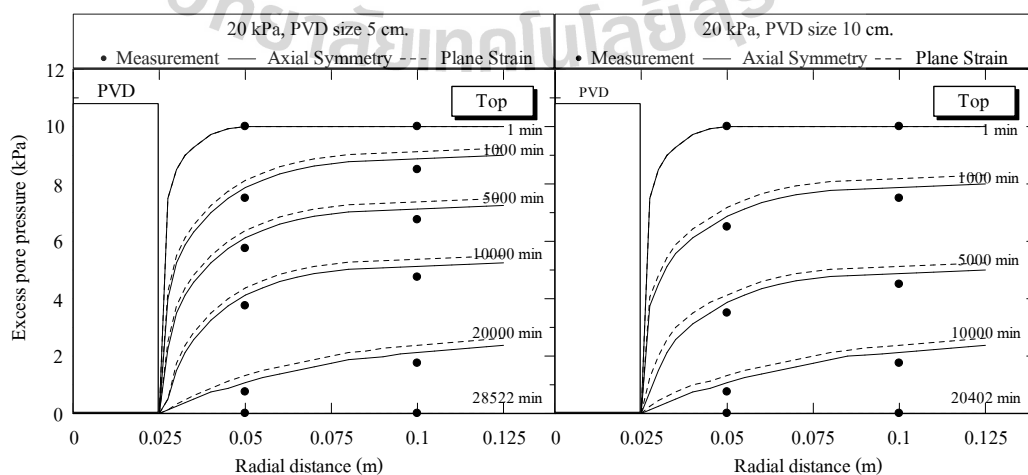
Figure 4.14 The relation between the applied vertical pressure and time; the settlement and time of the ultra-soft mud with 10 cm PVD.

4.4.2 Relation between the excess pore water pressure and time

Figures 4.15 to 4.18 show the relationship between the excess pore water pressure versus the radial distance at different consolidation times under various applied vertical stresses of 20, 40, 80 and 120 kPa. Since the drainage condition of the model ground is double drainage, the excess pore water pressures at the positions close to the top (PPC6 and PPC5) and bottom (PPC2 and PPC1) of the model ground

dissipate faster than that at the middle (PPC4 and PPC3) of the model ground. The comparison of the different positions of the excess pore water pressure shows that the dissipation of excess pore water pressure at the position close to the PVD is faster than that at other positions faraway.

A comparison of the excess pore water pressure between the measured results and finite element results from axial symmetry model and plane strain model indicates that the axial symmetry model and plane strain model give slightly higher excess pore water pressure than the measured result. Immediately after applying the vertical load on the model ($t=0$), the excess pore water pressure equals the applied vertical stress. The water in the void spaces of the clay layer is then squeezed out and flowed toward highly permeable sand layers and PVD, thereby reducing the excess pore water pressure until the end of the consolidation. The axial symmetry model can nearly match with the measured result rather than the plane strain model. The horizontal permeability coefficients (k_h) of axial symmetry model are 1.75×10^{-3} , 3.0×10^{-3} m/day for 5 and 10 cm PVD, respectively and of plane strain model was 2.3×10^{-4} and 2.9×10^{-4} m/day for 5 and 10 cm PVD, respectively. $r_e - r_w$ (diameter of model ground) of 5 and 10 cm PVD is 0.237 and 0.225, respectively.



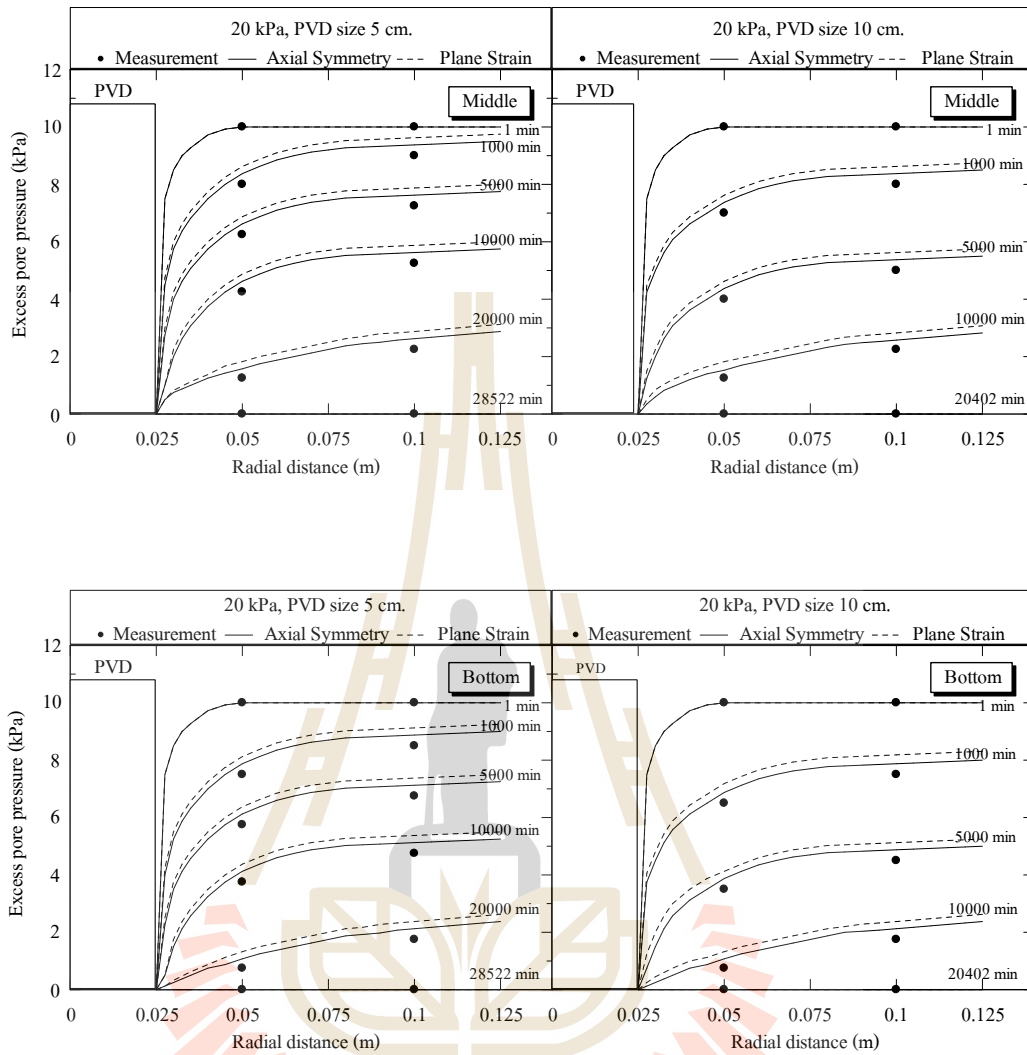


Figure 4.15 The change of the excess pore water pressure and the radial distance of PVD sized 5 and 10 cm respectively at 20 kPa.

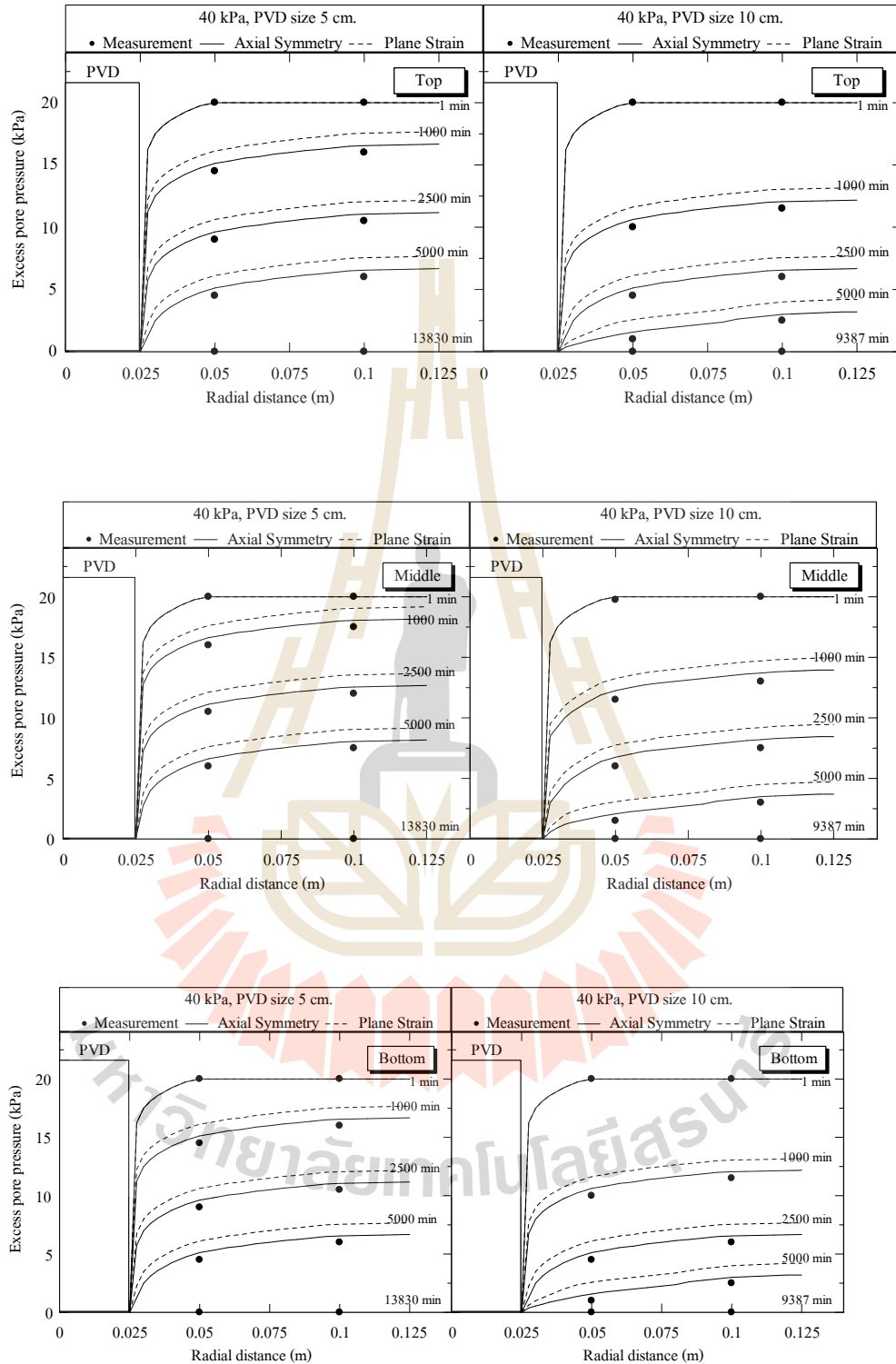


Figure 4.16 The change of the excess pore water pressure and the radial distance of PVD sized 5 and 10 cm respectively at 40 kPa.

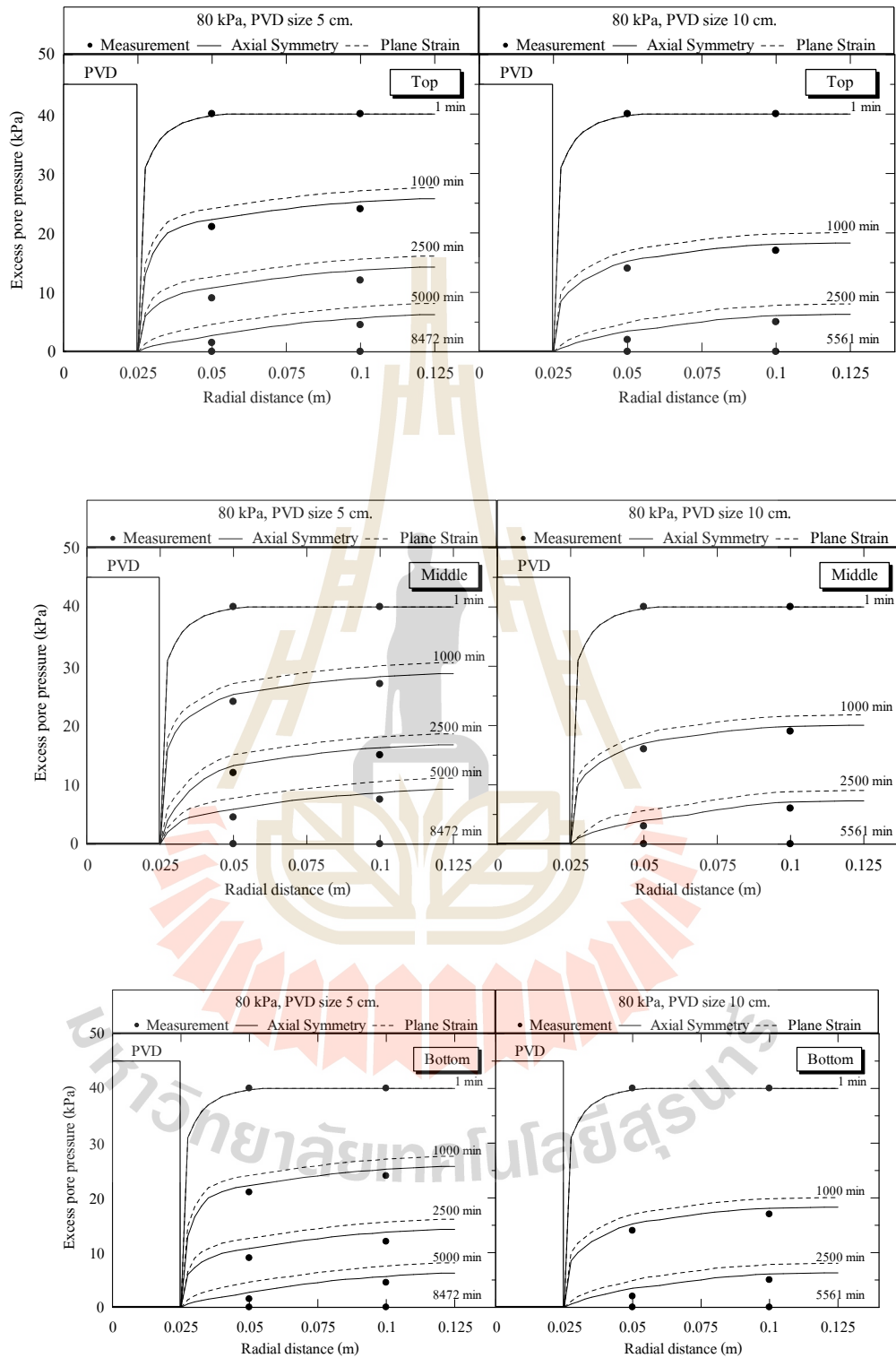


Figure 4.17 The change of the excess pore water pressure and the radial distance of PVD sized 5 and 10 cm respectively at 80 kPa.

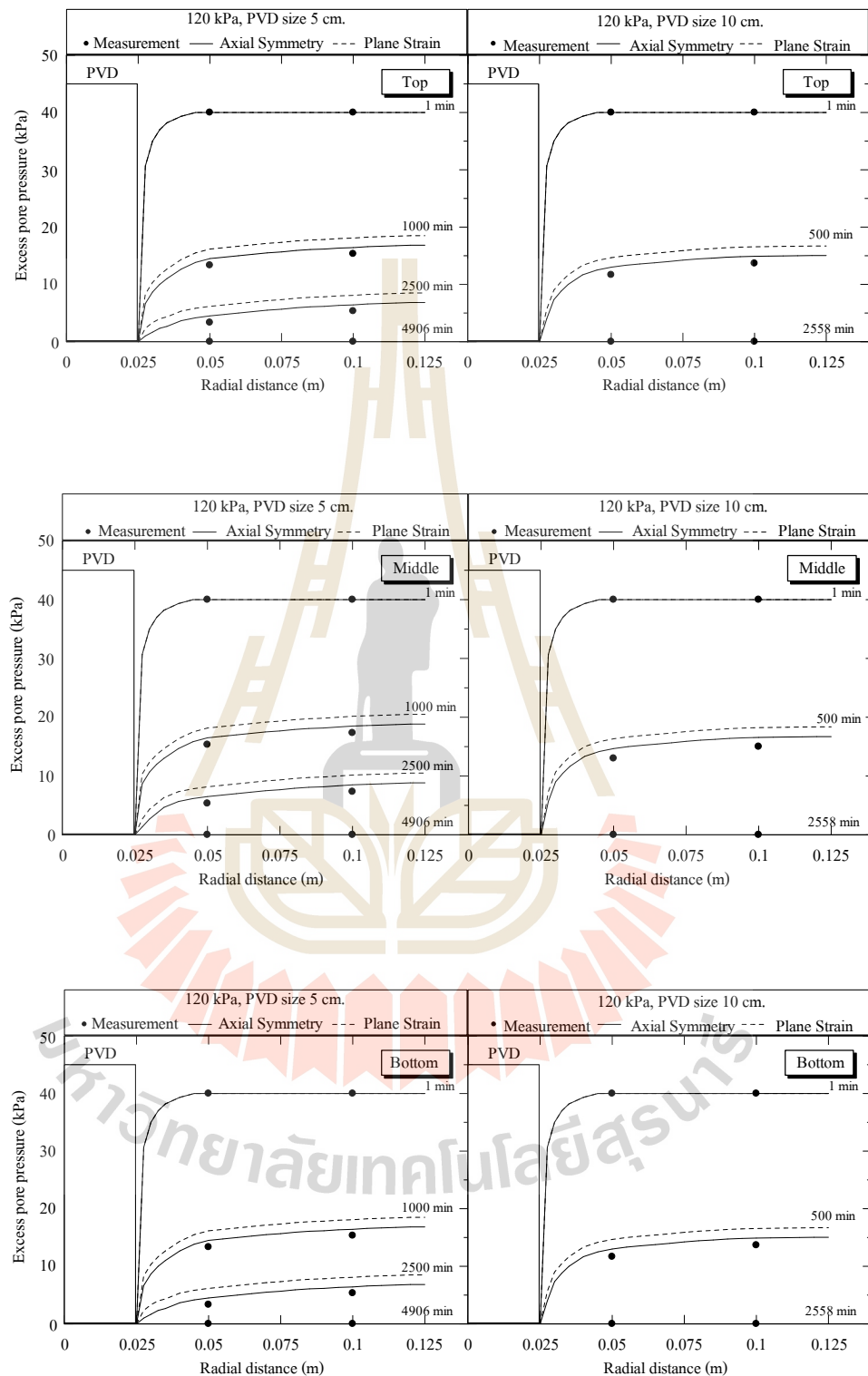
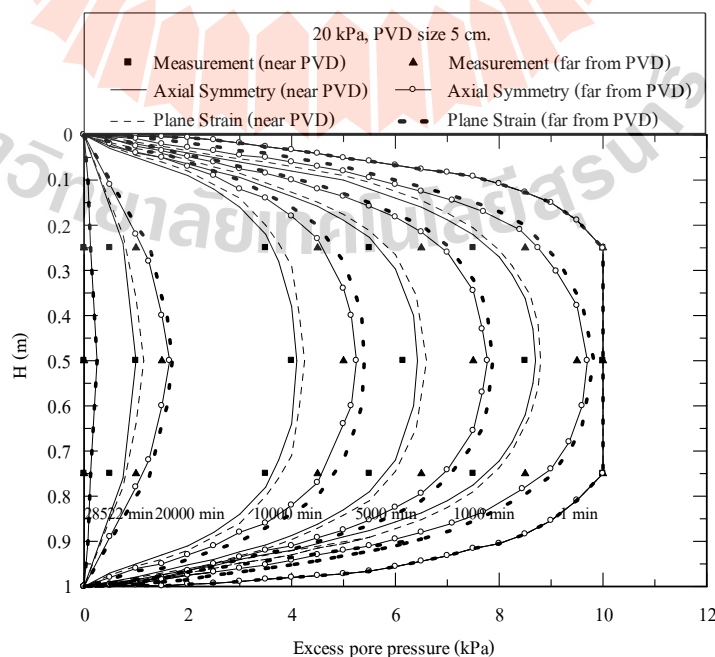


Figure 4.18 The change of the excess pore water pressure and the radial distance of PVD sized 5 and 10 cm respectively at 120 kPa.

Figures 4.19 to 4.22 show the relationship between the excess pore water pressure versus depth at different consolidation times, under applied vertical stress of 20, 40, 80 and 120 kPa. Pore water pressure cells were installed at the depth of 0.25, 0.5 and 0.75 m in the model ground as shown in Figure 3.6. The measured values from pore pressure cells PPC6 and PPC5 (Top) at 0.25 m depth and PPC2 and PPC1 (Bottom) at 0.75 m depth are similar result because the distance from the pore water pressure cells to the sand layer are the same. Therefore, the excess pore water pressures at the position close to the top and bottom of the model ground (double drainage) are almost the same. While the measured excess pore water pressure at the middle of the physical model test (PPC4 and PPC3) is found to have the largest because of the longest distance to the drainage layer. At the same location of pore water pressure cell and consolidation time, excess pore water pressure dissipation of 10 cm PVD is faster than that of 5 cm PVD. Comparing the numerical simulation using axial symmetry model and plane strain model, it was found that axial symmetry model yields a better results when compared with the measured result.



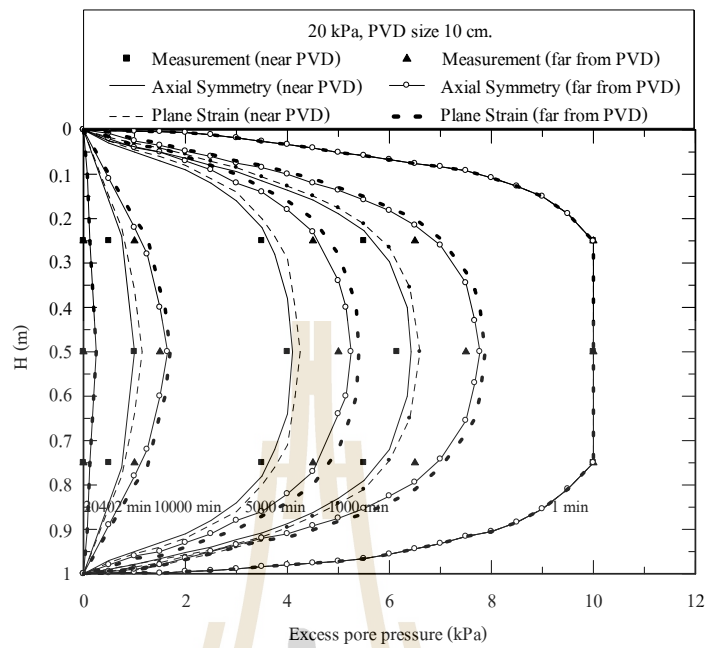
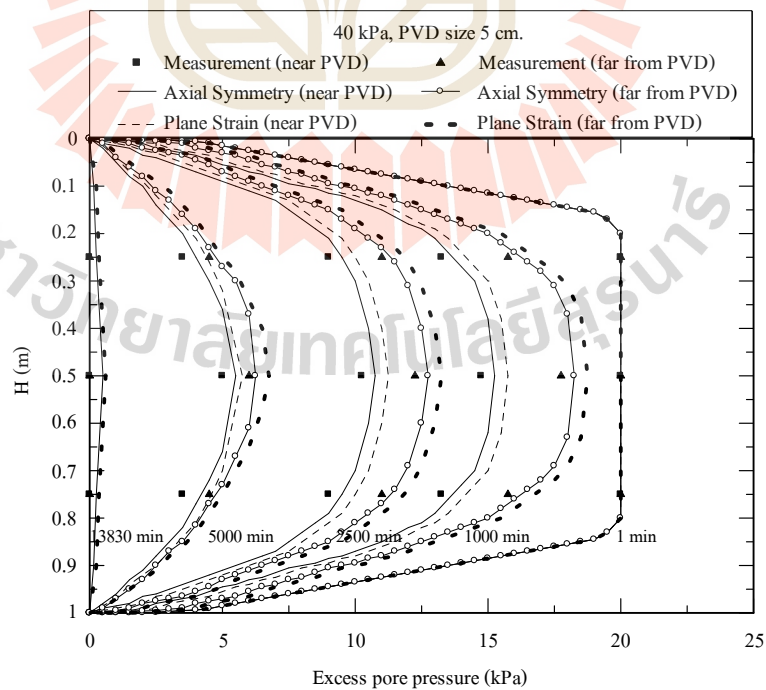


Figure 4.19 The relationship between the excess pore water pressure and depth of the soft mud with PVD sized 5 and 10 cm respectively at 20 kPa.



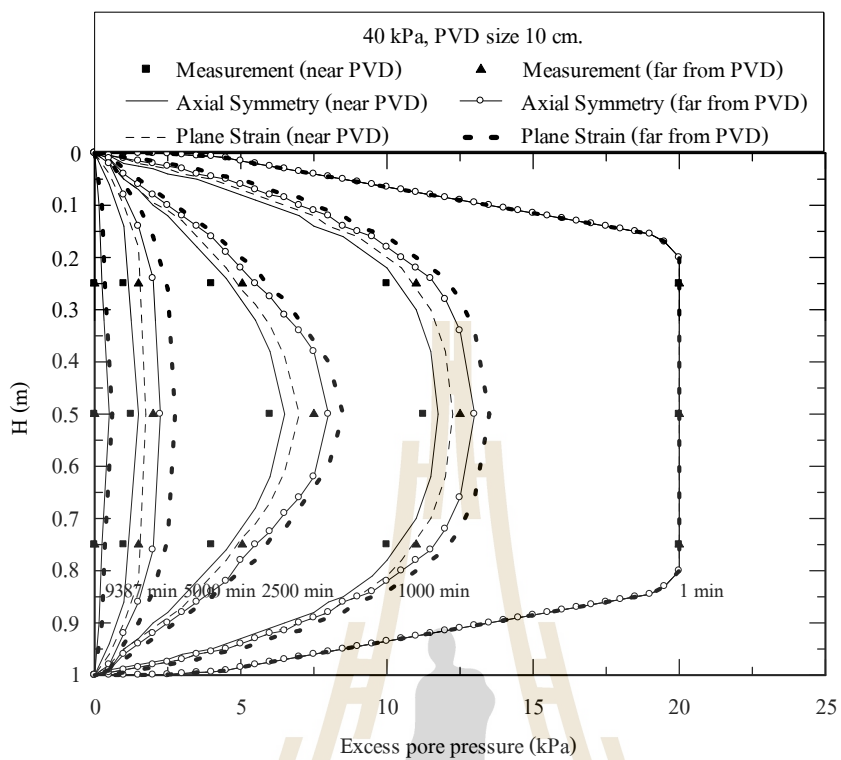


Figure 4.20 The relationship between the excess pore water pressure and depth of the soft mud with PVD sized 5 and 10 cm respectively at 40 kPa.

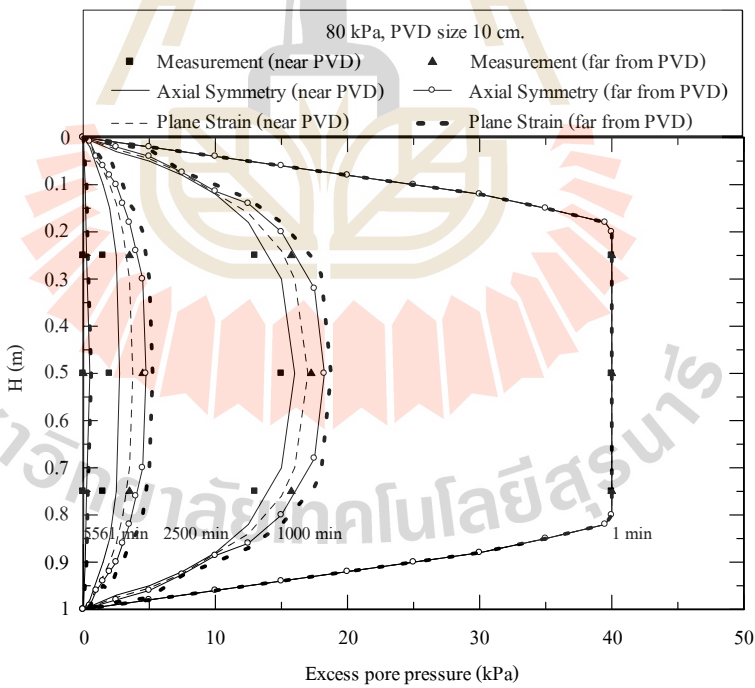
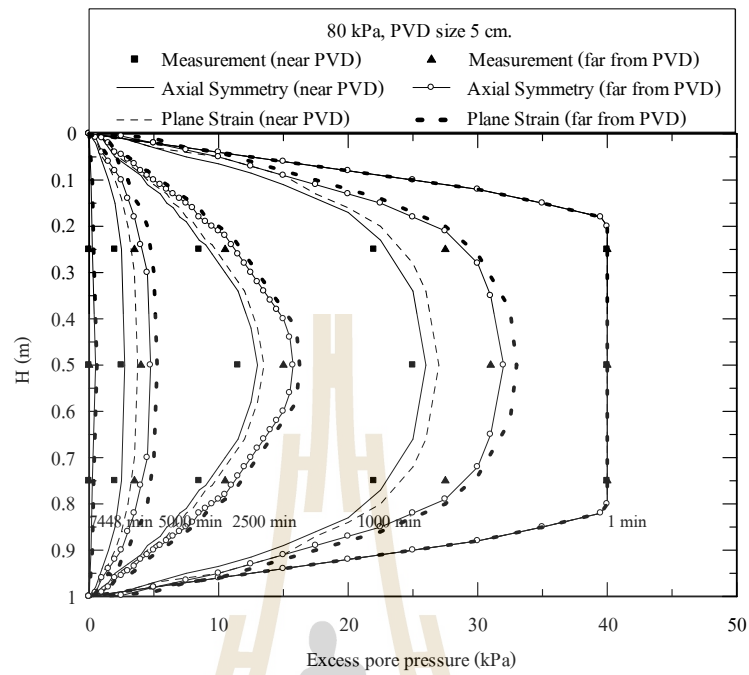


Figure 4.21 The relationship between the excess pore water pressure and depth of the soft mud with PVD sized 5 and 10 cm respectively at 80 kPa.

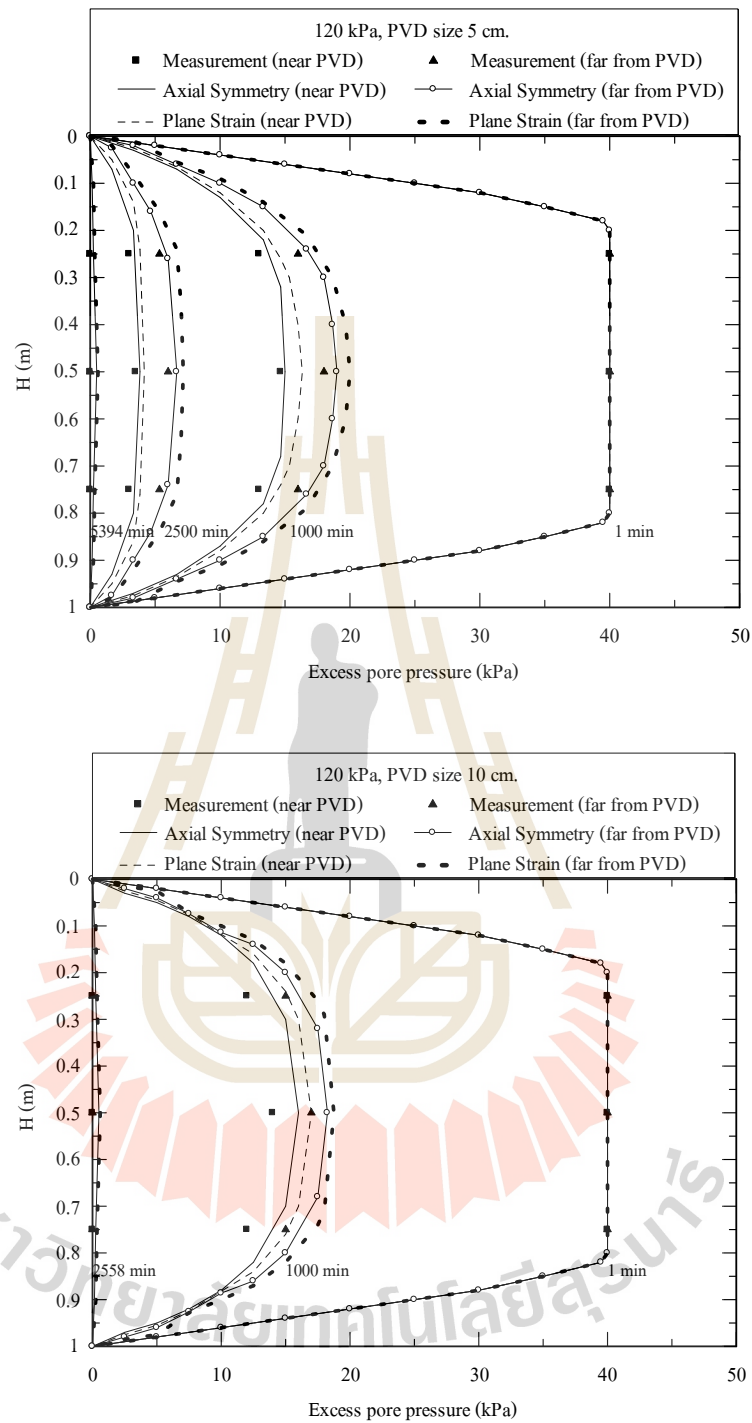


Figure 4.22 The relationship between the excess pore water pressure and depth of the soft mud with PVD sized 5 and 10 cm respectively at 120 kPa.

4.5 Analysis and Discussion

In term of settlement, PVD only accelerated the settlement of the ultra-soft mud while the final settlement is essentially the same. Comparing the measured settlement to the simulated settlement using 4 methods; 1.Hansbo Theory 2. Axial symmetry model 3. Plane strain model and 4.Chai's method, the settlement from Hansbo's theory is slightly higher than the measured result. For Chai's method and plane strain model, the calculated settlement is slightly lower than the measured result. However, the difference between measured and calculated result is acceptable within engineering range and therefore all the models can be used to simulate consolidation settlement with time.

In term of excess pore water pressure, from the relationship between the excess pore water pressure versus the radial distance and the relationship between the excess pore water pressure versus depth, the comparison between the measured result and Finite element results shows that the axial symmetry model provides the best simulated excess pore water pressure.

The consolidation of the ultra-soft mud with the prefabricated vertical drains was 1-D consolidation could be used for the settlement estimation in case of knowing the coefficient of consolidation (c_v) of composite ground. And Figure 4.23 show the ultra-soft mud with the prefabricated vertical drains sized 5 cm had c_v at 20, 40, 80 and 120 kPa were equal to 0.0108, 0.0075, 0.0064 and 0.057 m^2/day respectively. And ultra-soft mud with the prefabricated vertical drains sized 10 cm had c_v at 20, 40, 80 and 120 kPa were equal to 0.0156, 0.0109, 0.0091 and 0.0084 m^2/day respectively.

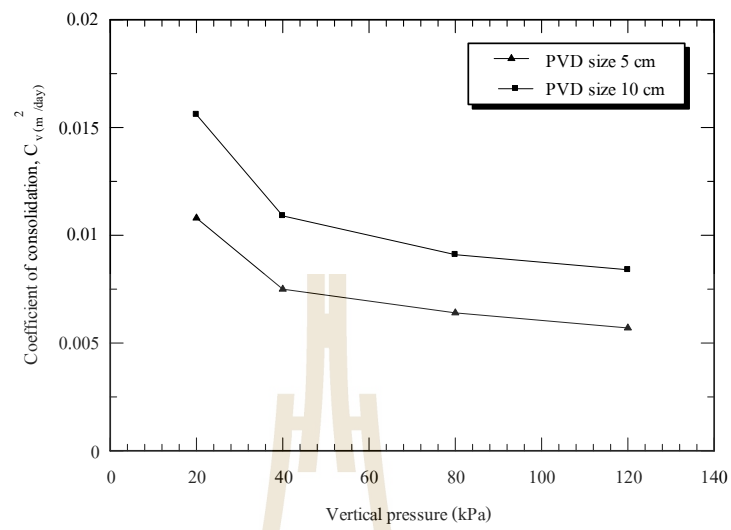


Figure 4.23 The relationship between coefficient of consolidation and applied vertical pressure.

CHAPTER 5

CONCLUSIONS

5.1 Summery

This study attempted to investigate the visibility of using PVD to improve engineering properties of ultra-soft mud in Mae Moh mine. The simulated consolidation settlement and excess pore water pressure using various finite element models were compared with the measured results from the model ground. The following conclusions can be drawn:

5.1.1 The consolidation of the ultra-soft mud with PVD

The settlement increases as the increase in applied vertical stress until the end of the consolidation and the final settlement is approximately 66 centimeters. When applying the load, the excess pore water pressure rapidly increases. The excess pore water pressure decreases rapidly with time due to the consolidation via the PVD. The rapid dissipation of excess pore water pressure is clearly observed at the top and bottom of the model ground (double drainage). The highest the excess pore water pressure is found at the middle of the model ground where the excess pore pressure close to the PVD is lower than that far away from the PVD.

5.1.2 Numerical Analysis

All the 4 models; 1. Hansbo's theory 2. Chai's method 3. Axial symmetry model and 4. Plane strain model can be used to simulate the rate of consolidation (settlement versus time relationship). While, excess pore water pressure can be fairly simulated by using both the axial symmetry and the plane strain models.

5.2 Suggestion

This research studied the consolidation behavior of the PVD improved ultra-soft mud in term of the settlement, rate of consolidation, and the excess pore water pressure using the physical model test and compared with the Finite element analysis (Plaxis 2D). The application of PVD to improve ultra-soft mud should be applied in the real condition with full instrumentation and finite element analysis.



REFERENCES

- B.H.C Sutton (1993). **Solving problems in soil mechanics**. Malaysia: Longman
- Bo Myint Win, V. Choa, A. Arulrajah and Y.M. Na (1999). "One dimension compression of slurry with radial drainage" **Soils and Foundation**, Vol.39, No.4, pp. 9-17.
- Bunopas & Wella. (1992). **Geotectonics and Geologic Evolution of Thailand**. **Bangkok** : Department of Mineral Resources.
- Charusiri. (1997). **Tectonic Evolution of Thailand : From Bunopas (1981)s to a new scenario**. Bangkok : Department of Mineral Resources.
- Cheng Liu and Jack B. Evett (2004). **Soil and foundations**. (6th edt.). Singapore: Person prentice hall.
- D.T. Bergado, L.R. Anderson, N. Miura and A.S. Balasubramaniam. **Soft ground improvement in lowland and other environments**. Thailand
- G.E. Barnes (1995). **Soil mechanics principle and practice**. London: Macmillan press Ltd.
- Jin-Chun Chai, Norihiko Miura, Saiichi Sakajo and Dennes Bergado (1995). "Behavior of vertical drains improved subsoil under embankment loading" **Soils and Foundation**, Vol.35, No.4, pp. 49-61.
- Jin-Chun Chai, Shui-Long Shen, Norihiko Miura and Dennes Bergado (2001). "Simple method of modeling PVD-improved subsoil" **Journal of**

geotechnical and geoenvironmental engineering, Vol. 127 NO. 11, pp. 22383.

Jin-Chun Chai, Bo Myint Win and A. Arulrajah (2009). “Reclamation of a slurry pond in Singapore” **Geotechnical engineering 162**, pp. 13-20.

Karl Terzaghi, Ralph B. Peck and Gholamreza Mesri (1996). **Soil mechanics in engineering practice**, (3rd ed.). United state of America.

M.J. Smith (1981). **Soil Mechanics**. (4th ed.) London: George godwin Ltd.

R. Whitlow (1995). **Basic soil mechanics**, (3rd ed.). Malaysia.

Suksun Horpibulsuk, Avirut Chinkulkijniwat, Arnon Cholphatsorn, Jirayut Suebsak and Martin D. Liu (2012). “Consolidation behavior of soil-cement column improved ground” **Computers and Geotectonics**

Thailand-Australia Lignite Mine Development Project. (1985). **Mae Moh Geotechnical Report**. Bangkok : EGAT

W. Sompong, G.M. Springbett and P.R. Evans. (1996). **Mae Moh Coal Deposit Geological Report**. Bangkok : EGAT

Y.K. Wong, Joseph. (2013). “Comparison of drainage line elements in plaxis 2D and 3D applied in consolidating marine clay deposits” **Soft soil Engineering**

International Conference. Young Townsend (1986). **Consolidation of soils testing and evaluation**. Baltimore

BIOGRAPHY

Miss Patsorn Wiwatthanatham was born on December 27th, 1989 in Bangkok. She studied at Satreburanawit School (Bangkok) for her elementary school. After that, she studied at Yothinburana School (Bangkok) for her high school. Then, she graduated from the Geology, Faculty of Science, Chulalongkorn University.

In 2012, she became the geologist in the Geotechnical Engineering and Hydrological Section, Geotechnical and Civil Engineering Department, Energy Resources Engineering Division, Electricity Generating Authority of Thailand. For the working life, she has the responsibility on the task which related to geology and geotechnical engineering. As time passes, the organization gave her a chance to study the master's degree in the field of Geotechnical Engineering. Due to the self-improvement and new knowledge, she decided to study the master's degree in Civil Engineering, Suranaree University of Technology in 2016.

During the master's degree, she will have the academic presentation in The 11th SEATUC SYMPOSIUM 2017 at Ho Chi Min University of Technology Vietnam, on March 13-14th 2017.